ESA Young Investigator Scientific Award Application 2025

Dr. Ben M. Lawrence
Early Career Postdoctoral researcher
The University of Melbourne

Endocrinology, 2025, **166**, bqaf078
https://doi.org/10.1210/endocr/bqaf078
Advance access publication 8 May 2025
Research Article

Functional Analysis of HSD17B3-Deficient Male Mice Reveals Roles for HSD17B7 and HSD17B12 in Testosterone Biosynthesis

Ben M. Lawrence,[1,2] Liza O'Donnell,[3,4] Anne-Louise Gannon,[1,5] David A. Skerrett-Byrne,[1,5,6,7,8] Shanmathi Parameswaran,[1] Imogen Abbott,[1] Sarah Smith,[1] David J. Handelsman,[9] Diane Rebourcet,[1,10,*] and Lee B. Smith[3,*]

[1]College of Engineering, Science and Environment, The University of Newcastle, Callaghan, New South Wales 2308, Australia
[2]School of BioSciences, The University of Melbourne, Parkville, Victoria 3010, Australia
[3]Office of the Deputy Vice-Chancellor (Research), Griffith University, Southport, Queensland 4222, Australia
[4]Hudson Institute of Medical Research and Department of Molecular and Translational Sciences, School of Clinical Sciences, Monash University, Clayton, Victoria 3168, Australia
[5]Infertility and Reproduction Research Program, Hunter Medical Research Institute, New Lambton, New South Wales 2305, Australia
[6]College of Health, Medicine and Wellbeing, The University of Newcastle, Callaghan, New South Wales 2308, Australia
[7]Institute of Experimental Genetics, Helmholtz Zentrum München, German Research Center for Environmental Health, Neuherberg 85764, Germany
[8]German Center for Diabetes Research (DZD), Neuherberg 85764, Germany
[9]University of Sydney and Andrology Department, ANZAC Research Institute, Concord Hospital, Sydney, New South Wales 2139, Australia
[10]Irset (Institut de recherche en santé, environnement et travail)-UMR_S 1085, Univ Rennes, Inserm, EHESP, Rennes 35065, France

Correspondence: Lee B. Smith, PhD, Building G34, Office for Research, Griffith University, 1 Parklands Drive, Southport, Queensland 4222, Australia.
Email: lee.smith@griffith.edu.au.
*Co-senior author.

Abstract

Historically, 17β-hydroxysteroid dehydrogenase type 3 (HSD17B3) was thought to be the key enzyme responsible for testicular testosterone production. In humans, loss-of-function mutations in *HSD17B3* impair testosterone production during prenatal life leading to impaired development of androgen-dependent tissues in 46,XY individuals. However, male mice with HSD17B3 deficiency exhibit normal testicular testosterone concentrations, normal development of reproductive organs and are fertile, suggesting that mice express other hydroxysteroid dehydrogenase enzymes capable of testicular testosterone synthesis. This study aimed to investigate whether 17β-hydroxysteroid dehydrogenase type 12 (HSD17B12), which can convert androstenedione to testosterone in mice but not in humans, compensates for the lack of HSD17B3 in *Hsd17b3* knockout (KO) mice. We used CRISPR/Cas9 to substitute the amino acid in mouse HSD17B12 that is responsible for its ability to convert androstenedione to testosterone with the amino acid of the human enzyme that prevents androstenedione being used as a substrate. When this *Hsd17b12* mutation was introduced into *Hsd17b3* KO mice, males exhibited normal reproductive tracts but reduced testicular testosterone production with a consequential reduction in seminal vesicle weight. This suggests HSD17B12 contributes toward testosterone production in the absence of HSD17B3, but other enzymes must also contribute. We therefore quantified other testicular hydroxysteroid dehydrogenases, finding that HSD17B7 mRNA and protein was markedly upregulated in *Hsd17b3* KO testes. We confirmed that mouse, but not human, HSD17B7 can produce testosterone in vitro. We conclude that compared to humans, mice exhibit increased plasticity in testosterone production via hydroxysteroid dehydrogenase enzymes to support androgen action and male fertility.

Key Words: testosterone, male fertility, androgens, testis, hydroxysteroid dehydrogenase

Abbreviations: 3α-diol, 5α-androstane-3α,17β-diol; 3β-diol, 5α-androstane-3β,17β-diol; AGD, anogenital distance; DHT, dihydrotestosterone; DMSO, dimethylsulfoxide; eGFP, enhanced green fluorescent protein; gDNA, genomic DNA; hCG, human chorionic gonadotropin; HSD17B12, 17β-hydroxysteroid dehydrogenase type 12; HSD17B3, 17β-hydroxysteroid dehydrogenase type 3; KO, knockout; PCR, polymerase chain reaction; qRT-PCR, quantitative reverse transcriptase polymerase chain reaction; WT, wild-type.

The production and action of the androgens testosterone and dihydrotestosterone (DHT) are essential for male sexual development and function, including fertility (1, 2). Hydroxysteroid 17β dehydrogenases convert 17-ketosteroids to 17β-hydroxysteroids, and 17β-hydroxysteroid dehydrogenase type 3 (HSD17B3), expressed in humans solely in the testis, is the primary enzyme responsible for the conversion of androstenedione to testosterone in the Leydig cells of the testis, culminating in testosterone secretion. Loss-of-function mutations to the human *HSD17B3* gene results in HSD17B3 deficiency whereby individuals with XY chromosomes exhibit androgen-deficient (hypogonadal) external genitalia but masculinized internal Wolffian structures at birth (1, 3-5). In contrast, *Hsd17b3* knockout (KO) mice develop with normal testosterone production and male reproductive function, including fertility when mature (6, 7). In

Received: 26 February 2025. **Editorial Decision:** 15 April 2025. **Corrected and Typeset:** 8 May 2025

Hsd17b3 KO mice, testosterone levels remain much higher in the testes than in circulation and other peripheral tissues including the adrenal glands, epididymis, prostate, and white adipose tissue, suggesting that the continued testosterone production in these mice originates from the testis (6, 7). Although the adrenal glands contribute a small proportion to androgen biosynthesis in human males (8), rodent adrenals do not produce androgens due to a lack of CYP17A1 enzyme expression (9, 10). Since steroidogenic enzyme expression in the mouse adrenal glands can change following orchidectomy (11), a previous study investigated whether the adrenal glands could contribute to testosterone production in *Hsd17b3* KO mice (7). Adrenalectomized *Hsd17b3* KO mice did not result in a decrease in circulating androstenedione, testosterone or DHT (7). These findings strongly suggest that the continued testosterone production in the testes of adult *Hsd17b3* KO mice is due to the expression of alternative testosterone synthesizing enzymes in the testis. However, the identity of these enzyme(s) is unknown.

Other hydroxysteroid dehydrogenase enzymes can catalyze the conversion of androstenedione to testosterone. HSD17B5 (also known as AKR1C3) can perform this conversion (12, 13) but is undetectable in the mouse testis of both wild-type and *Hsd17b3* KO adult mice (6, 14). HSD17B1 is expressed in fetal mouse Sertoli cells and contributes to testosterone production during fetal development (15, 16) and it can compensate for a lack of HSD17B3 during fetal development (17). However, in adulthood, *Hsd17b1* is undetectable in the testis in wild-type and *Hsd17b3* KO mice and cannot compensate for *Hsd17b3* deficiency (6, 17). Therefore, HSD17B1 and HSD17B5 are unlikely to contribute to testicular testosterone production in adult *Hsd17b3* KO mice.

HSD17B12 can convert androstenedione to testosterone in mice but not in humans (18), and produces 11-ketotestosterone, the predominant androgen in some fish (19). *Hsd17b12* encodes an enzyme that converts the estrogenic precursor estrone to the biologically active estrogen, estradiol (20), and catalyzes reactions involved in fatty acid elongation (21, 22) which is essential for early embryonic development (21, 23, 24). HSD17B12 was suggested as a potential candidate to compensate for a lack of HSD17B3 in *Hsd17b3* KO mice because it is expressed by adult Leydig cells (6).

Important functional differences exist between mouse and human HSD17B12. The differences in substrate specificity between the mouse and human enzymes regarding testosterone production is due to a key amino acid at position 234 on the amino acid sequence (18). In human and primate HSD17B12, a bulky phenylalanine amino acid at this location prevents the entrance of C19-steroids into the active site of the enzyme (20). In contrast, in mouse HSD17B12, the leucine amino acid at position 234 is smaller, and allows C19-steroids to enter the active site of the enzyme more readily than in humans (18). These data suggest that the inability of human HSD17B12 to make testosterone means it cannot compensate for the absence of HSD17B3 in conditions of human HSD17B3 deficiency. However, it is possible that HSD17B12 could maintain testosterone biosynthesis in the absence of *Hsd17b3* in mice.

The current study aimed to investigate the mechanisms by which testosterone production continues in adult *Hsd17b3* KO mice, with a focus on HSD17B12. As the loss of *Hsd17b12* is embryonically lethal in mice (21, 23), we used CRISPR/Cas9 to produce a novel mouse model in which we substituted the leucine amino acid in mouse HSD17B12 that is responsible for its ability to produce testosterone from androstenedione with phenylalanine, the amino acid in the human enzyme that prevents androstenedione being used as a substrate. We cross-bred this mutation into a homozygous *Hsd17b3* KO line to determine whether mouse HSD17B12 contributes to testosterone production in *Hsd17b3* KO mouse testes.

Materials and Methods

Transgenic Mice

Transgenic mice were generated at the MEGA Genome Engineering Facility at the Garvan Institute of Medical Research, Darlinghurst, NSW. CRISPR/Cas9 was used to generate a 7-base pair deletion at the end of exon 1 of *Hsd17b3* resulting in a frameshift mutation. These mice exhibited a phenotype indistinguishable from our previously generated *Hsd17b3* KO line (6, 14).

CRISPR/Cas9 was also used to generate the mutated *Hsd17b12* transgenic mouse line. Homologous repair using a template containing the desired mutation in the DNA sequence altered the 234th amino acid in the mouse HSD17B12 protein sequence. At this location, the DNA coding sequence for a leucine amino acid was altered to code for a phenylalanine amino acid to mimic the human HSD17B12 (referred as L234F).

A male C57BL/6 mouse carrying the homozygous KO of *Hsd17b3* was mated to a female C57BL/6 mouse carrying the homozygous L234F mutation to generate a double transgenic mouse line. The breeding strategy used thereafter to test the impact of the mutated HSD17B12 protein in *Hsd17b3* KO mice involved mating mice that were homozygous *Hsd17b3* KO and heterozygous *Hsd17b12* mutation.

Mice were exposed to a 12-hour day/night cycle and had access to water and soy-free chow, ad libitum. All procedures were approved by The University of Newcastle's Animal Care and Ethics Committee (ACEC), approval number #A-2018-820. All animal experiments were performed in accordance with the Australian code of practice for the care and use of animals for scientific purposes by the National Health and Medical Research Council of Australia.

In Vivo Treatments

Mice were injected intraperitoneally with a hyper-stimulating dose (20 IU) of human chorionic gonadotropin (hCG; Sigma-Aldrich, Australia) 16 hours prior to tissue collection (6).

Tissue Collection

Day-80 adult mice were euthanized by CO_2 inhalation. Blood was collected via cardiac puncture, centrifuged at 10 000*g* for 10 minutes at 4 °C, and serum was then collected and snap-frozen. Mice were weighed and anogenital distance (AGD) was measured using digital calipers (Adelab Scientific, Thebarton, SA, Australia). Androgen-dependent tissues were excised and weighed. Serum and tissues were either snap-frozen and stored at −80 °C until used for later analysis or fixed in Bouin's solution for 6 hours for histological analysis.

Genotyping

Genotyping was performed on ear biopsies after weaning and confirmation of genotype was performed again postmortem on tail tissue. Genomic DNA (gDNA) was digested in

Table 1. Details of genotyping assays

Assay	Reagent	Volume per reaction (μL)	Annealing temperature (°C)	Product size (bp)
Hsd17b3	Type-it Mastermix (2×)	5	55	WT-150
	Hsd17b3 forward primer (20 μM)	0.1		
	Hsd17b3 WT-reverse primer (20 μM)	0.1		Heterozygous-144 and 150
	Hsd17b3 del-reverse primer (20 μM)	0.1		
	dH_20	3.7		Homozygous-144
	gDNA	1		
Hsd17b12 WT	Type-it Mastermix (2×)	5	63	*Hsd17b12* WT-436
	Hsd17b12 WT-forward primer (20 μM)	0.1		
	Hsd17b12 WT-reverse primer (20 μM)	0.1		
	Il2 forward primer (20 μM)	0.1		*Il2* Control-324
	Il2 reverse primer (20 μM)	0.1		
	dH_20	3.6		
	gDNA	1		
Hsd17b12 Mutant	Type-it Mastermix (2×)	5	63	*Hsd17b12* Mut-432
	Hsd17b12 mut-forward primer (20 μM)	0.1		
	Hsd17b12 mut-reverse primer (20 μM)	0.1		
	Il2 forward primer (20 μM)	0.1		*Il2* Control-324
	Il2 reverse primer (20 μM)	0.1		
	dH_20	3.6		
	gDNA	1		

Table 2. Primers used for genotyping assays

Gene	Forward primer(s)	Reverse primer(s)
Hsd17b3	*Hsd17b3* forward: ggagaagctcttcattgctg	*Hsd17b3* WT-reverse: cttacctgcccattgtcccat *Hsd17b3* del-reverse: cttacctgtcccattgatcg
Hsd17b12	*Hsd17b12* WT-forward: acattagaaacctcacgctgct *Hsd17b12* mut-forward: acattagaaacctcacgctgct	*Hsd17b12* WT-reverse: ttgccagttttgtagctacaagg *Hsd17b12* Mut-forward: cagttttgtcgcgacgaa
Interleukin-2 (*Il2*) (Positive control gene)	*Il2* forward: ctaggccacagaattgaaagatct	*Il2* reverse: gtaggtggaaattctagcatcatcc

Tris-EDTA-Tween, pH 8, and Proteinase K for 1 hour at 55 °C, and then for 7 minutes at 95 °C to denature remaining Proteinase K. The digested samples were diluted 1:10 in DEPC-treated DNase- and RNase-free sterile water. The genotype of transgenic mice was identified by transgene-specific polymerase chain reaction (PCR) assays. PCR was performed on gDNA extracts using a Type-it Mutation Detect PCR Kit (QIAGEN, VIC, Australia). Details of primers used are shown in Tables 1 and 2. PCR products were detected using a QIAxcel DNA high resolution kit on the QIAxcel Advanced System and analyzed by QIAxcel ScreenGel Software (QIAGEN, VIC, Australia). *Il2* primers were included when genotyping *Hsd17b12* as a positive control for the PCR.

Transformation and Purification of Plasmids

Plasmids were transformed into NEB® Stable Competent *E. coli* (C3040I) cells following the NEB high efficiency transformation protocol (New England BioLabs, Notting Hill, VIC, Australia). In brief, 50 to 100 ng of plasmid DNA was added to NEB® Stable Competent *E. coli* and incubated on ice for 30 minutes, before being heat shocked at 42 °C for 30 seconds, then placed back on ice for 5 minutes. NEB® 10-beta/Stable outgrowth medium (New England BioLabs, Notting Hill, VIC, Australia) was added to each sample followed by incubation at 30 °C for 60 minutes, with constant shaking at 250 rpm. Cells were then spread over ampicillin-selective agar plates and incubated for 16 hours at 37 °C.

Transformed bacterial colonies were grown and purified following the QIAGEN Plasmid Maxi Kit Purification Handbook. Following purification of plasmid DNA, air-dried pellets were resuspended in DEPC-treated DNase- and RNase-free sterile water (Thermo Fisher Scientific, Vic, Australia). The yield of plasmid DNA was measured using the NanoDrop Lite Spectrophotometer (Thermo Fisher Scientific, VIC, Australia). Plasmids were stored at −30 °C.

Site-Directed Mutagenesis

Mouse *Hsd17b12* plasmid (details in Table 3) was altered by inducing a mutation that substituted the leucine amino acid at position 234 to a phenylalanine amino acid. The mutation and plasmid transformation were performed using an Agilent QuikChange II XL Site-Directed Mutagenesis Kit (Integrated Sciences, Chatswood, NSW, Australia). Primers were designed as recommended to induce a mutation to the mouse *Hsd17b12* (forward primer- gcagagtgtcatgccata**ctt**cg-tagctacaaaactggc; reverse primer- gccagttttgtagctacg**aag**tatgg-catgacactctgc, with bold and underlined regions indicating the point mutations) (Sigma-Aldrich, Australia). Manufacturer positive control and samples were prepared following manufacturer guidelines and cycled on a MasterCycler X50s. Amplified parental (nonmutated) products were digested with 10 U of *Dpn I* restriction enzyme at 37 °C for 1 hour. *Dpn I*-treated DNA was then added to XL10-GOLD ultra-competent cells and incubated on ice for 30 minutes, followed by heat-shock at 42 °C for 30 seconds, then placed back on ice to transform the cells with plasmid DNA. Cells were grown briefly in NZY^+ broth at 37 °C for 1 hour before being spread onto LB-ampicillin-selective agar plates containing 5-bromo-4-chloro-3-indolyl-β-D-galactopyranoside (X-gal) and isopropyl β-D-1-thiogalactopyranoside (IPTG). Plates were incubated for 16 hours at 37 °C and single colonies

Table 3. Details of plasmids used to transfect HEK-293T cells

Plasmid	Developer	Product ID	Tag/Reporter	Antibiotic resistance
e*GFP* control	GeneCopoeia	EX-NEG-M61	N/A	Ampicillin
Mouse *Hsd17b3*	GeneCopoeia	EX-Mm33978-M61	IRES2-eGFP	Ampicillin
Mouse *Hsd17b12*	GeneCopoeia	EX-Mm07555-M61	IRES2-eGFP	Ampicillin
Human *HSD17B12*	GeneCopoeia	EX-V1191-M61	IRES2-eGFP	Ampicillin
Mouse *Hsd17b7* (variant 2)	GeneCopoeia	EX-Mm30153-M61	IRES2-eGFP	Ampicillin
Human *HSD17B7* (variant 1)	Vector Builder	pDNA(VB220915-1259dkg)	eGFP	Ampicillin

containing the mutated plasmid were grown. The mutated plasmid was grown and purified following the QIAGEN Plasmid Maxi Kit Purification Handbook.

DNA Sequencing

The successful mutation of a leucine to a phenylalanine amino acid at site 234 in the *Hsd17b12* plasmid and in the humanized mouse line was confirmed by Sanger sequencing by the Australian Genome Research Facility (Westmead, Sydney, Australia). The desired point mutation was confirmed (Figs. 1A, 2A). Two separate point mutations were also induced in the mouse line; however, neither of these altered the amino acid sequence (Fig. 2A).

Cell Culture

HEK-293T cells were cultured in DMEM/F12 (Thermo Fisher Scientific, VIC, Australia) supplemented with 10% FCS (CellSera Australia, Rutherford, NSW, Australia) and 1% penicillin-streptomycin (Sigma-Aldrich, Australia). Cells received fresh culture medium approximately every 2 to 3 days and were incubated at 37 °C with 5% CO_2.

Transfections and Cell Treatments

HEK-293T cells (ATCC, Manassas, Virginia, USA) were transfected with plasmids to test the function of genes (Table 3), using a Lipofectamine™ 3000 transfection reagent kit (Thermo Fisher Scientific, VIC, Australia) as per manufacturer guidelines. One day prior, cells were seeded at 65% confluency in a 96-well plate, and 30 minutes prior to transfection, cells were washed and medium was replaced with Opti-MEM™ medium (Thermo Fisher Scientific, VIC, Australia) supplemented with 1% penicillin-streptomycin (Sigma-Aldrich, Australia), and incubated at 37 °C with 5% CO_2. A mastermix containing 0.1 µg plasmid DNA, 0.15 µL Lipofectamine™ 3000 reagent, 0.2 µL P3000™ Reagent (2 µL/µg DNA), and 10 µL Opti-MEM™ medium, per well was added to each well. Culture plates were placed on an orbital shaker for 5 minutes at 100 rpm to ensure plasmids were spread evenly across cells, followed by incubating at 37 °C with 5% CO_2. Transfection was confirmed after 24 hours by the presence of enhanced green fluorescent protein (eGFP) using the EVOS M5000 Imaging System (Thermo Fisher Scientific, Vic, Australia).

After transfection, cells were washed and medium replaced with phenol red free DMEM/F12, supplemented with 10% FCS and 1% penicillin-streptomycin. At 72 hours post transfection, cells were treated with either diluted dimethylsulfoxide (DMSO; Sigma-Aldrich, Australia) as a vehicle control or with 150 ng/mL of androstenedione (Cayman Chemical Company, Ann Arbor, MI, USA). Androstenedione was initially prepared as a 10 mg/mL stock concentration in DMSO. Stock androstenedione was then diluted in complete phenol red free DMEM/F12 medium. DMSO vehicle controls were diluted by the same factor. Each treatment group was performed in triplicate. Treated cells were incubated for 24 hours at 37 °C with 5% CO_2 followed by media being collected from cells and stored at −80 °C until steroid analysis.

Histology

Testis and epididymis tissues fixed in Bouin's solution were processed and embedded in paraffin wax. Then 5-µm sections were prepared, dewaxed in xylene (Sigma-Aldrich, Australia), and rehydrated through a decreasing gradient of ethanol. Tissue sections were stained with hematoxylin and eosin (Sigma-Aldrich, Australia). Light microscopy images of tissues were captured using a Zeiss AXIO Imager.A2 microscope (Carl Zeiss AG, Germany) with Olympus cellSens imaging software (Olympus, Macquarie Park, NSW, Australia).

Quantitative Reverse Transcriptase PCR

RNA was extracted from whole testis tissue using the RNeasy Mini kit (QIAGEN, VIC, Australia) as per manufacturer's instructions, incorporating RNase-free DNase on-column digestion (QIAGEN, VIC, Australia). An external Luciferase RNA control (Promega, Alexandria, NSW, Australia) was added at 1 ng/20 mg tissue to the homogenized tissue during the RNA extraction. RNA concentration was measured using a NanoDrop Lite Spectrophotometer (Thermo Fisher Scientific, VIC, Australia). Extracted RNA was reverse transcribed to cDNA using the SuperScipt VILO cDNA Synthesis Kit (Thermo Fisher Scientific, VIC, Australia) as per manufacturer instructions. Water (no template) and reverse transcriptase negative (-RT) controls were included in all reverse transcriptions. For quantitative reverse transcriptase (qRT)-PCR, target-specific primers and corresponding specific probes were identified and selected using the online Roche Universal Probe Library (UPL) Assay Design Centre. The qRT-PCR was performed on the LightCycler 96 system (Millenium Science, Mulgrave, VIC, Australia). Primers used to assess mouse *Hsd17b7* include: forward- gctcactgtgacaccgtacaa, and reverse- ctccggtttttggtggaag, along with UPL probe 81. Luciferase external control was detected using the primers: forward- gcacatatcgaggtgaacatcac, and reverse- gccaaccgaacggacattt, and a TaqMan Probe (tacgcggaatacttc).

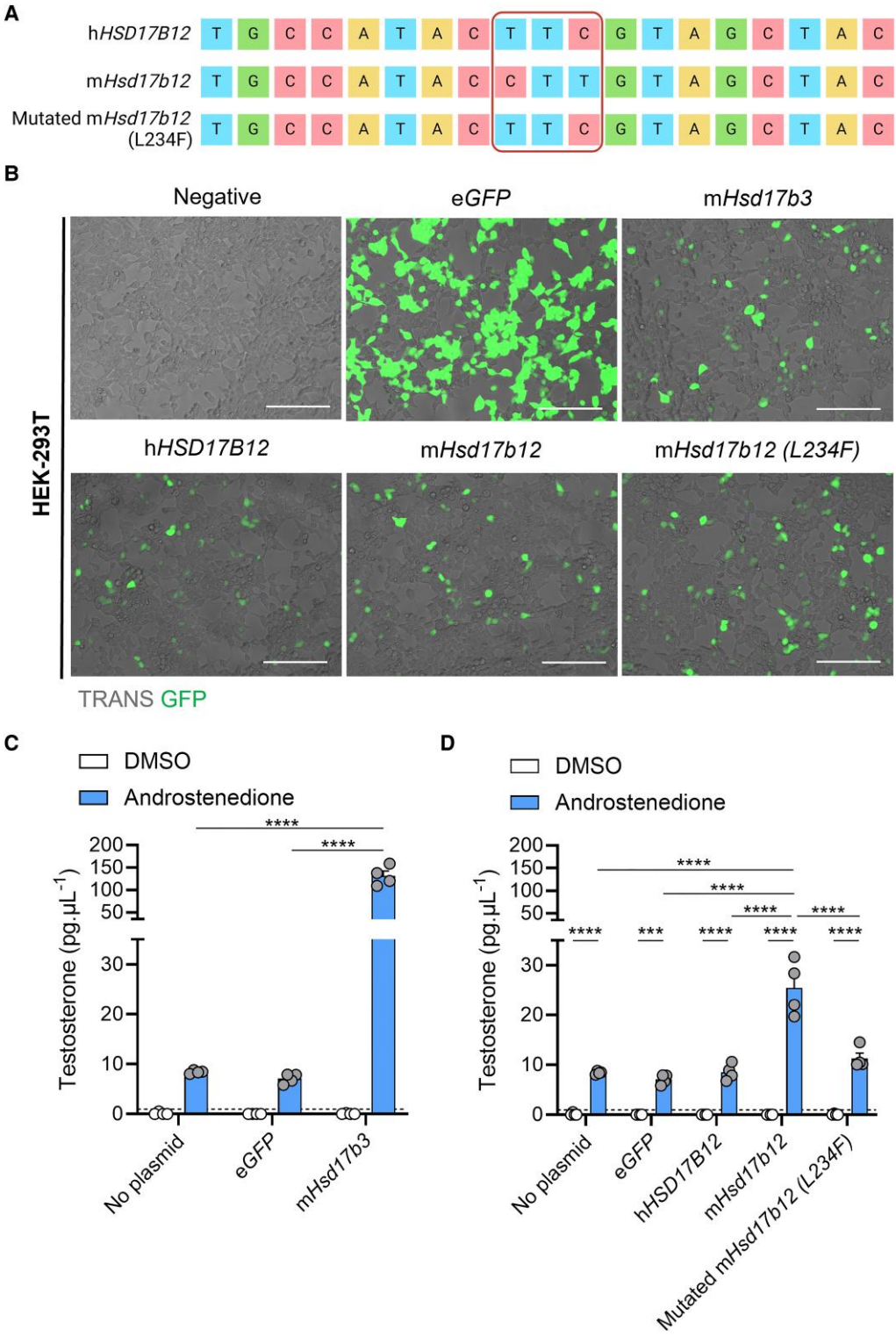

Figure 1. The presence of a leucine residue at amino acid position 234 in mouse HSD17B12 enables the conversion of androstenedione to testosterone. (A) Site-directed mutagenesis was performed on plasmids containing the genetic sequence of mouse (m)*Hsd17b12* to alter a single leucine amino acid to a phenylalanine (L234F). Plasmids containing the genetic sequence for human (h) *HSD17B12*, m*Hsd17b12*, and mutated m*Hsd17b12* (L234F) were sequenced by Sanger sequencing. Created with BioRender.com. (B) HEK-293T cells were transfected with plasmids carrying the e*GFP* reporter gene and steroidogenic enzyme genes, and testosterone in the culture media was quantified by mass spectrometry. Cells were transfected and treated with either DMSO (vehicle, open bars) or 150 ng/mL androstenedione (blue bars) for 24 hours. Representative images of HEK-293T cells that were transfected with plasmids expressing eGFP (green) alone (eGFP), or plasmids expressing eGFP, and either m*Hsd17b3*, h*HSD17B12*, m*Hsd17b12*, or a mutated m*Hsd17b12* which had a leucine amino acid substituted with a phenylalanine amino acid (L234F). Scale bar: 150 µm. TRANS: transillumination (C) Testosterone produced by cells transfected with m*Hsd17b3* were used as a positive control for the conversion of androstenedione to testosterone. (D) Testosterone produced by cells transfected with wild-type m*Hsd17b12*, h*HSD17B12*, and m*Hsd17b12* carrying the L234F mutation. Testosterone limit of detection = 0.98 pg/mL and is denoted by the dotted black line on the *y*-axis. Technical triplicates were averaged and plotted as biological replicates (n = 4). Two-way ANOVA, Tukey's multiple comparisons test, data shown as mean ± SEM. Significant differences between groups are indicated as *** = $P \leq .001$, **** = $P \leq .0001$.

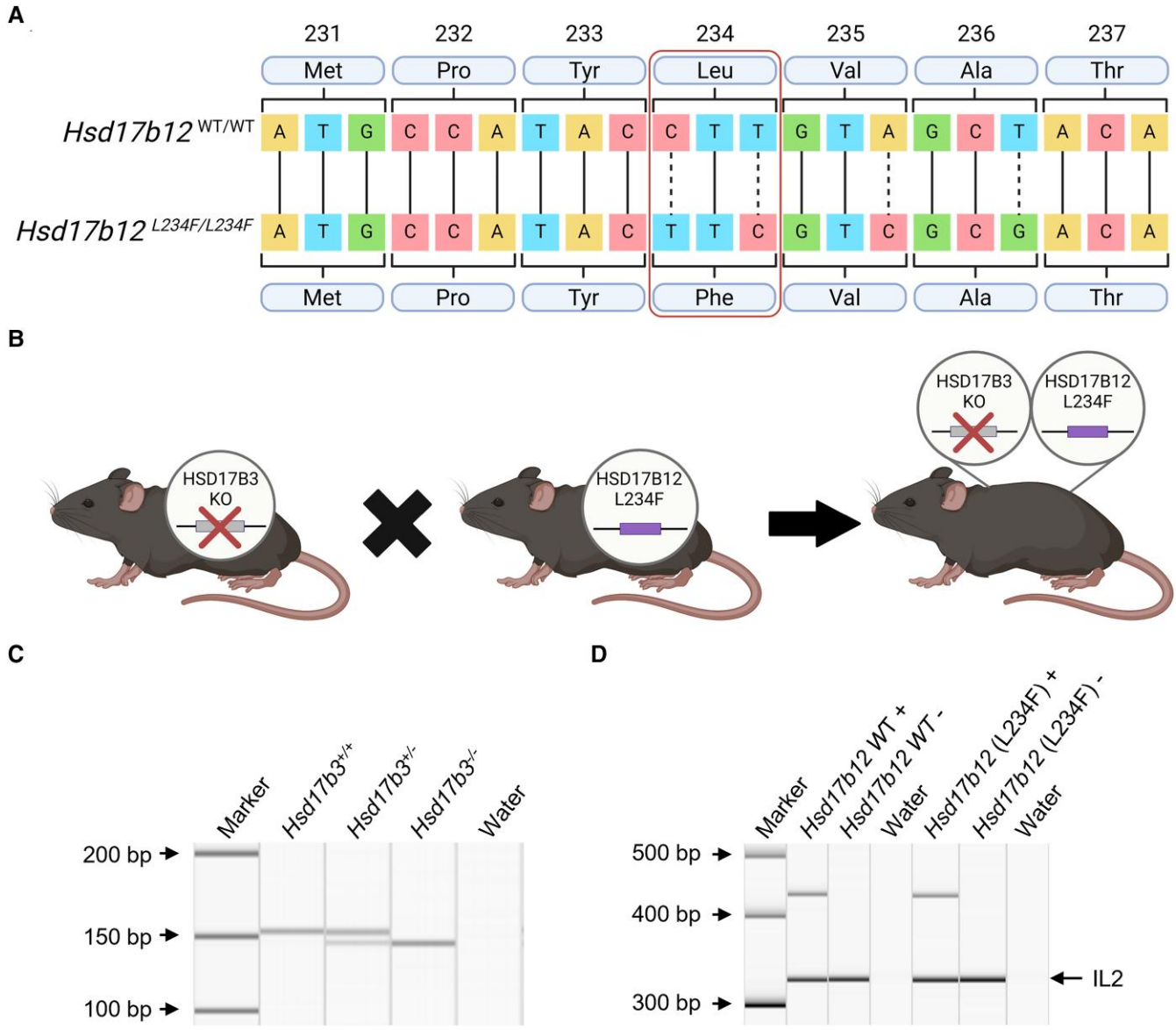

Figure 2. Generation and validation of *Hsd17b3* knockout (KO) mice expressing HSD17B12^{L234F}, with a mutation in amino acid position 234 that prevents its ability to convert androstenedione to testosterone. (A) Sanger sequencing of mouse *Hsd17b12* in wild-type and mutated animals. Point mutations in the DNA sequence were made to change the leucine (Leu) amino acid to a phenylalanine (Phe) amino acid, altering the amino acid sequence to replicate that seen in the human protein sequence. The mutated sequence is referred to as L234F. Created with BioRender.com. (B) Mutated *Hsd17b12* mice (*Hsd17b12*^{L234F}) were cross-bred with *Hsd17b3* KO mice to generate a mouse line incorporating both the *Hsd17b3* null allele and the *Hsd17b12* mutation. Created with BioRender.com. (C, D) Genotypes of mice were determined using standard PCR. (C) Presence of the *Hsd17b3*$^{+/+}$ (wild-type) allele was indicated by a 153-base pair (bp) band. The *Hsd17b3*$^{-/-}$ (*Hsd17b3* KO) allele was indicated by a 7-bp deletion which showed a 146-bp band. (D) The presence or absence (+ or –) of the *Hsd17b12* wild-type gene and the mutated *Hsd17b12* (L234F) gene was identified by PCR products that were 436 and 432 bp, respectively. Interleukin-2 (IL-2) was used as a positive control in amplified samples, shown by a 324-bp band.

Quantification of mRNA expression was calculated using the $2^{-\Delta\Delta Ct}$ method. Gene expression was determined relative to the external housekeeping Luciferase gene in adult tissues (Roche, AU). Each sample was run in triplicate and an average of the Ct value was taken.

Measurement of Testosterone in Cell Culture Media

Testosterone produced in vitro was quantified by liquid chromatography–mass spectrometry (LC-MS) using a QTRAP® 6500 LC-MS/MS System (SCIEX, Toronto, Canada) by the Central Analytical Facility at The University of Newcastle. Testosterone (Cayman Chemical Company, Ann Arbor, MI, USA) used for standards was resuspended in DMSO (Sigma-Aldrich, Australia) to make a stock concentration of 1 mg/mL. A testosterone working concentration of 1000 pg/µL was made using stock testosterone and fresh culture media (DMEM/F12 + 10% FBS). A 1:2 serial dilution was performed and used to make a standard curve with the lowest standard being 0.98 pg/mL.

Circulating and Intratesticular Steroid Analysis

Circulating and intratesticular steroids were quantified by LC-MS. Fragments of adult mouse testes (20-40 mg) were homogenized in 50 mM Tris pH 7.4, 0.01% SDS, 1%

deoxycholate, containing cOmplete Mini Protease Inhibitor Cocktail (Sigma-Aldrich, Australia) and PhosSTOP (Sigma-Aldrich, Australia) at a concentration of 20 µL/mg of tissue. Samples were homogenized using a TissueLyser II (QIAGEN, VIC, Australia) for 4 × 30-second intervals at 25 Hz. Samples were placed on ice for 1 minute after each 30-second interval to avoid samples overheating. LC-MS analysis was performed at the ANZAC Research Institute, Concord Hospital, NSW.

Proteomics

Sample preparation

Proteomics was performed on fragments of whole testes from adult (day 80) wild-type and *Hsd17b3* KO mice that were generated in a previous study (14). The *Hsd17b3* KO mice used for proteomics were also heterozygous for a null allele of the *Srd5a1* gene (14); however, these mice showed an identical endocrine and reproductive phenotype as previously generated *Hsd17b3* KO mouse lines (6, 7, 14). Testis fragments were homogenized as described above in ice cold lysis buffer containing 0.1M Na_3CO_3 pH 11 (Sigma-Aldrich, Australia), 10mM Na_3VO_4 (Sigma-Aldrich, Australia), 2.5% Protease inhibitor cocktail (Sigma-Aldrich, Australia), and one tablet of PhosSTOP (Sigma-Aldrich, Australia) per 10 mL (25-27). Samples were sonicated for 4 × 10-second intervals, with samples incubated on ice for 20 seconds between each interval to prevent protein denaturation. Total protein was quantified by the Pierce™ BCA Protein Assay kit (Thermo Fisher Scientific, Vic, Australia) and 500 µg of protein from each sample was mixed 1:1 with urea/thiourea to reach a final concentration of 6M urea/2M thiourea. Proteins were reduced by the addition of dithiothreitol (DTT) (Sigma-Aldrich, Australia) to a final concentration of 10 mM and incubated at room temperature for 30 minutes, shaking at 400 rpm. Proteins were then alkylated by adding iodoacetamide (Sigma-Aldrich, Australia) to a final concentration of 20mM and incubated in the dark at room temperature for 30 minutes with 400 rpm shaking. Protein samples were subsequently digested with a 1:12.875 ratio of 1 µg/µL trypsin/Lys-C Mix (Promega, Alexandria, NSW, Australia), incubated at room temperature for 3 hours with shaking at 400 rpm. Urea concentration was diluted to below 1M using 50mM of triethylammonium bicarbonate (TEAB) buffer (Sigma-Aldrich, Australia), pH 7.8, and incubated at 37 °C for 16 hours with shaking at 1000 rpm. Lipids were precipitated by adding formic acid (Sigma-Aldrich, Australia) to make a final concentration of 2%, and then centrifuged at 14 000*g* for 10 minutes at room temperature. The supernatant containing the peptides was stored at −80 °C until samples were desalted.

Peptide samples were cleaned and desalted using commercial desalting columns (Oasis, Waters Corporation, Milford MA, USA). Clean peptides were eluted through the equilibrated desalting columns using a vacuum pump. Peptides were quantified using a Qubit 2.0 fluorometer (Thermo Fisher Scientific, Vic, Australia) and 10 µg of sample peptides were lyophilized using a RVC 2-25 SpeedyVac (Martin Christ, Gefriertrocknungsanlagen GmbH, Germany) set at 45 °C for 2.5 hours. Lyophilized peptides were stored at −80 °C until required for mass spectrometry analysis.

Nano-liquid chromatography–mass spectrometry

Lyophilized clean peptides were resuspended in 2% acetonitrile (Thermo Fisher Scientific, VIC, Australia), 0.1% TFA to a final concentration of 1 µg/µL. Reverse phase nano-LC-MS was performed using an Orbitrap Eclipse Tribrid MS equipped with a front-end field asymmetric ion mobility spectrometry (FAIMS), coupled to a Vanquish Neo ultra high-performance liquid chromatography system UHPLC System (Thermo Fisher Scientific, Waltham, MA, US). Samples were loaded onto an Acclaim PepMap 100 C18 75 µm × 20 mm trap column (Thermo Fisher Scientific, Vic, Australia) for pre-concentration and online de-salting. Separation was then achieved using an EASY-Spray PepMap C18 75 µm × 250 mm column (Thermo Fisher Scientific, Vic, Australia), employing a linear gradient of acetonitrile (2%-40%) over 85 minutes. Full MS/data dependent acquisition MS/MS mode was utilized on Xcalibur (Thermo Fisher Scientific; version 4.6.67.17) with an automatic cycle between 3 compensations voltages (CV; −50, −65, and −80). The Orbitrap mass analyzer was set at a resolution of 1 200 000, to acquire full MS with an m/z range of 375-1500, with a normalized automatic gain control target set to standard and maximum fill times set to auto. The 20 most intense multiply charged precursors were selected for higher-energy collision dissociation fragmentation with a collisional energy of 35%. MS/MS fragments were measured using the Ion Trap, with the scan rate set to rapid, using standard mode for automatic gain control target and automatic maximum fill times.

Proteomic data processing and analysis

As per previous proteomic studies (25, 28, 29), database searching of raw files were performed using Proteome Discoverer 2.5 (Thermo Fisher Scientific), utilizing SEQUEST HT to search against the UniProt Mus musculus database (25 444 sequences, downloaded November 29, 2022). Database searching parameters included up to 2 missed cleavages, a precursor mass tolerance set to 10 ppm and fragment mass tolerance of 0.02 Da. Trypsin was designated as the digestion enzyme. Cysteine carbamidomethylation was set as a fixed modification while acetylation (K, N-terminus) and oxidation (M) were designated as dynamic modifications. Interrogation of the corresponding reversed database was also performed to evaluate the false discovery rate (FDR) of peptide identification using Percolator based on q-values, which were estimated from the target-decoy search approach. To filter out target peptide spectrum matches over the decoy-peptide spectrum matches, a fixed FDR of 1% was set at the peptide level.

Statistical Analysis

Statistical analyses were performed using GraphPad Prism software, versions 8.4.3 and 10.2.3 (GraphPad Software, San Diego, CA, USA). Gaussian distribution was assessed by the Shapiro-Wilk normality test to determine if downstream analyses would be performed using appropriate parametric or nonparametric statistical testing. Datasets which passed normality testing underwent parametric statistical tests including unpaired *t* tests, one-way ANOVA with Tukey's post hoc test, or two-way ANOVA with Tukey's post hoc test. Datasets which did not pass the normality test underwent nonparametric statistical testing including Kruskal-Wallis test with Dunn's post hoc test.

Significance testing and comparisons associated with the proteomic analysis of testis tissue were calculated by Proteome Discoverer 2.5 using a non-nested pairwise ratio approach, whereby the program calculates the peptide group ratios as the geometric median of all combinations of ratios

from all the replicates for each group. Protein ratios were subsequently calculated as the geometric median of the peptide group ratios and statistical testing was completed using a Student's *t* test. Proteomic data was considered significantly different when the *P* value ≤.05.

Results

Replacement of Leucine With Phenylalanine at Position 234 Inhibits Testosterone Biosynthesis in Mouse HSD17B12

We first aimed to confirm that mouse HSD17B12, but not human HSD17B12, can use androstenedione as a substrate to produce testosterone, and this is due to the reduced size of the amino acid at position 234.

Substitution of the leucine (Leu) amino acid with a phenylalanine (Phe) amino acid at position 234 (L234F) was confirmed through Sanger sequencing (Fig. 1A). The *Hsd17b12* sequences in both the mouse and human *Hsd17b12* plasmids matched exactly to previously published data (18). To assess the ability of mouse and human HSD17B12 to synthesize testosterone, we transfected HEK-293T cells with plasmids expressing GFP reporters and steroidogenic enzymes (Fig. 1B). Non-transfected cells and eGFP controls produced low levels of testosterone upon addition of androstenedione, suggesting some endogenous hydroxysteroid dehydrogenase activity in HEK-293T cells (Fig. 1C and 1D). Transfection with mouse *Hsd17b3* induced a >15-fold increase in testosterone compared to controls (Fig. 1C), indicating that these cells can be used to assess 17β-hydroxysteroid dehydrogenase activity.

The inability of human HSD17B12 to utilize androstenedione as a substrate (18) was confirmed by the unchanged amount of testosterone produced by cells transfected with human *HSD17B12* compared to controls (Fig. 1D). In contrast, transfection of cells with mouse *Hsd17b12* caused a significant increase in testosterone production (Fig. 1D), confirming species-dependent 17β-hydroxysteroid dehydrogenase activity.

Introduction of the L234F mutation into mouse *Hsd17b12* transfected cells significantly reduced its ability to produce testosterone compared to the nonmutated mouse *Hsd17b12* transfected cells (Fig. 1D). Testosterone concentrations in androstenedione-treated cells transfected with the mutated mouse *Hsd17b12* were not different to cells transfected with human *HSD17B12* (Fig. 1D). These results confirm the functional differences between the mouse and human HSD17B12 enzymes in their ability to convert androstenedione to testosterone (18) and demonstrate that the ability of mouse HSD17B12 to produce testosterone can be inhibited by the introduction of a phenylalanine amino acid at residue 234.

The Generation of *Hsd17b3*-Deficient Mice Expressing a Mutated *Hsd17b12*

We hypothesized that the maintenance of masculinization and fertility in *Hsd17b3* KO male mice could be due to the ability of endogenous HSD17B12 to maintain testicular testosterone concentrations. Complete deletion of *Hsd17b12* in mice is embryonically lethal (23) so CRISPR/Cas9 technology was used to generate a mouse line in which *Hsd17b12* was mutated from a leucine amino acid to a phenylalanine amino acid to mimic the human HSD17B12 (denoted $Hsd17b12^{L234F}$ mice). The L234F mutation was confirmed by Sanger sequencing (Fig. 2A). This mutation prevents the ability to convert androstenedione to testosterone (Fig. 1D) but is unlikely to prevent HSD17B12's ability to convert estrone to estradiol (18). If HSD17B12 is the sole enzyme producing testosterone in *Hsd17b3*-deficient adult mice, then the introduction of this mutation should cause a phenotype of androgen insufficiency in adult males.

$Hsd17b12^{L234F}$ mice were cross-bred with *Hsd17b3* KO mice to generate a mouse line incorporating both mutations (Fig. 2A and 2B). Genotyping confirmed mice were homozygous for the *Hsd17b3* KO ($Hsd17b3^{-/-}$) by a single band that contained a 7-bp deletion (146 bp) compared to wild-type (WT; $Hsd17b3^{+/+}$) and heterozygous ($Hsd17b3^{+/-}$) which had a single 153 bp band or 2 bands, respectively (Fig. 2C). Separate PCRs were used to assess the presence or absence of the *Hsd17b12* WT and mutated genes for each mouse (Fig. 2D). The genotype of mice with a KO of *Hsd17b3* and expressing a mutated *Hsd17b12* with a L234F amino acid substitution is referred to as $Hsd17b3^{-/-}$; $Hsd17b12^{L234F/L234F}$.

Male *Hsd17b3*-Deficient Mice Expressing Mutated *Hsd17b12* Have Smaller Seminal Vesicles but Remain Fertile

The impact of the *Hsd17b12* L234F mutation on the phenotype of *Hsd17b3* KO male mice was characterized in adult (day 80) mice. Both males and females were examined to investigate whether a phenotype of under-virilization or disordered sexual development was evident (Fig. 3). All male reproductive tissues were present, including the testes, epididymides, vas deferens, seminal vesicles and prostate (Fig. 3A). All females had ovaries and uteri present in all genotypes (Fig. 3B). These results indicate that androgen bioactivity in male *Hsd17b3* KO mice expressing a mutated *Hsd17b12* continues during development. No change in body weight was observed between $Hsd17b3^{-/-}$; $Hsd17b12^{WT/WT}$, $Hsd17b3^{-/-}$; $Hsd17b12^{WT/L234F}$ and $Hsd17b3^{-/-}$; $Hsd17b12^{L234F/L234F}$ groups (Fig. 3C). While there was no change in the anogenital distance (AGD) between any group (Fig. 3D), there was a decrease in the anogenital index (AGI), which is a standardized assessment of AGD (30), in $Hsd17b3^{-/-}$; $Hsd17b12^{L234F/L234F}$ compared to $Hsd17b3^{-/-}$; $Hsd17b12^{WT/WT}$ (Fig. 3E). There was a significant reduction in seminal vesicle weight in $Hsd17b3^{-/-}$; $Hsd17b12^{L234F/L234F}$ mice compared to $Hsd17b3^{-/-}$; $Hsd17b12^{WT/WT}$ controls (Fig. 3F), which is known to be sensitive to reductions in androgens (31). There was a slight but significant reduction in testis weight of $Hsd17b3^{-/-}$; $L234F^{L234F/L234F}$ compared to $Hsd17b3^{-/-}$; $L234F^{WT/L234F}$ mice, but not compared to $Hsd17b3^{-/-}$; $L234F^{WT/WT}$ controls (Fig. 3G). No significant differences were detected in the weight of the epididymis (Fig. 3H), kidney (Fig. 3I), or spleen (Fig. 3J). There was also a significant increase in gonadal fat weight in $Hsd17b3^{-/-}$; $Hsd17b12^{L234F/L234F}$ mice compared to the $Hsd17b3^{-/-}$; $Hsd17b12^{WT/WT}$ controls (Fig. 3K).

Gross testis histology was unchanged in $Hsd17b3^{-/-}$; $Hsd17b12^{L234F/L234F}$ mice, with seminiferous tubules and interstitial cells resembling other genotypes (Fig. 4A) and the cauda epididymis contained abundant sperm (Fig. 4B). In a small number of test matings between $Hsd17b3^{-/-}$; $Hsd17b12^{L234F/L234F}$ males and control females, live viable offspring were obtained.

Testicular Testosterone Production Is Reduced in *Hsd17b3*-Deficient Mice Expressing Mutated *Hsd17b12*

We next investigated the impact of the L234F mutation in mouse HSD17B12 on testicular testosterone production in

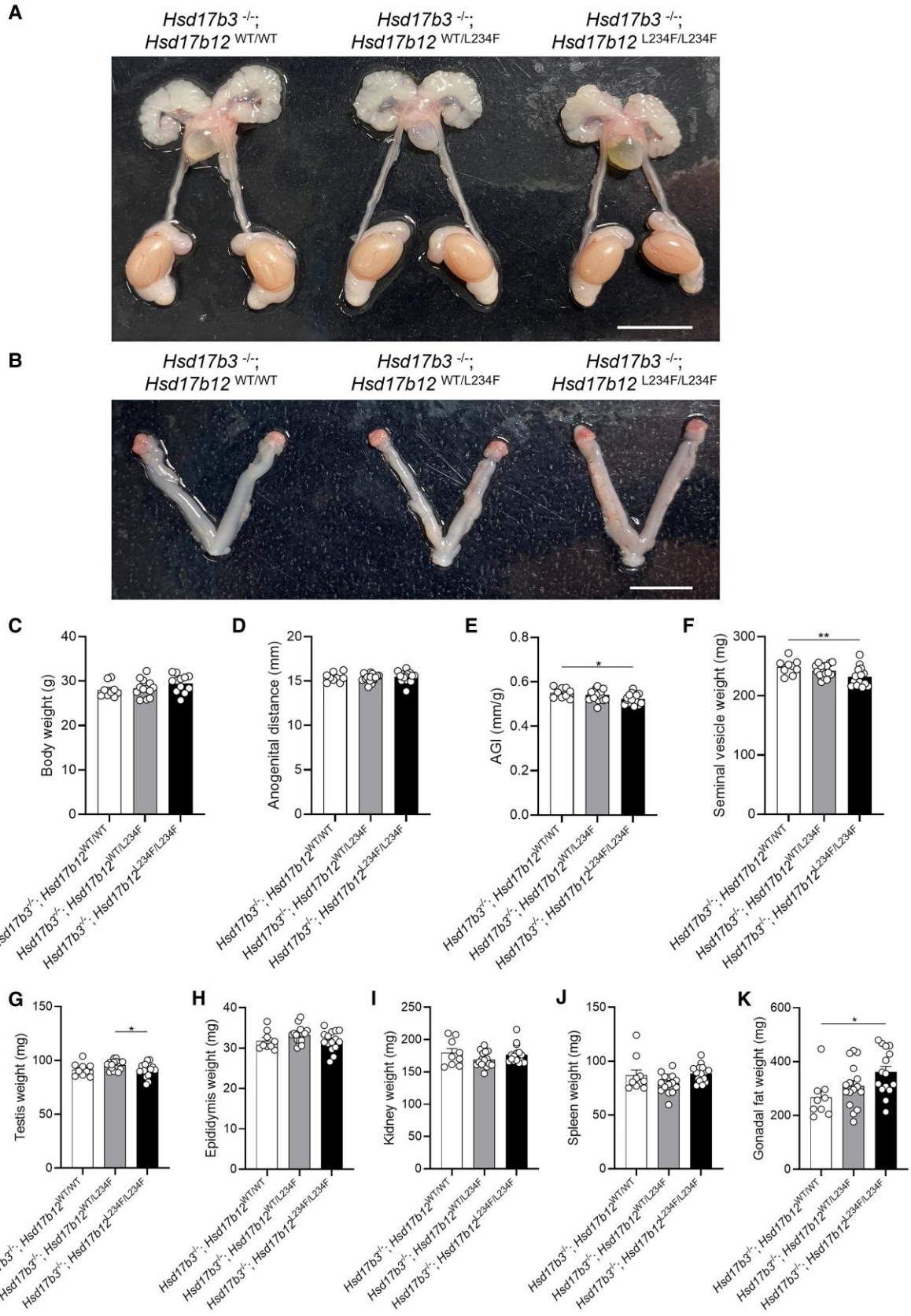

Figure 3. Characterization of the reproductive tract in adult (day 80) male *Hsd17b3* knockout (*Hsd17b3*$^{-/-}$) mice expressing the mutant *Hsd17b12*$^{L234F/L234F}$ allele. (A) Representative images of male and (B) female reproductive tracts of *Hsd17b3*$^{-/-}$; *Hsd17b12*$^{WT/WT}$, *Hsd17b3*$^{-/-}$; *Hsd17b12*$^{WT/L234F}$ and *Hsd17b3*$^{-/-}$; *Hsd17b12*$^{L234F/L234F}$ mice. Scale bars: 10 mm. (C) Total body weight, (D) anogenital distance, (E) anogenital index (AGI) (standardization of anogenital distance relative to body weight), (F) seminal vesicle, (G) testis, (H) epididymis, (I) kidney, (J) spleen, and (K) gonadal fat weights of male mice. One-way ANOVA, Tukey's test where $P \leq .05$, data shown as mean ± SEM with n = 9-16. Significant differences between groups are indicated as * = $P \leq .05$, ** = $P \leq .01$.

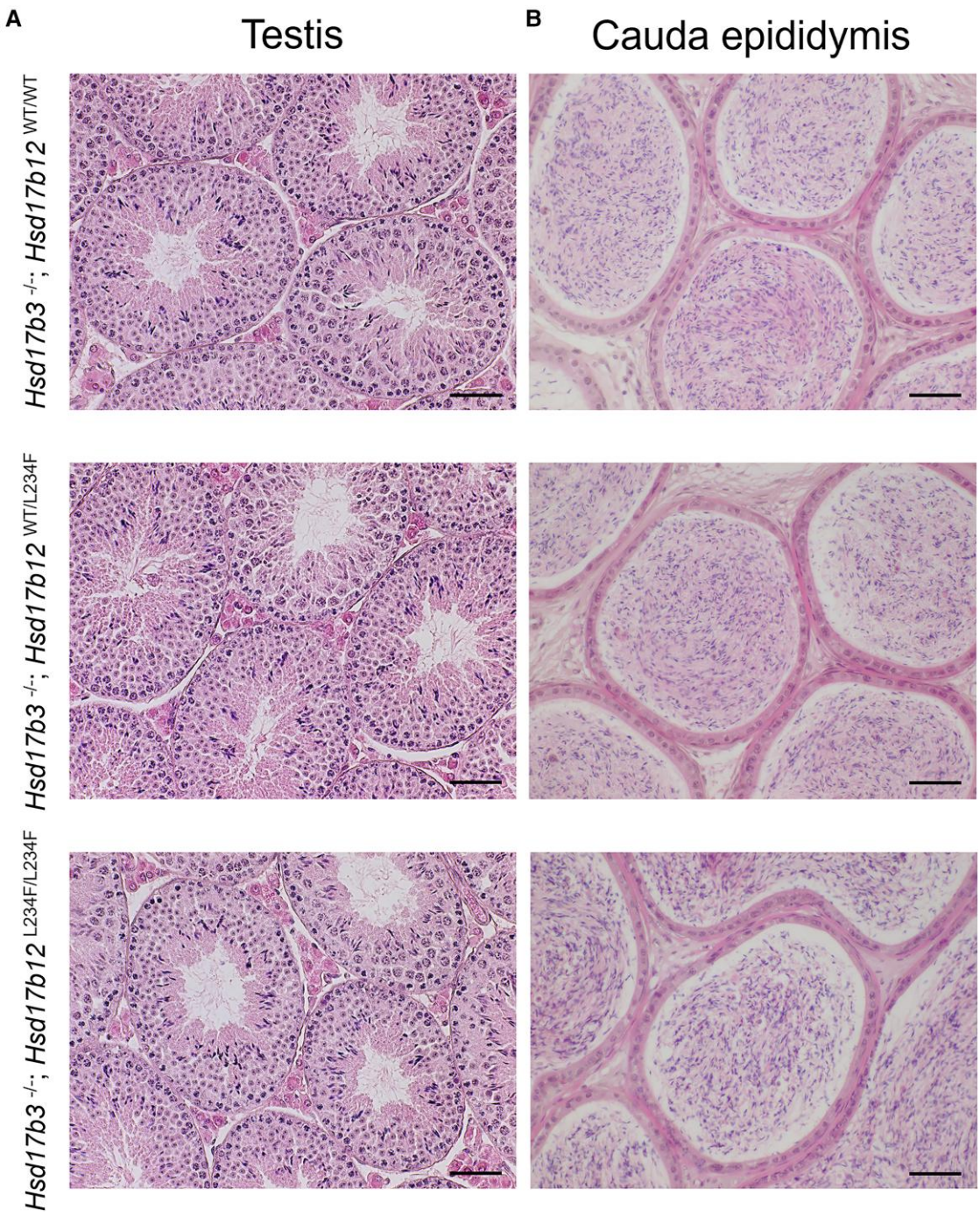

Figure 4. Testis and cauda epididymis histology in adult (day 80) male *Hsd17b3* knockout (*Hsd17b3*$^{-/-}$) mice expressing either the mouse *Hsd17b12* wild-type allele (*Hsd17b12*$^{WT/WT}$), heterozygous for the mutant allele (*Hsd17b12*$^{WT/L234F}$) or homozygous for the humanized *Hsd17b12* mutant allele (*Hsd17b12*$^{L234F/L234F}$). (A) Representative hematoxylin and eosin (H&E) staining of adult the testis and (B) cauda epididymis. Scale bars: 50 μm.

Hsd17b3 KO mice in vivo. Adult mice were treated with hCG to stimulate maximal androgen production and intratesticular steroids were measured by LC-MS.

Within the canonical pathway of androgen biosynthesis, pregnenolone, progesterone, 17-OH progesterone, dehydroepiandrosterone (DHEA), androstenedione, and androstenediol concentrations were unchanged in the testis (Fig. 5A, 5B, 5E, 5G, 5H, and 5K). Increased concentrations of 17-OH pregnenolone were observed in *Hsd17b3*$^{-/-}$; *Hsd17b12*$^{L234F/L234F}$ compared to *Hsd17b3*$^{-/-}$; *Hsd17b12*$^{WT/WT}$ (Fig. 5D), pointing to other roles for the L234 residue in steroid metabolism. Importantly, *Hsd17b3* KO mice with the *Hsd17b12* L234F mutation showed a significant (~16%) reduction in intratesticular testosterone concentrations compared to *Hsd17b3*$^{-/-}$; *Hsd17b12*$^{WT/WT}$ mice (Fig. 5L). These data suggest that HSD17B12 contributes to testosterone biosynthesis in the testes of *Hsd17b3* KO mice, but it is not solely responsible for the continued testosterone production. While there was a reduction in testosterone concentration, no changes in DHT were observed (Fig. 5M).

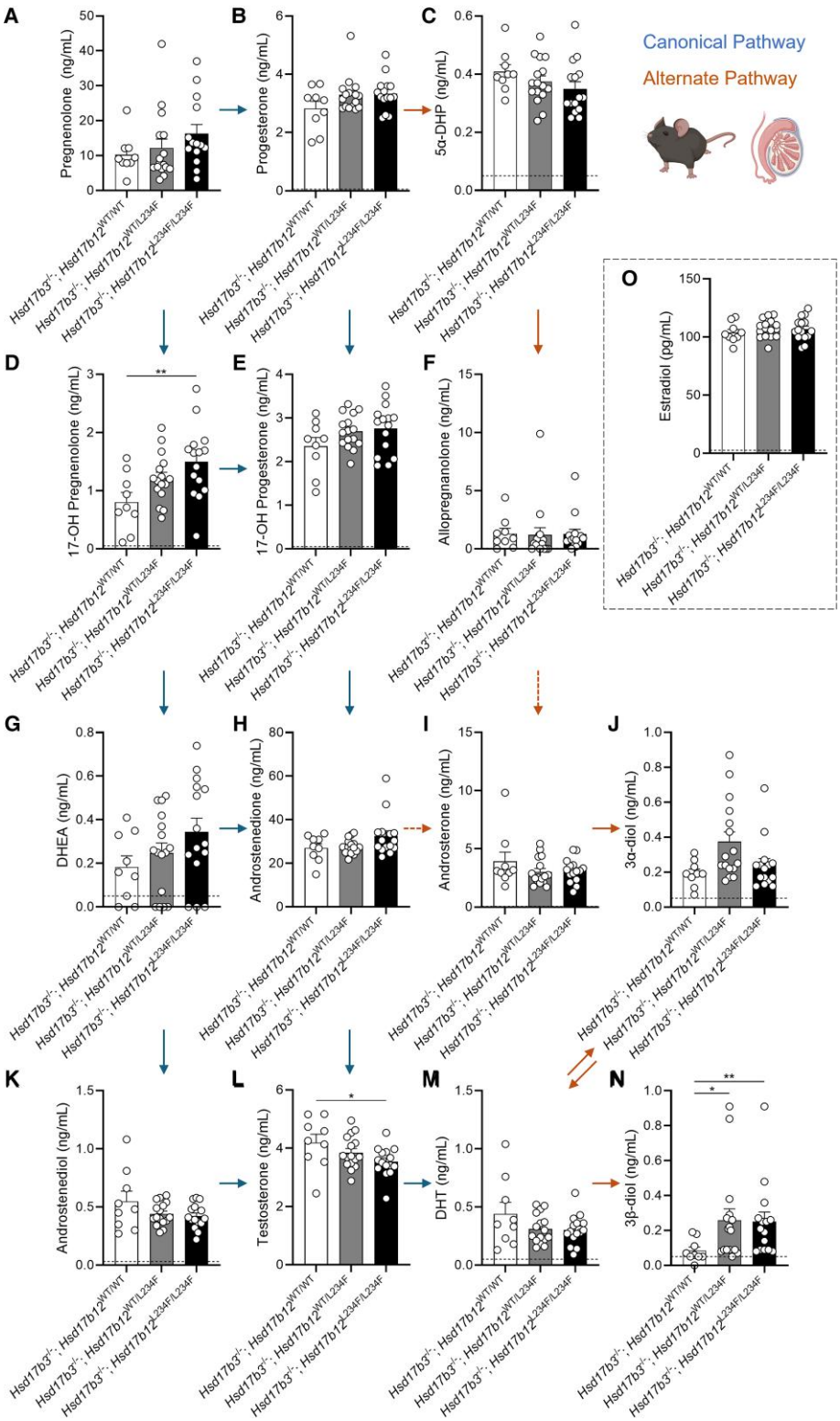

Figure 5. Intratesticular steroid concentrations in adult (day 80) male *Hsd17b3* knockout (*Hsd17b3*$^{-/-}$) mice expressing the mutant *Hsd17b12*^{L234F} allele(s). Mice were treated with human chorionic gonadotrophin (hCG) to stimulate maximal steroidogenesis. Androgens and androgen precursors include (A) pregnenolone, (B) progesterone, (C) 5α-dihydroprogesterone (5α-DHP) (D) 17-OH pregnenolone, (E) 17-OH progesterone (F) allopregnanolone (G) dehydroepiandrosterone (DHEA), (H) androstenedione, (I) androsterone, (J) 5α-androstane-3α, 17β-diol (3α-diol), (K) androstenediol, (L) testosterone, (M) dihydrotestosterone (DHT), and (N) 5α-androstane-3β, 17β-diol (3β-diol). The arrows indicate the direction of the canonical and alternate androgen production pathways. Dotted arrows indicate an indirect conversion. Biological replicates that were below the limit of detection were recorded as 0 ng/mL. Limit of detection ranged from 0.01 ng/mL to 0.05 ng/mL depending on the analyte and is indicated by a dotted black line on *y*-axis. One-way ANOVA, Tukey's test (for parametric data) or Kruskal-Wallis test (for nonparametric data), where $P \leq .05$, data shown as mean ± SEM with n = 9-16 per group. Significant differences between groups are indicated as * = $P \leq .05$, ** = $P \leq .01$. (O) Intratesticular estradiol levels. Limit of detection = 2.5 pg/mL and is indicated by the dotted black line on *y*-axis, One-way ANOVA, Tukey's test where $P \leq .05$, data shown as mean ± SEM with individual values for n = 9-16 biological replicates per group.

We also measured the impact of the L234F mutation in HSD17B12 on intratesticular androgen precursors within the alternate pathway of androgen biosynthesis, including 5α-dihydroprogesterone (5α-DHP), allopregnanolone, androsterone, 5α-androstane-3α,17β-diol (androstanediol [3α-diol]) and 5α-androstane-3β,17β-diol (3β-diol) (Fig. 5C, 5F, 5I, 5J, and 5N). No significant changes were seen in these steroids except for an increase in 3β-diol in both *Hsd17b3*$^{-/-}$; *Hsd17b12*$^{L234F/L234F}$ and *Hsd17b3*$^{-/-}$; *Hsd17b12*$^{WT/L234F}$ testes (Fig. 5N), perhaps suggestive of alterations in 3β-diol production in mice with the mutated *Hsd17b12* allele.

Intratesticular concentrations of the estrogens estrone (E1) and estradiol (E2) were also quantified. While estrone was undetectable in all samples, no changes were observed in intratesticular estradiol between all genotypes (Fig. 5O).

Taken together, the results suggest that mouse HSD17B12 can contribute to testicular testosterone biosynthesis in *Hsd17b3* KO mice; however, it is not the sole enzyme responsible for the maintenance of adult testicular testosterone production in the absence of HSD17B3.

Circulating Testosterone Concentrations Are Unchanged in *Hsd17b3*-Deficient Mice Expressing a Mutated *Hsd17b12*

We also investigated circulating steroids in hCG-treated adult *Hsd17b3* KO male mice expressing the L234F mutation, as *Hsd17b12* is ubiquitously expressed (18). Within the canonical pathway of androgen biosynthesis, no significant changes were observed in pregnenolone, progesterone, 17-OH pregnenolone, androstenedione, or androstenediol (Fig. 6A, 6B, 6D, 6H, and 6K). 17-OH progesterone concentrations were significantly increased in *Hsd17b3*$^{-/-}$; *Hsd17b12*$^{L234F/L234F}$ compared to *Hsd17b3*$^{-/-}$; *Hsd17b12*$^{WT/WT}$ mice (Fig. 6E). Dehydroepiandrosterone (DHEA) was undetectable (Fig. 6G) suggesting that the Δ4 canonical pathway remains the preferred route for androgen biosynthesis in mice lacking *Hsd17b3*. Importantly, no differences were observed in circulating concentrations of testosterone or DHT among any of the genotypes (Fig. 6L and 6M).

In the alternate pathway of androgen biosynthesis, *Hsd17b3*$^{-/-}$; *Hsd17b12*$^{L234F/L234F}$ mice showed reduced concentrations of 5α-dehydroepiandrosterone (5α-DHP) in circulation compared to *Hsd17b3*$^{-/-}$; *Hsd17b12*$^{WT/L234F}$ mice (Fig. 6C). Both *Hsd17b3*$^{-/-}$; *Hsd17b12*$^{WT/L234F}$ and *Hsd17b3*$^{-/-}$; *Hsd17b12*$^{L234F/L234F}$ mice exhibited reduced concentrations of allopregnanolone compared to *Hsd17b3*$^{-/-}$; *Hsd17b12*$^{WT/WT}$ mice (Fig. 6F). Interestingly, *Hsd17b3*$^{-/-}$; *Hsd17b12*$^{L234F/L234F}$ mice showed a statistically significant reduction in circulating concentrations of allopregnanolone compared to controls (Fig. 6F), suggesting that the mutated HSD17B12 may impact on the biosynthesis of allopregnanolone in peripheral tissues, but not in the testis (Fig. 5F). No differences were observed in the other alternate androgen precursors, including androsterone, 3α-diol, and 3β-diol (Fig. 6I, 6J, and 6N).

Androstenedione and testosterone are aromatized to estrone and estradiol, respectively, and mouse HSD17B12 can convert estrone to the more potent estrogen, estradiol (18). No significant differences were observed in estrone concentrations among the groups; however, there is high variability in the data of the *Hsd17b3*$^{-/-}$; *Hsd17b12*$^{WT/L234F}$ and *Hsd17b3*$^{-/-}$; *Hsd17b12*$^{L234F/L234F}$ cohorts (Fig. 6O). Circulating estradiol concentrations were increased in *Hsd17b3* KO mice expressing either the heterozygous or homozygous L234F *Hsd17b12* allele compared to *Hsd17b3* KO mice expressing wild-type *Hsd17b12* (Fig. 6P); however, whether this is a direct result of altered enzyme activity in converting estrone to estradiol, or via another mechanism remains to be established.

Identification of HSD17B7 as Another Mouse Hydroxysteroid Dehydrogenase Enzyme that Can Synthesize Testosterone

The above results suggest that other enzyme(s) contribute to testosterone synthesis in the adult testis of mice lacking HSD17B3. We therefore investigated other hydroxysteroid dehydrogenase family proteins in the testes of *Hsd17b3* KO mice by LC-MS. HSD3B1, HSD3B6, HSD17B4, HSD17B7, HSD17B8, HSD17B10, and hydroxysteroid dehydrogenase-like 2 (HSDL2) were detected and the protein abundance between WT and *Hsd17b3* KO testes was compared (Fig. 7A). HSD17B7 was detected at low levels in 2 of the 3 WT samples and was undetectable in a third (Fig. 7A) but showed a ~20-fold increase in *Hsd17b3* KO testes (Fig. 7A and 7B).

We then interrogated testicular *Hsd17b7* mRNA expression and showed that it was significantly increased in adult *Hsd17b3* KO mice (Fig. 7C), as previously observed (7). These results suggest that increased *Hsd17b7* mRNA and protein in the testis is a feature of *Hsd17b3* deficiency.

Next, we investigated the ability of HSD17B7 to convert androstenedione to testosterone. Two earlier studies suggested it does not utilize androstenedione as a substrate under different experimental conditions (32, 33); however, we sought to re-assess these observations using LC-MS to measure testosterone production.

HEK-293T cells were transfected with plasmids expressing GFP reporters and steroidogenic enzymes, and 17β-hydroxysteroid dehydrogenase activity was assessed as the ability to convert androstenedione to testosterone. Successful transfection was confirmed by eGFP expression (Fig. 8A). Cells were treated with either DMSO (vehicle) or with androstenedione, and testosterone in the media was quantified. Cells transfected with mouse *Hsd17b3* were used as a positive control for testosterone synthesis, and a significant increase in testosterone production was observed in androstenedione-treated cells transfected with *Hsd17b3* compared to non-transfected or e*GFP* controls (Fig. 8B). Importantly, androstenedione-treated cells transfected with mouse *Hsd17b7* showed a significant increase in testosterone concentrations compared to androstenedione-treated, non-transfected and e*GFP* control cells (Fig. 8C). These data demonstrate that mouse HSD17B7 can synthesize testosterone from androstenedione under these conditions.

Finally, we examined the ability of human HSD17B7 to produce testosterone. Cells transfected with human *HSD17B7* had unchanged testosterone concentrations compared to non-transfected and e*GFP* controls and were significantly lower than the amounts produced by cells transfected with mouse *Hsd17b7* (Fig. 8C).

Discussion

HSD17B3 has long been thought to be the canonical enzyme responsible for testicular testosterone production. In humans, loss-of-function mutations in *HSD17B3* cause disordered prepubertal testosterone production with consequent effects

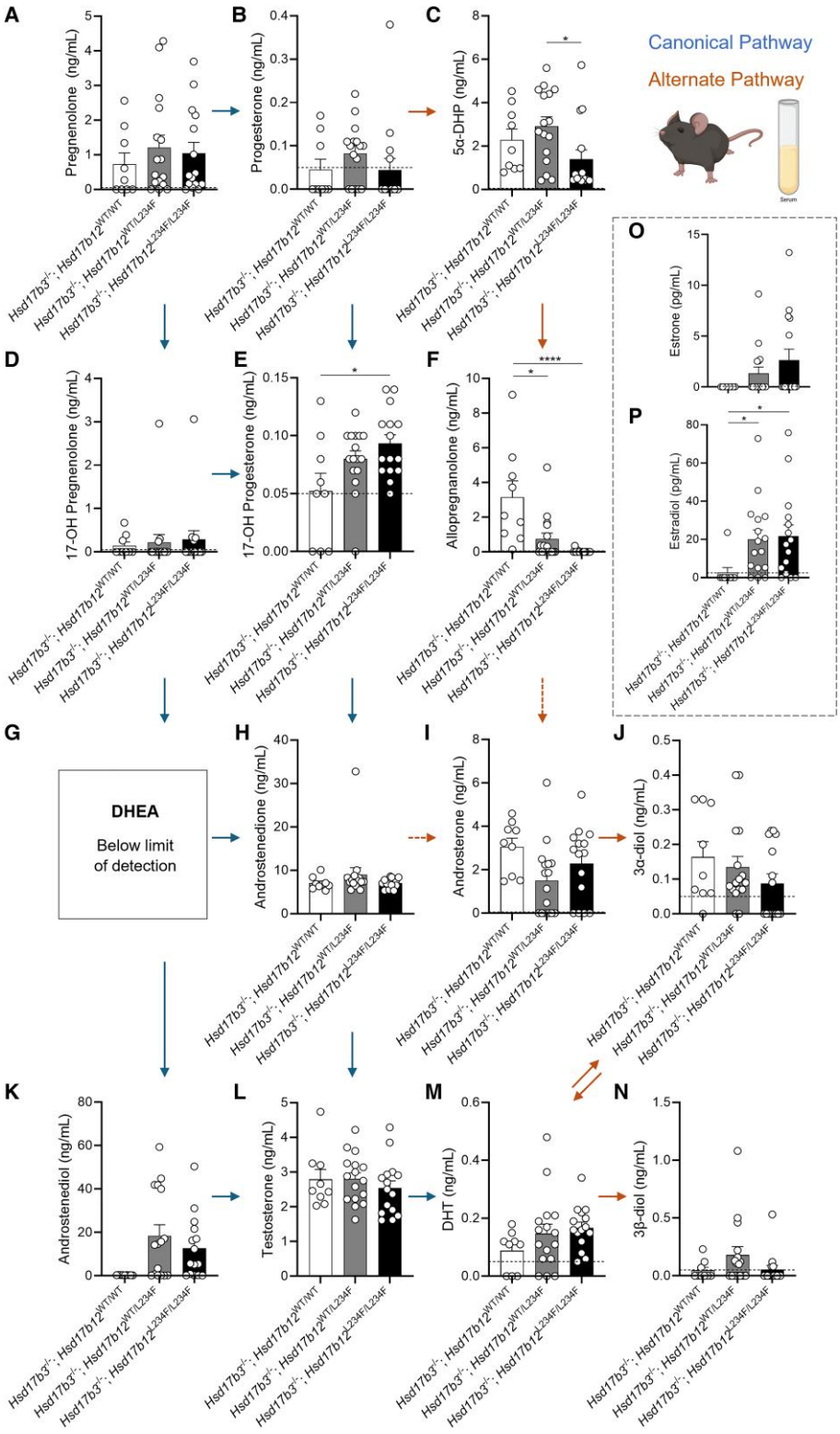

Figure 6. Circulating steroid concentrations in adult (day 80) male *Hsd17b3* knockout (*Hsd17b3*$^{-/-}$) mice expressing the mutant *Hsd17b12*^{L234F} allele. Mice were treated with human chorionic gonadotrophin (hCG) to stimulate maximal steroidogenesis. Androgens and androgen precursors include (A) pregnenolone, (B) progesterone, (C) 5α-dihydroprogesterone (5α-DHP) (D) 17-OH pregnenolone, (E) 17-OH progesterone (F) allopregnanolone (G) dehydroepiandrosterone (DHEA), (H) androstenedione, (I) androsterone, (J) 5α-androstane-3α, 17β-diol (3α-diol), (K) androstenediol, (L) testosterone, (M) dihydrotestosterone (DHT), and (N) 5α-androstane-3β, 17β-diol (3β-diol). Steroids were quantified from the serum collected from mice. The arrows indicate the direction of the canonical and alternate androgen production pathways. Dotted arrows indicate an indirect conversion. Biological replicates that were below the limit of detection were recorded as 0 ng/mL. The limit of detection ranged from 0.01 ng/mL to 0.05 ng/mL depending on the analyte and is indicated by a dotted black line on *y*-axis. One-way ANOVA, Tukey's test (for parametric data) or Kruskal-Wallis test (for nonparametric data), where $P \leq .05$, data shown as mean ± SEM with n = 9-16 per group. Significant differences between groups are indicated as * = $P \leq .05$, **** = $P \leq .0001$. (O) Quantification of estrone and (P) estradiol concentrations in serum. Limit of detection = 2.5 pg/mL and is indicated by the dotted black line on *y*-axis, One-way ANOVA, Kruskal-Wallis test where $P \leq .05$, data shown as mean ± SEM with individual values for n = 9-16 biological replicates per group.

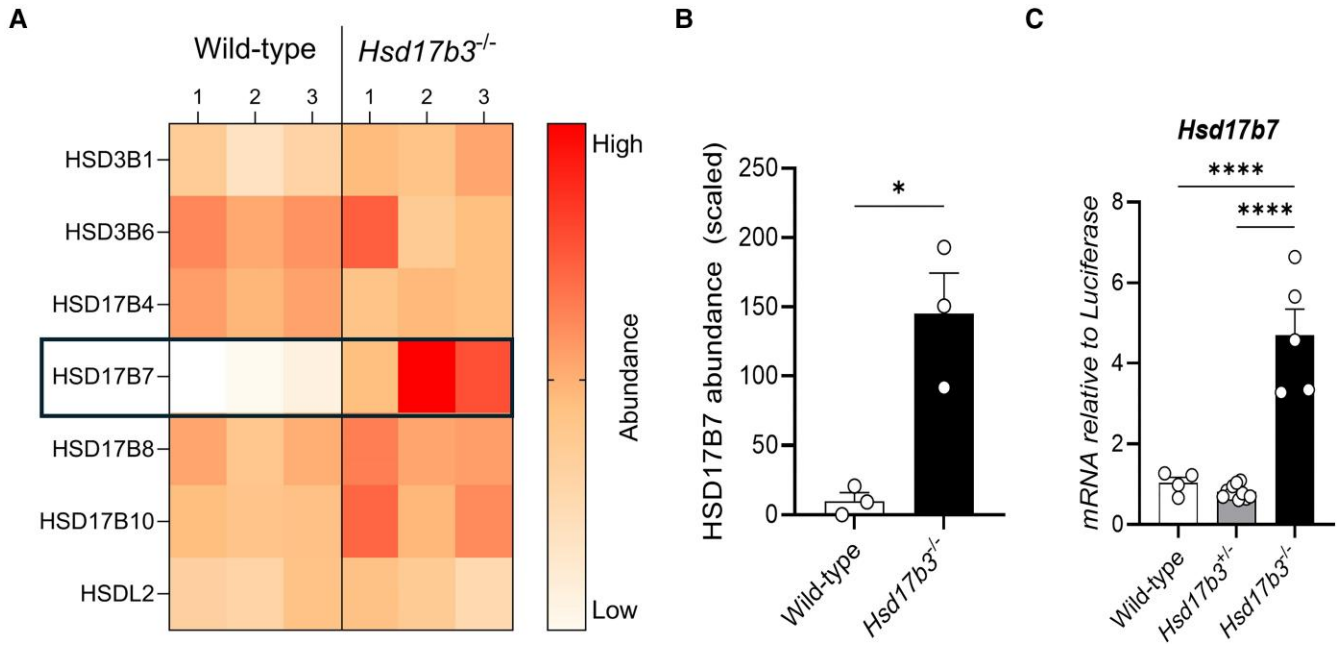

Figure 7. Upregulation of HSD17B7 protein and mRNA in HSD17B3-deficient mice. (A) Heat map representing the protein abundance of all hydroxysteroid dehydrogenases detected in wild-type and *Hsd17b3* knockout (KO; *Hsd17b3*$^{-/-}$) mice. The color scale indicates protein abundance. (B) Scaled abundance values of HSD17B7 in wild-type and *Hsd17b3* KO mice. Data shown as scaled in relation to whole abundance of proteins detected. Scaling of data was performed on Proteome Discoverer 2.5 software for interpretation. Limit of detection on mass spectrometer was 0.2 (scaled). Biological replicates that were below the limit of detection were recorded as 0. One-way ANOVA, Tukey's test where $P \leq .05$, data shown as mean ± SEM with n = 3 biological replicates per group. Significant differences between groups are indicated as * = $P \leq .05$. (C) *Hsd17b7* mRNA transcript levels in adult testes of wild-type (*Hsd17b3*$^{+/+}$), heterozygous (*Hsd17b3*$^{+/-}$) or homozygous (*Hsd17b3*$^{-/-}$) mice. One-way ANOVA, Tukey's test where $P \leq .05$, data shown as mean ± SEM with n = 5-8 biological replicates per group. Significant differences between groups are indicated as * = $P \leq .05$, **** = $P \leq .0001$.

impairing reproductive organ development, with 46,XY individuals exhibiting impaired masculinization of external genitalia with internal male reproductive structures at birth (1, 3). However, mice with HSD17B3 deficiency exhibit normal male sexual development and fertility and continue to produce testosterone in the testis (4, 6, 7, 14), suggesting the existence of other enzymes that can produce testosterone in the absence of *Hsd17b3*.

HSD17B12 is a multifunctional enzyme which can utilize androstenedione as a substrate in mice to produce testosterone (18). We previously demonstrated that the HSD17B12 enzyme is expressed by the adult Leydig cells and there is a small but significant upregulation in testicular expression of *Hsd17b12* in *Hsd17b3* KO mice (6) and HSD17B12 has been hypothesized to contribute to testicular testosterone production in the absence of HSD17B3 (4, 6). Studies introducing mutations into residue 234 of the HSD17B12 enzyme showed that the presence of a phenylalanine amino acid blocks C19 steroids into the active site, preventing testosterone biosynthesis, however, smaller amino acids at position 234, such as alanine or leucine, enable testosterone biosynthesis (18, 20).

Transfection of HEK-293T cells confirmed that mouse HSD17B12 was able to produce testosterone in vitro but the human enzyme was not. Following substitution of the leucine amino acid at residue 234 in mouse HSD17B12 to a phenylalanine amino acid, as in human HSD17B12, we confirmed previous observations that the L234F substitution in mouse HSD17B12 reduced testosterone production to basal levels in HEK-293T cells (18, 20). Therefore, the L234F mutation in the mouse HSD17B12 enzyme provides an opportunity to inhibit HSD17B12's ability to use androstenedione as a substrate to produce testosterone but preserving expression of this enzyme throughout development.

We therefore used this mutation strategy to investigate whether HSD17B12 contributes to the maintenance of testicular testosterone production in the absence of HSD17B3 in mice. We generated a "humanized" L234F-mutated HSD17B12 mouse line and cross-bred this line with *Hsd17b3* KO mice. All male and female *Hsd17b3* KO mice expressing the mutated *Hsd17b12* developed the appropriate male and female reproductive tracts, respectively.

As *Hsd17b3* and *Hsd17b12* are expressed by the fetal testis during development (17, 34), the ablation of the androgenic function of these proteins in the context of continued normal development indicates the presence of one or more additional testosterone synthesizing enzymes during fetal development, with a recent publication indicating that a key contributor to this is HSD17B1 (17). Our observations are consistent with this previous study demonstrating that HSD17B1 is the predominant enzyme able to compensate for HSD17B3 deficiency during mouse fetal development (17). However, the testes of *Hsd17b1* + *Hsd17b3* double KO mice continue to produce lower but detectable levels of testosterone at birth (17). As HSD17B12 is expressed in the fetal testis (34), we propose that HSD17B12 activity could also contribute to the continued testosterone production observed in *Hsd17b1* + *Hsd17b3* double KO mice (17).

The alternate pathway of androgen biosynthesis can synthesize DHT independently of testosterone (14). Alternate pathway precursors including androsterone, 3α-diol and 3β-diol are increased in the circulation of adult *Hsd17b3* KO mice, but not in the testes (14). Similarly, DHT and alternate

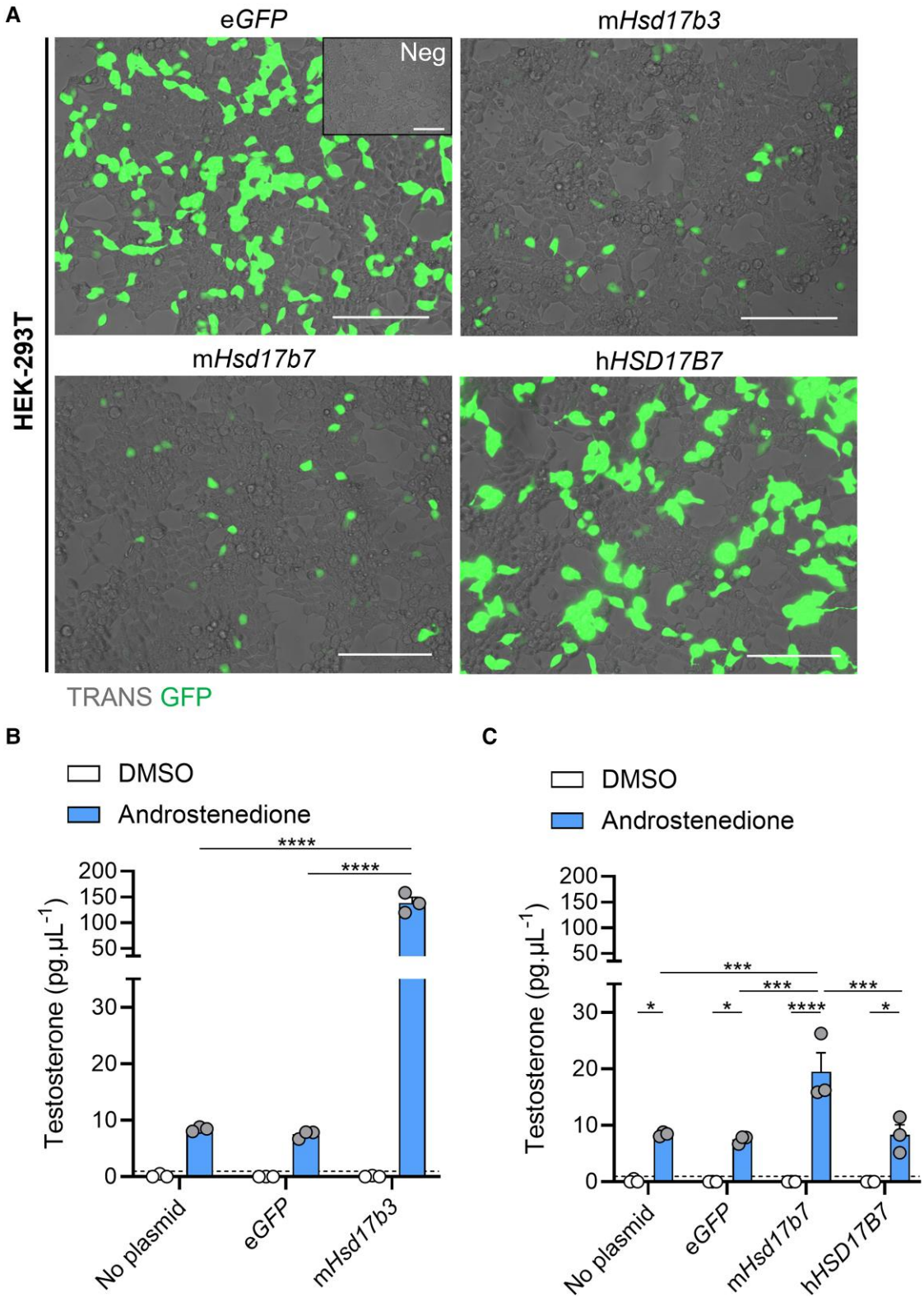

Figure 8. Mouse HSD17B7 can synthesize testosterone from androstenedione whereas human HSD17B7 cannot. (A) Representative images of HEK-293T cells transfected with either no plasmid (Neg), eGFP alone, or plasmids containing mouse (m) *Hsd17b3*, mouse m*Hsd17b7*, or human (h)*HSD17B7* with an e*GFP* reporter. Transfected cells indicated by eGFP expression (green). Scale bar: 150 µm. TRANS: transillumination. (B, C) Testosterone levels in culture media post transfection and following 24 hours of DMSO (vehicle, open bars) or 150 ng/mL androstenedione treatment (blue bars). Testosterone limit of detection = 0.98 pg/mL and is denoted by the dotted black line on the *y*-axis. Technical triplicates were averaged and plotted as biological replicates (n = 3). Two-way ANOVA, Tukey's test, data shown as mean ± SEM. Significant differences between groups are indicated as * = $P \leq .05$, *** = $P \leq .001$, **** = $P \leq .0001$.

pathway precursors were unchanged in the testes of *Hsd17b3* KO mice expressing the mutated HSD17B12 enzyme compared to *Hsd17b3* KO mice expressing the WT HSD17B12, suggesting that the *Hsd17b12* mutation does not impact the ability of DHT production via the alternate pathway in the testes.

In adult *Hsd17b3* KO mice, introduction of the mutated HSD17B12 enzyme caused a small but significant decrease in testicular, but not circulating, testosterone and suggested that HSD17B12 contributes to ~16% testicular testosterone synthesis in *Hsd17b3* KO mice. Significant decreases in seminal vesicle and testis weights were also observed, suggesting a small reduction in androgen bioactivity. However, testis and epididymal histology was unchanged with abundant sperm in the cauda epididymis, indicating that the loss of HSD17B12's ability to produce testosterone does not have a major impact on androgen bioactivity, sexual development, and adult reproductive function in male mice. Thus, we conclude that HSD17B12 does contribute to testicular testosterone production in mice, but it is not the sole enzyme responsible for the continued testicular testosterone production in *Hsd17b3* KO mice.

Therefore, the protein abundance of other 17-ketosteroid reductase enzymes in the testes of wild-type and *Hsd17b3* KO adult mice were investigated. HSD17B1 was not detected in the testes, aligning with previous studies demonstrating that HSD17B1 is down-regulated postnatally (35) and cannot compensate for HSD17B3 deficiency in adulthood (6, 17). HSD17B7 was deemed to be a strong candidate because both mRNA (7) and protein are significantly increased in *Hsd17b3* KO testes compared to wild-type, with the protein showing a particularly marked (~20 fold) increase. HSD17B7 is a multifunctional enzyme that can utilize estrone, DHT and zymosterone as substrates (36-38). The mouse enzyme was first cloned in 1998 (32) and can convert the less active estrone to estradiol, a potent estrogen (32, 33). It also converts DHT into 3α-diol and, to a lesser extent, 3β-diol (33). However, previous studies suggested that the mouse enzyme is unable to convert androstenedione into testosterone (32, 33).

Our results revealed that, in transfected HEK-293T cells, mouse HSD17B7, but not human HSD17B7, can convert androstenedione to testosterone. Two earlier studies concluded that mouse HSD17B7 did not perform this conversion (32, 33); however, those studies employed reduced concentrations of substrate and shorter incubation times, which may have influenced the observed outcomes. Extrapolating from our findings, we suggest that HSD17B7 is unlikely to contribute to androgen bioactivity in 46,XY individuals with HSD17B3 deficiency (1, 3-5) but the mouse enzyme may be able to contribute to testosterone biosynthesis in *Hsd17b3* KO mice (6, 7, 17) in both fetal and postnatal life (34, 39). The KO of *Hsd17b7* in mice is embryonically lethal due to a defect in de novo cholesterol biosynthesis (36, 40). Because HSD17B7 is a multifunctional enzyme with various roles in steroidogenesis (36-38), future studies on its ability to contribute to testosterone biosynthesis in *Hsd17b3* KO mice would first require the identification of the specific amino acid residues responsible for the conversion of androstenedione to testosterone, as has been defined for HSD17B12 (18). Once such residues are defined, site-directed mutations and CRISPR/Cas9 technology could be used to produce mice carrying mutated *Hsd17b7* that is unable to produce testosterone. Introduction of the mutated *Hsd17b7* into *Hsd17b3* KO mice homozygous for *Hsd17b12*^{L234F} could then be used to determine the contribution of HSD17B7 to testosterone synthesis.

We conclude that in the absence of the testosterone-biosynthetic enzyme HSD17B3, mice continue to produce basal testicular testosterone (6, 7), facilitated through the activity of other 17-ketosteroid reductase enzymes which contribute to the maintenance of testosterone biosynthesis. Our results show that mouse HSD17B12 can convert androstenedione to testosterone and, in mice lacking HSD17B3 function, HSD17B12 contributes to ~16% of testicular testosterone production. However, testosterone production continues in mice lacking androgenic functions of both HSD17B3 and HSD17B12, suggesting that one or more further 17-ketosteroid reductase enzyme also contributes. Our results also show a marked increase in the testicular expression of HSD17B7 in the absence of *Hsd17b3*, and demonstrate that HSD17B7 can convert androstenedione to testosterone in vitro, suggesting that HSD17B7 may contribute to testosterone production in HSD17B3-deficient mice. The identification of 2 additional hydroxysteroid dehydrogenase enzymes that can synthesize testosterone in mice, but not humans, contributes toward a clearer understanding of the phenotypic differences between mouse and human HSD17B3 deficiency, where sexual development and fertility is preserved in mice, but disordered sexual development is seen in humans. These results suggest that the existence of multiple hydroxysteroid dehydrogenase enzymes capable of testosterone synthesis in mice is a safeguard for male sexual development and fertility in this species. These findings are consistent with the hypothesis that mice have increased plasticity in steroidogenic enzymes and multiple redundancies within steroidogenesis pathways. However, human orthologs have lost this plasticity, making humans more vulnerable to disordered sexual development following the loss of HSD17B3 function.

Acknowledgments

The authors acknowledge Robert Brink for the development of the mouse lines and the BioResearchers Facility (BRF) at the University of Newcastle and Australian BioResources (ABR) for their assistance in animal husbandry and maintaining the mouse colonies. The authors would like to thank Dr. Reena Desai from the ANZAC Research Institute for the analysis of testicular and circulating steroids, and Nathan Smith from the Central Analytical Facility (CAF) at the University of Newcastle for assistance with LC-MS/MS mass spectrometry. We thank the Academic and Research Computing Support team, The University of Newcastle, who provided High Performance Computing Infrastructure to support the bioinformatics analyses.

Funding

This work was funded by the National Health and Medical Research Council (NHMRC), grant number APP1158344 and funding from the University of Newcastle (awarded to L.B.S.) and Griffith University (awarded to L.B.S.). D.J.H. was funded by an NHMRC Investigator grant.

Author Contributions

B.M.L., D.R., and L.B.S. conceived and designed the study. B.M.L., D.A.S.B., S.P., I.A., and S.S. carried out the experiments.

B.M.L. analyzed the results and designed the figures. B.M.L., L.O.D., and L.B.S. wrote the manuscript, B.M.L., L.O.D., A.L.G, D.H., D.R., and L.B.S. revised the manuscript. L.B.S. provided funding for the study. All authors have read and agreed to the published version of the manuscript.

Disclosures

D.J.H. is an editorial board member for *Endocrinology* and played no role in the journal's evaluation of the manuscript. There are no other disclosures to make.

Data Availability

Original data generated and analyzed during this study are included in this published article or in data repositories. The mass spectrometry proteomics data have been deposited to the ProteomeXchange Consortium via the PRIDE partner repository (41) with the dataset identifier PXD050748 and 10.6019/PXD050748.

References

1. Geissler WM, Davis DL, Wu L, *et al.* Male pseudohermaphroditism caused by mutations of testicular 17β–hydroxysteroid dehydrogenase 3. *Nat Genet*. 1994;7(1):34-39.
2. O'Hara L, Smith LB. Androgen receptor roles in spermatogenesis and infertility. *Best Pract Res Clin Endocrinol Metab*. 2015;29(4):595-605.
3. Gonçalves CI, Carriço J, Bastos M, Lemos MC. Disorder of sex development due to 17-beta-hydroxysteroid dehydrogenase type 3 deficiency: a case report and review of 70 different HSD17B3 mutations reported in 239 patients. *Int J Mol Sci*. 2022;23(17):10026.
4. Lawrence BM, O'Donnell L, Smith LB, Rebourcet D. New insights into testosterone biosynthesis: novel observations from HSD17B3 deficient mice. *Int J Mol Sci*. 2022;23(24):15555.
5. Mendonca BB, Gomes NL, Costa EM, *et al.* 46,XY disorder of sex development (DSD) due to 17β-hydroxysteroid dehydrogenase type 3 deficiency. *J Steroid Biochem Mol Biol*. 2017;165(Pt A):79-85.
6. Rebourcet D, Mackay R, Darbey A, *et al.* Ablation of the canonical testosterone production pathway via knockout of the steroidogenic enzyme HSD17B3, reveals a novel mechanism of testicular testosterone production. *FASEB J*. 2020;34(8):10373-10386.
7. Sipilä P, Junnila A, Hakkarainen J, *et al.* The lack of HSD17B3 in male mice results in disturbed Leydig cell maturation and endocrine imbalance akin to humans with HSD17B3 deficiency. *FASEB J*. 2020;34(5):6111-6128.
8. Naamneh Elzenaty R, du Toit T, Flück CE. Basics of androgen synthesis and action. *Best Pract Res Clin Endocrinol Metab*. 2022;36(4):101665.
9. van Weerden WM, Bierings HG, van Steenbrugge GJ, de Jong FH, Schröder FH. Adrenal glands of mouse and rat do not synthesize androgens. *Life Sci*. 1992;50(12):857-861.
10. Gannon AL, O'Hara L, Mason JI, *et al.* Androgen receptor signalling in the male adrenal facilitates X-zone regression, cell turnover and protects against adrenal degeneration during ageing. *Sci Rep*. 2019;9(1):10457.
11. Huhtaniemi R, Oksala R, Knuuttila M, *et al.* Adrenals contribute to growth of castration-resistant VCaP prostate cancer Xenografts. *Am J Pathol*. 2018;188(12):2890-2901.
12. Adeniji AO, Chen M, Penning TM. AKR1C3 as a target in castrate resistant prostate cancer. *J Steroid Biochem Mol Biol*. 2013;137:136-149.
13. Byrns MC, Mindnich R, Duan L, Penning TM. Overexpression of aldo-keto reductase 1C3 (AKR1C3) in LNCaP cells diverts androgen metabolism towards testosterone resulting in resistance to the 5α-reductase inhibitor finasteride. *J Steroid Biochem Mol Biol*. 2012;130(1-2):7-15.
14. Lawrence BM, O'Donnell L, Gannon AL, *et al.* Compensatory mechanisms that maintain androgen production in mice lacking key androgen biosynthetic enzymes. *FASEB J*. 2024;38(22):e70177.
15. Sha J, Baker P, O'Shaughnessy PJ. Both reductive forms of 17 beta-hydroxysteroid dehydrogenase (types 1 and 3) are expressed during development in the mouse testis. *Biochem Biophys Res Commun*. 1996;222(1):90-94.
16. Whiley PAF, O'Donnell L, Moody SC, *et al.* Activin A determines steroid levels and composition in the fetal testis. *Endocrinology*. 2020;161(7):bqaa058.
17. Junnila A, Zhang FP, Martínez Nieto G, *et al.* HSD17B1 compensates for HSD17B3 deficiency in fetal mouse testis but not in adults. *Endocrinology*. 2024;165(6):bqae056.
18. Blanchard PG, Luu-The V. Differential androgen and estrogen substrates specificity in the mouse and primates type 12 17beta-hydroxysteroid dehydrogenase. *J Endocrinol*. 2007;194(2):449-455.
19. Suzuki H, Ozaki Y, Ijiri S, Gen K, Kazeto Y. 17β-Hydroxysteroid dehydrogenase type 12a responsible for testicular 11-ketotestosterone synthesis in the Japanese eel, Anguilla japonica. *J Steroid Biochem Mol Biol*. 2020;198:105550.
20. Luu-The V, Tremblay P, Labrie F. Characterization of type 12 17beta-hydroxysteroid dehydrogenase, an isoform of type 3 17beta-hydroxysteroid dehydrogenase responsible for estradiol formation in women. *Mol Endocrinol*. 2006;20(2):437-443.
21. Bellemare V, Phaneuf D, Luu-The V. Target deletion of the bifunctional type 12 17β-hydroxysteroid dehydrogenase in mice results in reduction of androgen and estrogen levels in heterozygotes and embryonic lethality in homozygotes. *Horm Mol Biol Clin Investig*. 2010;2(3):311-318.
22. Mazza C, Breton R, Housset D, Fontecilla-Camps JC. Unusual charge stabilization of NADP+in 17beta-hydroxysteroid dehydrogenase. *J Biol Chem*. 1998;273(14):8145-8152.
23. Rantakari P, Lagerbohm H, Kaimainen M, *et al.* Hydroxysteroid (17{beta}) dehydrogenase 12 is essential for mouse organogenesis and embryonic survival. *Endocrinology*. 2010;151(4):1893-1901.
24. Saloniemi T, Jokela H, Strauss L, Pakarinen P, Poutanen M. The diversity of sex steroid action: novel functions of hydroxysteroid (17beta) dehydrogenases as revealed by genetically modified mouse models. *J Endocrinol*. 2012;212(1):27-40.
25. Skerrett-Byrne DA, Trigg NA, Bromfield EG, *et al.* Proteomic dissection of the impact of environmental exposures on mouse seminal vesicle function. *Mol Cell Proteomics*. 2021;20:100107.
26. Skerrett-Byrne DA, Bromfield EG, Murray HC, *et al.* Time-resolved proteomic profiling of cigarette smoke-induced experimental chronic obstructive pulmonary disease. *Respirology*. 2021;26(10):960-973.
27. Skerrett-Byrne DA, Anderson AL, Hulse L, *et al.* Proteomic analysis of koala (Phascolarctos cinereus) spermatozoa and prostatic bodies. *Proteomics*. 2021;21(19):e2100067.
28. Skerrett-Byrne DA, Anderson AL, Bromfield EG, *et al.* Global profiling of the proteomic changes associated with the post-testicular maturation of mouse spermatozoa. *Cell Rep*. 2022;41(7):111655.
29. Smyth SP, Nixon B, Anderson AL, *et al.* Elucidation of the protein composition of mouse seminal vesicle fluid. *Proteomics*. 2022;22(9):e2100227.
30. Mitchell RT, Mungall W, McKinnell C, *et al.* Anogenital distance plasticity in adulthood: implications for its use as a biomarker of fetal androgen action. *Endocrinology*. 2015;156(1):24-31.
31. Mahendroo MS, Cala KM, Hess DL, Russell DW. Unexpected virilization in male mice lacking steroid 5 alpha-reductase enzymes. *Endocrinology*. 2001;142(11):4652-4662.
32. Nokelainen P, Peltoketo H, Vihko R, Vihko P. Expression cloning of a novel estrogenic mouse 17 beta-hydroxysteroid dehydrogenase/17-ketosteroid reductase (m17HSD7), previously described as

a prolactin receptor-associated protein (PRAP) in rat. *Mol Endocrinol*. 1998;12(7):1048-1059.
33. Torn S, Nokelainen P, Kurkela R, *et al.* Production, purification, and functional analysis of recombinant human and mouse 17beta-hydroxysteroid dehydrogenase type 7. *Biochem Biophys Res Commun*. 2003;305(1):37-45.
34. Tan K, Song HW, Wilkinson MF. Single-cell RNAseq analysis of testicular germ and somatic cell development during the perinatal period. *Development*. 2020;147(3):dev183251.
35. O'Shaughnessy PJ, Baker PJ, Heikkila M, Vainio S, McMahon AP. Localization of 17beta-hydroxysteroid dehydrogenase/17-ketosteroid reductase isoform expression in the developing mouse testis–androstenedione is the major androgen secreted by fetal/neonatal leydig cells. *Endocrinology*. 2000;141(7):2631-2637.
36. Jokela H, Rantakari P, Lamminen T, *et al.* Hydroxysteroid (17beta) dehydrogenase 7 activity is essential for fetal de novo cholesterol synthesis and for neuroectodermal survival and cardiovascular differentiation in early mouse embryos. *Endocrinology*. 2010;151(4):1884-1892.
37. Liu H, Robert A, Luu-The V. Cloning and characterization of human form 2 type 7 17beta-hydroxysteroid dehydrogenase, a primarily 3beta-keto reductase and estrogen activating and androgen inactivating enzyme. *J Steroid Biochem Mol Biol*. 2005;94(1-3):173-179.
38. Marijanovic Z, Laubner D, Moller G, *et al.* Closing the gap: identification of human 3-ketosteroid reductase, the last unknown enzyme of mammalian cholesterol biosynthesis. *Mol Endocrinol*. 2003;17(9):1715-1725.
39. Jameson SA, Natarajan A, Cool J, *et al.* Temporal transcriptional profiling of somatic and germ cells reveals biased lineage priming of sexual fate in the fetal mouse gonad. *PLoS Genet*. 2012;8(3):e1002575.
40. Shehu A, Mao J, Gibori GB, *et al.* Prolactin receptor-associated protein/17beta-hydroxysteroid dehydrogenase type 7 gene (Hsd17b7) plays a crucial role in embryonic development and fetal survival. *Mol Endocrinol*. 2008;22(10):2268-2277.
41. Perez-Riverol Y, Bai J, Bandla C, *et al.* The PRIDE database resources in 2022: a hub for mass spectrometry-based proteomics evidences. *Nucleic Acids Res*. 2022;50(D1):D543-d552.

Professor Lee Smith
Deputy Vice Chancellor (Research)

Telephone +61 (0) 7 5552 7211

dvcr@griffith.edu.au
www.griffith.edu.au

Leneen Forde Chancellery
Office of the Vice Chancellor
Gold Coast campus
Griffith University QLD 4222
Australia

7th July, 2025

Letter of Support: Dr Ben M. Lawrence

Dear Sir/Madam,

I am very pleased to endorse the application of Dr Ben Lawrence for the ESA Young Investigator Scientific Article Award.

Ben is first author of the article '**Functional Analysis of HSD17B3-Deficient Male Mice Reveals Roles for HSD17B7 and HSD17B12 in Testosterone Biosynthesis**', that has been published in the Q1 journal *Endocrinology*. This publication was then selected to be the featured article for the journal in June 2025.

I can personally attest that Ben contributed significantly to all aspects relating to this manuscript.

Ben joined my research team in the infancy of this research project. Ben was heavily involved in discussions surrounding the project and contributed to the research design by proposing relevant experiments. Ben's suggestion of assessing the testosterone synthesising ability of human HSD17B7 was an important advance in demonstrating that mice have multiple steroidogenic enzymes with increased plasticity compared to humans.

Furthermore, Ben was the lead researcher performing the experiments involved in this study. Along with assistance from co-authors, Ben did the majority of plasmid bulking and plasmid extractions, tissue collections and genotyping. Ben prepared the samples that were used for mass spectrometry (steroid analysis and testis proteomics). Ben also directed the management of the transgenic mouse colony and was responsible for the site-directed mutagenesis of plasmids, sample preparation for sequencing, cell culture experiments, animal treatments, histology and data analysis.

In conjunction with Dr. Liza O'Donnell and myself, Ben was heavily involved in the preparation of this manuscript, contributing across all aspects including writing, figure preparation, draft revision, feedback integration and responding to reviewer comments.

Ben's scientific drive and self-motivation goes above and beyond as evidenced by his contributions to this outstanding publication. In short, I give my unreserved support for Ben's application for this award and strongly attest that he would be a worthy recipient.

Yours sincerely,

Professor Lee Smith
Deputy Vice Chancellor (Research)

Co-author signatures:

x  x 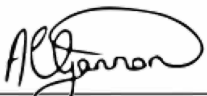

Dr. Liza O'Donnell | Dr. Anne-Louise Gannon

x  x 

Dr. David A. Skerrett-Byrne | Miss Shanmathi Parameswaran

x  x 

Miss Imogen Abbott | Mrs Sarah Smith

x 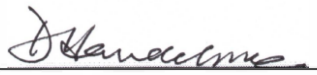 x 

Prof. David J. Handelsman | Dr. Diane Rebourcet

X 

Prof. Lee B. Smith

International Journal of
Molecular Sciences

MDPI

Review

New Insights into Testosterone Biosynthesis: Novel Observations from HSD17B3 Deficient Mice

Ben M. Lawrence [1,*], Liza O'Donnell [1], Lee B. Smith [1,2,3] and Diane Rebourcet [1,*]

[1] College of Engineering, Science and Environment, The University of Newcastle, Callaghan, NSW 2308, Australia
[2] Office for Research, Griffith University, Southport, QLD 4222, Australia
[3] MRC Centre for Reproductive Health, The Queen's Medical Research Institute, University of Edinburgh, Edinburgh EH16 4TJ, UK
* Correspondence: ben.lawrence@uon.edu.au (B.M.L.); diane.rebourcet@newcastle.edu.au (D.R.)

Abstract: Androgens such as testosterone and dihydrotestosterone (DHT) are essential for male sexual development, masculinisation, and fertility. Testosterone is produced via the canonical androgen production pathway and is essential for normal masculinisation and testis function. Disruption to androgen production can result in disorders of sexual development (DSD). In the canonical pathway, 17β-hydroxysteroid dehydrogenase type 3 (HSD17B3) is viewed as a critical enzyme in the production of testosterone, performing the final conversion required. HSD17B3 deficiency in humans is associated with DSD due to low testosterone concentration during development. Individuals with *HSD17B3* mutations have poorly masculinised external genitalia that can appear as ambiguous or female, whilst having internal Wolffian structures and testes. Recent studies in mice deficient in HSD17B3 have made the surprising finding that testosterone production is maintained, male mice are masculinised and remain fertile, suggesting differences between mice and human testosterone production exist. We discuss the phenotypic differences observed and the possible other pathways and enzymes that could be contributing to testosterone production and male development. The identification of alternative testosterone synthesising enzymes could inform the development of novel therapies to endogenously regulate testosterone production in individuals with testosterone deficiency.

Keywords: androgens; testosterone; HSD17B3; enzymes; canonical pathway

Citation: Lawrence, B.M.; O'Donnell, L.; Smith, L.B.; Rebourcet, D. New Insights into Testosterone Biosynthesis: Novel Observations from HSD17B3 Deficient Mice. *Int. J. Mol. Sci.* **2022**, *23*, 15555. https://doi.org/10.3390/ijms232415555

Academic Editor: Chuen Yan Cheng

Received: 8 November 2022
Accepted: 6 December 2022
Published: 8 December 2022

1. Background

Androgens are steroid hormones critical for male sexual development, masculinisation, spermatogenesis, and general lifelong male health [1–3]. Disruptions to androgen production at any point during life can result in complications contributing to lower quality of life and premature death [2,3].

Androgen biosynthesis is a complex process that occurs in the highly specialised Leydig cells, in the interstitial space of the testis. Androgen biosynthesis involves a succession of enzymatic reactions converting steroid precursors to the biologically active androgens testosterone and the more potent dihydrotestosterone (DHT). Like all steroid hormones, cholesterol is the initial precursor required to make androgens. Therefore, a constant supply is needed for the Leydig cells. Free cholesterol can be derived from (i) de novo cholesterol synthesis, (ii) from the hydrolysis of stored cholesterol esters in lipids, or (iii) from lipoproteins circulating in the serum. It has been demonstrated in mice and rats that the preferred source of cholesterol for steroidogenesis is de novo synthesis [4,5]. Sourcing free cholesterol allows the Leydig cells to begin the process of synthesising androgens.

The first step in steroidogenesis is the conversion of cholesterol into pregnenolone and this process occurs in the inner membrane of the mitochondria of the Leydig cells [6,7]. The binding of luteinising hormone (LH) to the luteinising hormone/choriogonadotropin

receptor (LHCGR) causes an increase in the phosphorylation of the steroidogenic acute regulatory (StAR) protein which regulates the transfer of cholesterol to the inner mitochondrial membrane. Cholesterol side-chain cleavage enzyme, CYP11A1 (P450scc), then converts cholesterol into pregnenolone (Figure 1) [7]. Pregnenolone leaves the mitochondria by passive diffusion and all subsequent androgen biosynthesis steps occur in the smooth endoplasmic reticulum of the cell [8].

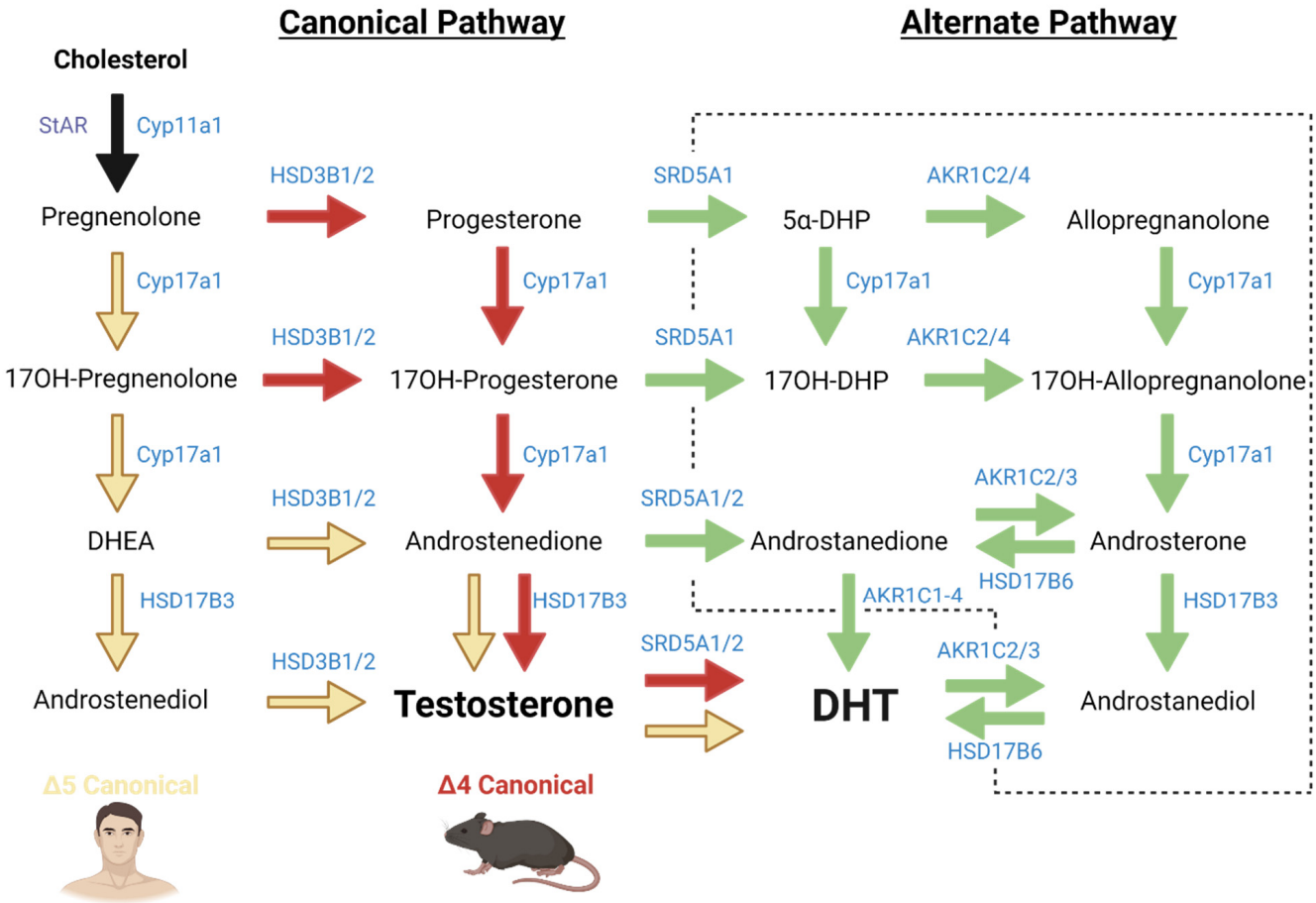

Figure 1. The current understanding of the canonical and alternate pathways of androgen biosynthesis. Independent of which pathway is used (black arrow), all androgens originate from cholesterol and are converted by multiple enzymes to produce the active androgens testosterone and dihydrotestosterone (DHT). The canonical pathway produces testosterone, which can act directly on the androgen receptor or be used as a precursor to the more potent androgen DHT. The alternate pathway (green arrows enclosed by the dotted line) can synthesise DHT, bypassing the need for testosterone synthesis. The canonical pathway includes Δ4 and Δ5 pathways; humans favour the Δ5 pathway (yellow arrows), whereas mice preference the Δ4 pathway (red arrows). Created with BioRender.com (accessed on 31 October 2022).

Within the canonical pathway of androgen biosynthesis (Figure 1), pregnenolone and progesterone are converted to 17OH-pregnenolone and 17OH-progesterone, respectively, by the 17α-hydroxylase activity of CYP17A1 [9]. The 17,20 lyase activity of CYP17A1 then converts 17OH-pregnenolone and 17OH-progesterone into DHEA and androstenedione, respectively [9,10]. HSD17B3, which is exclusively expressed in the testes, can convert DHEA into androstenediol, or androstenedione into the biologically active androgen testosterone. HSD3B1/2 can convert pregnenolone, 17OH-pregnenolone, DHEA and androstanediol into progesterone, 17OH-progesterone, androstenedione, and testosterone, respectively.

The canonical pathway can be divided into the Δ4 and Δ5 pathways, with primary usage depending on animal species (Figure 1). Humans and primates predominantly

use the Δ5 route for the conversions required from pregnenolone through to DHEA, with less contribution to the Δ4 route. This is due to the human 17,20 lyase activity of CYP17A1, which has a significantly higher preference towards 17OH-pregnenolone over 17OH-progesterone [10,11]. In contrast, rodents primarily utilize the Δ4 pathway as their CYP17A1 has a stronger affinity towards 17OH-progesterone [10,11].

Free testosterone diffuses into cells and binds to the androgen receptor (AR) to induce androgen-dependent genomic and non-genomic pathways [12]. It can also be transported in circulation by the carrier proteins, sex hormone binding globulin (SHBG) in humans [13], and androgen binding protein in rodents [14]. These proteins transport testosterone to androgen target organs where it can then be converted by steroid-5alpha-reductase (SRD5A) enzymes to DHT. The enzyme that produces DHT is dependent on the tissue as SRD5A1 is the major isoform detected in non-reproductive tissues, such as the liver and skin, whereas SRD5A2 is predominantly expressed in the reproductive organs [15]. Both SRD5A enzymes catalyse this reaction but differ in their substrate affinity and other biochemical properties [16].

While HSD17B3 is the critical enzyme for testosterone production, studies in mice have shown it is not expressed by fetal Leydig cells, and instead is expressed by fetal Sertoli cells during sexual development [17,18]. Therefore, in the mouse, fetal Leydig cells are responsible for producing the androgen precursor, androstenedione, and the fetal Sertoli cells are responsible for catalysing the conversion to testosterone [18]. During postnatal development however, Sertoli cells lose the expression of HSD17B3 and immature Leydig cells differentiate into adult Leydig cells [18]. Leydig cell differentiation results in the expression of steroidogenic enzymes, including HSD17B3, enabling the adult Leydig cells to become the primary site of testosterone synthesis under gonadotrophin stimulation from puberty and throughout adulthood [19,20].

2. Human HSD17B3 Deficiency

HSD17B3 deficiency is the most common disorder of androgen synthesis, with 70 reported mutations in humans that result in a disorder of sexual development (DSD) phenotype [21,22]. This disorder is caused by a genetic mutation in the *HSD17B3* gene and results in perturbed sexual differentiation in males as it prevents the sufficient reduction of androstenedione into testosterone. Whilst genetic testing can confirm *HSD17B3* loss-of-function mutations, hormone profiling is used as a diagnostic hallmark, where abnormally high androstenedione to testosterone ratios is seen, with androstenedione being 10 times higher than normal, indicative of reduced HSD17B3 function [21,23–25].

46,XY DSD humans with a loss-of-function mutation in *HSD17B3* present with external genitalia that are under-masculinised, appearing as either ambiguous or as female, with a blind vaginal pouch. As a result of the human body's default setting to develop female external structures without appropriate androgen action, many individuals with this condition are raised as female and diagnosis is often missed during infancy. Interestingly, internally testes are present, which are commonly smaller, undescended (cryptorchidism) and located in the inguinal or intraabdominal regions [21]. Wolffian structures are also present, including epididymis, vas deferens and seminal vesicles. As the Wolffian structures are androgen-dependent, this indicates that low levels of testosterone continue to be produced [21].

One of the more curious observations seen in individuals with HSD17B3 deficiency is that they, to some extent, undergo late-onset virilisation during puberty and it is at this time when most cases are diagnosed. At time of puberty, 46,XY individuals raised as female may seek medical attention due to amenorrhea or due to virilisation. The extent of virilisation at puberty can vary according to the mutation but may include developing male characteristics such as deepening of the voice, heightened body hair, defined male body structure and clitoromegaly, resembling a micropenis [21,25–27]. Due to these individuals having some level of androgen action during puberty and low levels of testosterone present, it is suggested that HSD17B3 is not solely responsible for testosterone production

in humans during puberty and there may be other 17β-hydroxysteroid dehydrogenase enzymes involved [21]. HSD17B5, also known as AKR1C3, is expressed in peripheral tissues and can be a source of peripheral conversion in some disease states, including prostate cancer [21,28,29]. Therefore, it has been postulated that the circulating testosterone present may be produced in peripheral tissues, rather than in the testes [21]. Another explanation for the late-onset virilisation is that not all HSD17B3 mutations render HSD17B3 completely inactive, and residual HSD17B3 may function to convert low amounts of androstenedione into testosterone, followed by SRD5A enzymes becoming more highly expressed at puberty where they can synthesise DHT [21,30].

Regardless of the extent of virilisation that occurs, HSD17B3-deficient individuals are infertile [31]. This highlights the importance of the human canonical pathway and the role of human HSD17B3 in male sexual development, testosterone production and testis function.

3. Transgenic Mouse Models of HSD17B3 Deficiency

Transgenic mouse models can be utilised to dissect androgen biosynthesis, the roles of steroidogenic enzymes, and provide hypotheses for testing in human disorders. The complexities of the steroidogenic pathways (Figure 1) make it challenging to predict outcomes of in vivo models. Development of in silico modelling using the modified Edinburgh pathway notation (mEPN), and the network editing softwares yED and BioLayout, has been useful in displaying the steroidogenesis pathway and for predicting logical hypotheses [32]. These tools have the potential to be used to model different signalling pathways in a multitude of contexts. Both human and rodent steroidogenic pathways in the testis have been modelled using this in silico approach and have been adapted to portray HSD17B3 deficiency [32,33]. In silico modelling of HSD17B3 deficiency in rodents predicted androstenedione production would increase as Leydig cells mature and no testosterone would be produced [32]. Therefore, a similar phenotype in rodents was expected to that seen in humans with HSD17B3 deficiency.

Since the in silico model establishment of the HSD17B3 deficiency in mice, two independent research groups have now reported the phenotypes of independently derived *Hsd17b3*-deficient mouse lines [17,34]. These models were designed to mimic the human mutation causing HSD17B3 deficiency by blocking the conversion of androstenedione to the active androgen testosterone, subsequently causing disruption to the canonical androgen production pathway.

Matching the diagnostic hallmark of HSD17B3 deficiency in human males, and the in silico model, HSD17B3 knockout (KO) male mice had a significantly higher androstenedione to testosterone ratio, indicating that the canonical pathway of androgen production was disrupted [17,34].

Surprisingly though, unlike in humans, male HSD17B3 KO mice remain virilised at birth and can be identified from female littermates [17,34]. Decreased anogenital distance is observed in HSD17B3 KO male mice compared to wild-type males, however, it is not reduced to that seen in females [17,34]. The smaller anogenital distance indicates that HSD17B3 KO mice have reduced, but not absent, androgen action during a key fetal developmental timepoint known as the masculinisation programming window [35].

Further examination of HSD17B3 KO mice revealed that unlike in human males with HSD17B3 deficiency, mice had no major impact on reproductive development [17,34]. Sipila et al. showed a decrease in seminiferous tubule diameter and in testis weight at ~1 and 3 months of age, however, in contrast Rebourcet et al. did not see any testis weight difference in adulthood [17,34]. As seminiferous tubules make up approximately 90% of the testis, a decrease in testis weight is a key indicator of reduced spermatogenesis. Surprisingly though and in contrast to humans, HSD17B3 KO male mice display normal spermatogenesis and remain fertile, something that has widely been accepted to be fundamentally dependent upon the 17-ketosteroid reductase activity of HSD17B3, and its ability to produce testosterone. The decrease in tubule diameter observed by Sipila and

colleagues was more prevalent in mice aged 4 weeks [34], prior to the commencement of spermatogenesis, compared to 3-month-old mice, suggesting that the development of the testis may be delayed, rather than spermatogenesis itself. As testosterone is absolutely required for spermatogenesis [36], this indicates that testosterone is being produced to acceptable levels in the HSD17B3 KO mice.

Hormone profiling of HSD17B3 KO adult male mice revealed a marked increase in circulating and intratesticular androstenedione, likely due to a reduced ability to convert this substrate into testosterone [17,34]. Other androgen precursors are also increased in HSD17B3 KO males, including progesterone and 17OH-progesterone, suggesting a backlog of androgen precursors within the pathway [17,34]. Importantly, intratesticular testosterone levels were unchanged, and circulating testosterone and DHT were significantly increased in HSD17B3 KO adult males [17,34]. Circulating LH was also increased, along with increased transcription of *Lhcgr*, *StAR*, *Cyp11a1* and *Cyp17a1* [17,34]. The increased circulating testosterone, LH, and upregulation of steroidogenic biosynthetic enzymes indicate that the hypothalamic-pituitary-gonadal axis, which functions as a negative feedback loop, is dysregulated in these mice. As the hypothalamic-pituitary-gonadal axis is programmed by actions of testosterone and kisspeptin signalling during fetal development, this negative feedback axis may be impacted due to abnormal androgen action during fetal development, however this proposition has not been confirmed [17,37,38].

As HSD17B3 KO males remain fertile, with quantitatively and qualitatively normal spermatogenesis [34], along with a maintenance of intratesticular testosterone [17,34], this suggests the existence of a compensatory mechanism in mice which maintains testosterone production in the absence of HSD17B3. However, the enzyme(s) responsible remains unknown.

The maintenance of testicular testosterone production in the absence of HSD17B3 in mice [17,34] contradicts the predicted testosterone levels portrayed by the in silico model [32], strongly suggesting the existence of other unrecognised androgen biosynthetic enzymes that contribute to testicular testosterone production. These results highlight the utility of transgenic mouse models for identifying and elucidating the roles of specific steroidogenic enzymes and androgens, and suggest that the in silico models of steroidogenesis need more information to accurately predict steroidogenic output in a given context.

The results of Sipila et al. and Rebourcet et al. demonstrate that HSD17B3 does not encapsulate the entirety of testosterone production in mice [17,34]. Other pathways or enzymes, particularly those within the HSD17B family, may influence or be involved in testosterone production, and are potential candidates that could compensate for the loss of HSD17B3 action.

4. Possible Explanations for Continued Testosterone Production in HSD17B3-Deficient Mice

4.1. The Role of the Adrenal Gland in Androgen Production

Whilst the majority of androgens are produced in the testis, approximately 5% of human androgens are synthesised in the zona reticularis of the human adrenal cortex. This is an alternative source for androgens, such as DHEA and androstenedione, however, these have a low affinity for AR and are considered to be weak androgens [39]. However, these androgen precursors can be transported to other tissues where they are metabolised via the canonical or alternate androgen pathways to produce more potent androgens, specifically testosterone and DHT (Figure 1). The human adrenal cortex can also synthesise 11-oxygenated 19-carbon steroids such as 11β-hydroxyandrostenedione and 11β-hydroxytestosterone utilising the enzyme CYP11B1 [40], however these are modifications of androstenedione and testosterone.

There are species differences between human and mouse adrenal function. In fact, the mouse adrenal is often overlooked as an androgen-producing organ because the CYP17A1 enzyme, important for 17,20 lyase activity in androgen production, is silenced early on in mouse development [41]. Therefore, while the human adrenal gland can produce some androgens, the lack of CYP17A1 in the mouse adrenal greatly reduces its capacity for andro-

gen production [41]. Further, 11-oxygenated steroids that are prevalent in humans, are at undetectable concentrations in mouse circulation [42]. It is however possible that the mouse adrenal gland could produce androgens from circulating testis-derived androstenedione. The adrenal gland expresses the enzyme HSD17B5, which could be involved in converting some of the high circulating androstenedione to testosterone.

To determine if the mouse adrenal gland can compensate for the lack of HSD17B3 by producing testosterone and DHT, Sipila et al. measured androgen concentrations after an adrenalectomy [34]. Surprisingly, the results showed that circulating testosterone and DHT in adrenalectomized HSD17B3 KO mice further increased, ruling out the adrenal gland as the site of continued androgen production [34]. This finding supports observations in human HSD17B3 deficiency cases, as adrenal steroid biosynthesis remains normal in males with HSD17B3 deficiency [43].

4.2. Androgen Biosynthesis in Peripheral Tissues

Local conversion of androgens also occurs in peripheral tissues, making them another potential source of androgen production [44]. SRD5A enzymes are expressed in peripheral tissues and can convert testosterone to the more potent androgen DHT.

11β-hydroxysteroids synthesised in the human adrenal gland can be converted to 11-keto androgens, predominantly occurring in peripheral tissues, and these can have androgen activity by acting on AR [45]. There is emerging evidence that the 11-keto androgens, including 11-ketotestosterone and 11-keto-DHT, play a role in male physiology in both humans and mice, however, whether they have a role in postnatal testis function is not established [40,46,47]. Whilst 11-keto-testosterone has been detected in both humans [45] and mice [48], 11-keto-testosterone is another modification of testosterone and therefore does not explain the testosterone synthesis in the HSD17B3 deficient mice [17,34]. However, the role of 11-keto androgens in mice may be amplified and contribute to some of the phenotypic characteristics observed in these mice.

The increased circulating testosterone with unchanged intratesticular levels suggests testosterone synthesis could be occurring in the peripheral tissue of HSD17B3 KO mice. Enzymes expressed in the periphery, such as HSD17B5, are potential candidates that may be responsible. HSD17B5 can convert androstenedione to testosterone and is the major enzyme that performs this conversion in the prostate [28]. HSD17B5 is overexpressed in cancers, including castrate-resistant prostate cancer, resulting in increased testosterone production [44]. Therefore, it can be postulated that HSD17B5 may become overexpressed in peripheral tissues following HSD17B3 ablation.

To further investigate the source of androgens, Sipila and colleagues also performed intra-tissue steroid analysis on the testis and peripheral tissues including epididymis, prostate, adrenal, liver, kidney, adipose tissue, and spleen [34]. These results demonstrated some, although minimal, testosterone levels in peripheral tissues of HSD17B3 KO mice, and high levels in the testis, indicating that testosterone synthesis in the absence of HSD17B3 is likely to be of testicular origin [34].

4.3. The Alternate "Backdoor" Pathway

The functionality of the canonical pathway is essential for testosterone production, however, it does not encapsulate the entirety of androgen biosynthesis. In 2003, Wilson et al. discovered a new androgen biosynthesis pathway in the tammar wallaby, where DHT is produced utilising steroid precursors, bypassing the need for testosterone synthesis (Figure 1) [49,50]. Since this discovery, the alternate pathway, commonly known as the backdoor pathway, has been identified in other species including both mice and humans [51–53].

Androgen precursors produced in the canonical pathway are converted into the alternate pathway by SRD5A1 and SRD5A2 enzymes (Figure 1). Although the canonical and alternate pathways have been investigated individually, it is unknown whether these pathways function independently, or in combination.

It is now clear that masculinisation during human fetal development is dependent on both the canonical and alternate androgen biosynthesis pathways [54]. Confirming the importance of the alternate pathway, Flück et al. demonstrated that mutations to enzymes specific for the alternate pathway (AKR1C2/4) show perturbed sexual development resulting in DSD, even when the canonical pathway remains intact [52,54,55]. Further, O'Shaughnessy et al. recently showed that androsterone, an alternate pathway androgen, was a major precursor found in human male fetuses, with significantly higher circulating concentration compared to females [56]. This study also demonstrated that during human fetal development, the alternate pathway predominantly functions in peripheral nongonadal tissues including the placenta, liver and adrenal, indicating that tissues other than the testes contribute to masculinisation [56]. Masculinisation gender differences during fetal development due to the alternate pathway is likely due to *CYP17A1* expression, with expression occurring in the testis and adrenal [56]. Taken together, these studies indicate that the alternate pathway is important in male physiology, as evidenced by its requirement during key developmental timepoints. As the conversion of testosterone to the more potent DHT is important for the development of external genitalia [57], the non-developed male genitalia in human HSD17B3 deficient individuals suggests that the alternate pathway alone cannot compensate for the canonical pathway during fetal life. Therefore, both the canonical and alternate pathways are required for appropriate male sexual development, however, the specific interactions are unclear.

As DHT is largely responsible for the virilisation of external tissues, the alternate pathway may be responsible for the virilisation of tissues during puberty, rather than the canonical pathway. This is a possible explanation for the virilisation observed in HSD17B3 deficient humans during puberty, as it does not require testosterone to be produced, however this hypothesis has not been tested.

Whether the alternate pathway compensates for the canonical pathway in the absence of HSD17B3 in mice is currently unknown. The increased DHT production in HSD17B3 KO male mice may suggest the alternate pathway could be compensating for the canonical pathway to promote androgen action, by maintaining peripheral levels of DHT that can support normal androgen function [34]. Unfortunately, alternate pathway androgen precursors were not measured in either model so this theory cannot be confirmed at this stage. Then again, the increased levels of DHT [34] could be a result of the increased levels of circulating testosterone [17,34] from the canonical pathway, being converted into DHT. Regardless of whether the alternate pathway is compensating or not, this does not explain the continued testosterone production in the HSD17B3 KO mice and their ability to reproduce [17,34].

4.4. Other 17β-hydroxysteroid Dehydrogenases: Implications for Testosterone Synthesis

The HSD17B family consists of multiple subtypes that either reduce and/or oxidise precursors to convert them into other steroids. The amino acid sequence of reductive HSD17B enzymes is generally well conserved across human and mouse species, indicating that they originated from a common ancestor (Table 1). Therefore, it seems likely that some HSD17B enzymes may have overlapping functions and could be candidates to be compensatory mechanisms during the loss of HSD17B3. The homology of protein sequences has been assessed using protein BLAST (https://blast.ncbi.nlm.nih.gov (accessed on 26 October 2022)) to compare the amino acid sequence of mouse HSD17B3 with other reductive mouse HSD17B enzymes (Table 2).

Table 1. Amino acid sequence homology of HSD17B enzymes between human and mouse.

HSD17B Subtype	Amino Acid Sequence Homology (%)	Preferred Functions
HSD17B1	68.29	Estrogen synthesis E1 → E2
HSD17B3	73.2	Androgen synthesis A4 → T
HSD17B5 (Human AKR1C3) (Mouse AKR1C6)	75.54	Prostaglandin synthesis
HSD17B7	78.01	Cholesterol synthesis Estrogen synthesis E1 → E2
HSD17B9 (Mouse HSD17B6)	47.17	Retinoid metabolism
HSD17B12	81.09	Fatty acid elongation Estrogen synthesis E1 → E2

E1 = Estrone, E2 = Estradiol, A4 = Androstenedione, T = Testosterone.

Table 2. Amino acid sequence homology of mouse HSD17B3 with other mouse HSD17B enzymes.

Mouse HSD17B Subtype	Amino Acid Sequence Homology Compared to Mouse HSD17B3 (% Identical)	Reductive Capacity	Shown to Convert A4 → T
HSD17B1	24.26	Yes [58]	Yes [59,60]
HSD17B5 (Mouse AKR1C6)	No significant similarity found	Yes [44]	Yes [28,44]
HSD17B7	26.85	Yes [61]	N/A
HSD17B9 (Mouse HSD17B6)	28.79	Yes [62]	N/A
HSD17B12	40.27	Yes [58]	Yes [63]

A4 = Androstenedione, T = Testosterone.

Current literature dictates that in the testis, the canonical pathway of androgen production employs HSD17B3 as the critical enzyme for androstenedione reduction to testosterone. However, there are other known HSD17B enzymes capable of performing this reaction, including; HSD17B1 [64], HSD17B5 [28] and HSD17B12 [63]. Although these enzymes can carry out this function, it is with less efficiency compared to HSD17B3 [65].

HSD17B1 is viewed largely as an estrogenic enzyme, with its major function being the enzyme that catalyses the conversion of estrone to the more potent estrogen, estradiol. However, it has also been shown to have testosterone synthesising capabilities [66]. While HSD17B3 in Leydig cells is considered as the predominant enzyme responsible for testosterone synthesis in males, the situation is more complex during fetal testis development with both fetal Sertoli cells and fetal Leydig cells being required for testosterone synthesis [64]. In the fetal mouse testis, there is increasing evidence supporting that HSD17B1 and HSD17B3 both contribute to testicular testosterone production [18,47,64,66]. Human HSD17B1 can also convert androstenedione into testosterone, however, is less efficient compared to the mouse enzyme [47,67]. Virilisation during fetal development in the HSD17B3 KO male mice could be a result of the fetal Sertoli cells expressing HSD17B1, and as mouse HSD17B1 is more efficient at synthesising testosterone compared to human HSD17B1, this may partly explain the differences in the phenotype amongst the species [64,66]. Whether

androgen action as a result of HSD17B1 activity is also true for the human fetal testis is unclear, however there is evidence for the preferential expression of *HSD17B1* and *HSD17B3* in human fetal Sertoli cells compared to Leydig cells [47]. While HSD17B1 is expressed in the mouse testis during fetal development, this expression is reduced to undetectable levels in adulthood [17,18,59,66]. Hakkarainen et al. demonstrated that HSD17B1 is required for normal steroid synthesis and spermatogenesis [66]. This study showed that in HSD17B1 KO male mice, HSD17B3 is up-regulated to compensate at 1 day postpartum and interestingly, continues to be up-regulated at 3 months of age (when HSD17B1 is normally undetectable) [66], likely to maintain testosterone production.

HSD17B5 is a multi-functional aldo-keto reductase enzyme that is involved in androgen, estrogen, progestin, and prostaglandin synthesis [68]. HSD17B5 is undetectable in the mouse testis and shows low expression in the human testis, yet is highly expressed in peripheral tissues [18,69]. While *Hsd17b5* was undetectable in the testis of HSD17B3 KO mice [17], its abundant expression in the periphery suggests HSD17B5 could be contributing to testosterone synthesis across multiple tissues as previously discussed. However, as a large proportion of testosterone in HSD17B3 KO adult mice is likely derived from the testis [34], HSD17B5 may be accompanied by other enzymes.

HSD17B12 is ubiquitously expressed throughout the body, including in the Leydig cells, throughout all life stages and is considered as a multi-functional enzyme predominantly involved in estradiol synthesis and the elongation of very long chain fatty acids [70]. Alongside HSD17B12's major functions, mouse HSD17B12 has been shown in vitro to convert androstenedione to testosterone, and HSD17B12 in the Japanese eel synthesises 11-ketotestosterone, a predominant androgen in fish, from 11-ketoandrostenedione, suggesting that this function is conserved across some species [71]. However, human HSD17B12 is less efficient at converting androstenedione into testosterone [58,63]. The human HSD17B12 protein is highly specific for reducing estrone to estradiol, however, a single amino acid change of a bulky phenylalanine to a smaller leucine in mouse HSD17B12 impacts the binding site, making mouse HSD17B12 less specific, allowing more substrates (including androstenedione) to enter the active site [63]. This amino acid difference could explain the phenotypic differences seen between mouse and human. Consistent with the suggestion from Rebourcet et al. that mouse HSD17B12 could be compensating for the loss of HSD17B3 activity in HSD17B3 KO males [17], mice heterozygous for HSD17B12 have reduced levels of circulating testosterone, however, this could be a biproduct as a result of HSD17B12's other functions [70]. *Hsd17b12* transcript expression in the testes of HSD17B3 KO males are slightly elevated [17]. However, as androstenedione and testosterone can be converted into estrogens by the enzyme aromatase (*Cyp19a1*), and because circulating androstenedione and testosterone is increased in HSD17B3 KO mice, this slight increase in *Hsd17b12* could also be due to a heightened conversion of estrogens, which is HSD17B12's primary function.

Other reductase enzymes including mouse HSD17B6 and HSD17B7 have not been shown to convert androstenedione into testosterone, however, their ability to produce testosterone cannot be ruled out and would require further investigation. There is also the possibility that there are undiscovered HSD17B enzymes in the mouse that could be catalysing the reaction forming testosterone.

5. Concluding Remarks and Future Perspective

HSD17B3 has long been thought to be the main testosterone biosynthetic enzyme in adult males and required for sexual development and fertility. *HSD17B3* loss-of-function mutations in humans results in perturbed male sexual differentiation [22], however, recent ground-breaking studies have revealed that ablation of the canonical pathway in transgenic mice deficient in HSD17B3, has little impact on male development and fertility [17,34]. These HSD17B3 KO mouse models demonstrate the presence of species differences in androgen production and highlight the challenges that scientists experience when trying to study human disorders. While mice function similarly to humans, future studies involv-

ing the modelling of human androgen-related disorders in mice must acknowledge and consider the species differences.

The preservation of testosterone production and fertility in mice lacking HSD17B3 highlights the complexity of androgen biosynthesis and that the current view of mouse testosterone production is incomplete. The phenotypic differences observed between mice and humans with HSD17B3 deficiency could be a result of one or a combination of mechanisms, such as adrenal or other peripheral tissue androgen production, alternate pathway compensation, or testosterone production due to other HSD17B enzymes. The identification of compensatory mechanisms for androgen production is required and could provide novel insights into how androgens, specifically testosterone, are synthesised, and this will allow for more accurate models of human androgen-related disorders to be developed.

Author Contributions: B.M.L. wrote the manuscript and designed the figure and tables. B.M.L., L.O., L.B.S. and D.R. conceived and contributed to editing the manuscript. All authors have read and agreed to the published version of the manuscript.

Funding: This work was funded by the Department of Health, National Health and Medical Research Council (NHMRC), grant number APP1158344. B.M.L. was funded by the University of Newcastle HDR Research Training Program.

Institutional Review Board Statement: Not applicable.

Informed Consent Statement: Not applicable.

Data Availability Statement: Schematic of androgen production pathway Created with BioRender.com, agreement number KK24L9P31C. Amino acid sequence comparison was determined using NCBI protein blast suite (https://blast.ncbi.nlm.nih.gov (accessed on 26 October 2022)).

Acknowledgments: We would like to thank Anne-Louise Gannon for helpful discussions.

Conflicts of Interest: The authors declare no conflict of interest.

References

1. Spitzer, M.; Huang, G.; Basaria, S.; Travison, T.G.; Bhasin, S. Risks and benefits of testosterone therapy in older men. *Nat. Rev. Endocrinol.* **2013**, *9*, 414. [CrossRef] [PubMed]
2. Shores, M.M. The implications of low testosterone on mortality in men. *Curr. Sex Health Rep.* **2014**, *6*, 235–243. [CrossRef] [PubMed]
3. Zarotsky, V.; Huang, M.Y.; Carman, W.; Morgentaler, A.; Singhal, P.K.; Coffin, D.; Jones, T.H. Systematic literature review of the risk factors, comorbidities, and consequences of hypogonadism in men. *Andrology* **2014**, *2*, 819–834. [CrossRef] [PubMed]
4. Azhar, S.; Menon, K.M. Receptor mediated gonadotropin action in gonadal tissues: Relationship between blood cholesterol levels and gonadotropin stimulated steroidogenesis in isolated rat Leydig and luteal cells. *J. Steroid Biochem.* **1982**, *16*, 175–184. [CrossRef] [PubMed]
5. Hou, J.W.; Collins, D.C.; Schleicher, R.L. Sources of cholesterol for testosterone biosynthesis in murine Leydig cells. *Endocrinology* **1990**, *127*, 2047–2055. [CrossRef] [PubMed]
6. O'Shaughnessy, P.J.; Murphy, L. Steroidogenic enzyme activity in the rat testis following Leydig cell destruction by ethylene-1,2-dimethanesulphonate and during subsequent Leydig cell regeneration. *J. Endocrinol.* **1991**, *131*, 451–457. [CrossRef] [PubMed]
7. Lambeth, J.D.; Stevens, V.L. Cytochrome P-450scc: Enzymology, and the regulation of intramitochondrial cholesterol delivery to the enzyme. *Endocr. Res.* **1984**, *10*, 283–309. [CrossRef]
8. Skinner, M.K. *Encyclopedia of Reproduction*; Academic Press: Cambridge, MA, USA, 2018.
9. Miller, W.L. Androgen biosynthesis from cholesterol to DHEA. *Mol. Cell Endocrinol.* **2002**, *198*, 7–14. [CrossRef]
10. Flück, C.E.; Miller, W.L.; Auchus, R.J. The 17,20-lyase activity of cytochrome p450c17 from human fetal testis favors the delta5 steroidogenic pathway. *J. Clin. Endocrinol. Metab.* **2003**, *88*, 3762–3766. [CrossRef]
11. Fevold, H.R.; Lorence, M.C.; McCarthy, J.L.; Trant, J.M.; Kagimoto, M.; Waterman, M.R.; Mason, J.I. Rat P450(17 alpha) from testis: Characterization of a full-length cDNA encoding a unique steroid hydroxylase capable of catalyzing both delta 4- and delta 5-steroid-17,20-lyase reactions. *Mol. Endocrinol.* **1989**, *3*, 968–975. [CrossRef]
12. Lucas-Herald, A.K.; Alves-Lopes, R.; Montezano, A.C.; Ahmed, S.F.; Touyz, R.M. Genomic and non-genomic effects of androgens in the cardiovascular system: Clinical implications. *Clin. Sci.* **2017**, *131*, 1405–1418. [CrossRef] [PubMed]
13. Zhu, J.L.; Chen, Z.; Feng, W.J.; Long, S.L.; Mo, Z.C. Sex hormone-binding globulin and polycystic ovary syndrome. *Clin. Chim. Acta* **2019**, *499*, 142–148. [CrossRef] [PubMed]

14. Reventos, J.; Sullivan, P.M.; Joseph, D.R.; Gordon, J.W. Tissue-specific expression of the rat androgen-binding protein/sex hormone-binding globulin gene in transgenic mice. *Mol. Cell Endocrinol.* **1993**, *96*, 69–73. [CrossRef] [PubMed]
15. Wei, R.; Zhong, S.; Qiao, L.; Guo, M.; Shao, M.; Wang, S.; Jiang, B.; Yang, Y.; Gu, C. Steroid 5α-Reductase Type I Induces Cell Viability and Migration via Nuclear Factor-κB/Vascular Endothelial Growth Factor Signaling Pathway in Colorectal Cancer. *Front. Oncol.* **2020**, *10*, 1501. [CrossRef] [PubMed]
16. Russell, D.W.; Wilson, J.D. Steroid 5 alpha-reductase: Two genes/two enzymes. *Annu. Rev. Biochem.* **1994**, *63*, 25–61. [CrossRef]
17. Rebourcet, D.; Mackay, R.; Darbey, A.; Curley, M.K.; Jørgensen, A.; Frederiksen, H.; Mitchell, R.T.; O'Shaughnessy, P.J.; Nef, S.; Smith, L.B. Ablation of the canonical testosterone production pathway via knockout of the steroidogenic enzyme HSD17B3, reveals a novel mechanism of testicular testosterone production. *FASEB J.* **2020**, *34*, 10373–10386. [CrossRef]
18. O'Shaughnessy, P.; Baker, P.; Heikkila, M.; Vainio, S.; McMahon, A. Localization of 17β-hydroxysteroid dehydrogenase/17-ketosteroid reductase isoform expression in the developing mouse testis—androstenedione is the major androgen secreted by fetal/neonatal Leydig cells. *Endocrinology* **2000**, *141*, 2631–2637. [CrossRef]
19. Ye, L.; Li, X.; Li, L.; Chen, H.; Ge, R.S. Insights into the Development of the Adult Leydig Cell Lineage from Stem Leydig Cells. *Front. Physiol.* **2017**, *8*, 430. [CrossRef]
20. Ge, R.S.; Hardy, M.P. Variation in the end products of androgen biosynthesis and metabolism during postnatal differentiation of rat Leydig cells. *Endocrinology* **1998**, *139*, 3787–3795. [CrossRef]
21. Mendonca, B.B.; Gomes, N.L.; Costa, E.M.; Inacio, M.; Martin, R.M.; Nishi, M.Y.; Carvalho, F.M.; Tibor, F.D.; Domenice, S. 46,XY disorder of sex development (DSD) due to 17β-hydroxysteroid dehydrogenase type 3 deficiency. *J. Steroid Biochem. Mol. Biol.* **2017**, *165*, 79–85. [CrossRef]
22. Gonçalves, C.I.; Carriço, J.; Bastos, M.; Lemos, M.C. Disorder of Sex Development Due to 17-Beta-Hydroxysteroid Dehydrogenase Type 3 Deficiency: A Case Report and Review of 70 Different HSD17B3 Mutations Reported in 239 Patients. *Int. J. Mol. Sci.* **2022**, *23*, 10026. [CrossRef] [PubMed]
23. Flück, C.E.; Pandey, A.V. Steroidogenesis of the testis–new genes and pathways. *Proc. Ann. D'Endocrinologie* **2014**, *75*, 40–47. [CrossRef] [PubMed]
24. Batista, R.L.; Costa, E.M.F.; Rodrigues, A.S.; Gomes, N.L.; Faria, J.A., Jr.; Nishi, M.Y.; Arnhold, I.J.P.; Domenice, S.; Mendonca, B.B. Androgen insensitivity syndrome: A review. *Arch. Endocrinol. Metab.* **2018**, *62*, 227–235. [CrossRef] [PubMed]
25. Geissler, W.M.; Davis, D.L.; Wu, L.; Bradshaw, K.D.; Patel, S.; Mendonca, B.B.; Elliston, K.O.; Wilson, J.D.; Russell, D.W.; Andersson, S. Male pseudohermaphroditism caused by mutations of testicular 17β–hydroxysteroid dehydrogenase 3. *Nat. Genet.* **1994**, *7*, 34–39. [CrossRef]
26. Mains, L.M.; Vakili, B.; Lacassie, Y.; Andersson, S.; Lindqvist, A.; Rock, J.A. 17beta-hydroxysteroid dehydrogenase 3 deficiency in a male pseudohermaphrodite. *Fertil. Steril.* **2008**, *89*, 228.e213–227. [CrossRef]
27. Hiort, O.; Marshall, L.; Birnbaum, W.; Wünsch, L.; Holterhus, P.M.; Döhnert, U.; Werner, R. Pubertal Development in 17Beta-Hydroxysteroid Dehydrogenase Type 3 Deficiency. *Horm. Res. Paediatr.* **2017**, *87*, 354–358. [CrossRef]
28. Byrns, M.C.; Mindnich, R.; Duan, L.; Penning, T.M. Overexpression of aldo-keto reductase 1C3 (AKR1C3) in LNCaP cells diverts androgen metabolism towards testosterone resulting in resistance to the 5α-reductase inhibitor finasteride. *J. Steroid. Biochem. Mol. Biol.* **2012**, *130*, 7–15. [CrossRef]
29. Fankhauser, M.; Tan, Y.; Macintyre, G.; Haviv, I.; Hong, M.K.; Nguyen, A.; Pedersen, J.S.; Costello, A.J.; Hovens, C.M.; Corcoran, N.M. Canonical androstenedione reduction is the predominant source of signaling androgens in hormone-refractory prostate cancer. *Clin. Cancer Res.* **2014**, *20*, 5547–5557. [CrossRef]
30. Andersson, S.; Moghrabi, N. Physiology and molecular genetics of 17β-hydroxysteroid dehydrogenases. *Steroids* **1997**, *62*, 143–147. [CrossRef]
31. Mah, L.W.; Chan, Y.Y.; Yang, J.H. Chapter 3—Gender Identity in Disorders of Sex Development. In *Principles of Gender-Specific Medicine*, 3rd ed.; Legato, M.J., Ed.; Academic Press: San Diego, CA, USA, 2017; pp. 27–43. [CrossRef]
32. O'Hara, L.; O'Shaughnessy, P.J.; Freeman, T.C.; Smith, L.B. Modelling steroidogenesis: A framework model to support hypothesis generation and testing across endocrine studies. *BMC Res. Notes* **2018**, *11*, 252. [CrossRef]
33. Livigni, A.; O'Hara, L.; Polak, M.E.; Angus, T.; Wright, D.W.; Smith, L.B.; Freeman, T.C. A graphical and computational modeling platform for biological pathways. *Nat. Protoc.* **2018**, *13*, 705–722. [CrossRef] [PubMed]
34. Sipilä, P.; Junnila, A.; Hakkarainen, J.; Huhtaniemi, R.; Mairinoja, L.; Zhang, F.P.; Strauss, L.; Ohlsson, C.; Kotaja, N.; Huhtaniemi, I.; et al. The lack of HSD17B3 in male mice results in disturbed Leydig cell maturation and endocrine imbalance akin to humans with HSD17B3 deficiency. *FASEB J.* **2020**, *34*, 6111–6128. [CrossRef] [PubMed]
35. Welsh, M.; Saunders, P.T.; Fisken, M.; Scott, H.M.; Hutchison, G.R.; Smith, L.B.; Sharpe, R.M. Identification in rats of a programming window for reproductive tract masculinization, disruption of which leads to hypospadias and cryptorchidism. *J. Clin. Invest.* **2008**, *118*, 1479–1490. [CrossRef] [PubMed]
36. O'Hara, L.; Smith, L.B. Androgen receptor roles in spermatogenesis and infertility. *Best Pract. Res. Clin. Endocrinol. Metab.* **2015**, *29*, 595–605. [CrossRef]
37. Kreisman, M.J.; Song, C.I.; Yip, K.; Natale, B.V.; Natale, D.R.; Breen, K.M. Androgens Mediate Sex-Dependent Gonadotropin Expression During Late Prenatal Development in the Mouse. *Endocrinology* **2017**, *158*, 2884–2894. [CrossRef]
38. Dungan, H.M.; Clifton, D.K.; Steiner, R.A. Minireview: Kisspeptin neurons as central processors in the regulation of gonadotropin-releasing hormone secretion. *Endocrinology* **2006**, *147*, 1154–1158. [CrossRef]

39. Rege, J.; Nakamura, Y.; Satoh, F.; Morimoto, R.; Kennedy, M.R.; Layman, L.C.; Honma, S.; Sasano, H.; Rainey, W.E. Liquid chromatography-tandem mass spectrometry analysis of human adrenal vein 19-carbon steroids before and after ACTH stimulation. *J. Clin. Endocrinol. Metab.* **2013**, *98*, 1182–1188. [CrossRef]
40. Naamneh Elzenaty, R.; du Toit, T.; Flück, C.E. Basics of androgen synthesis and action. *Best Pract. Res. Clin. Endocrinol. Metab.* **2022**, *36*, 101665. [CrossRef]
41. Van Weerden, W.; Bierings, H.; Van Steenbrugge, G.; De Jong, F.; Schröder, F. Adrenal glands of mouse and rat do not synthesize androgens. *Life Sci.* **1992**, *50*, 857–861. [CrossRef]
42. Rege, J.; Garber, S.; Conley, A.J.; Elsey, R.M.; Turcu, A.F.; Auchus, R.J.; Rainey, W.E. Circulating 11-oxygenated androgens across species. *J. Steroid Biochem. Mol. Biol.* **2019**, *190*, 242–249. [CrossRef]
43. Lee, Y.S.; Kirk, J.M.; Stanhope, R.G.; Johnston, D.I.; Harland, S.; Auchus, R.J.; Andersson, S.; Hughes, I.A. Phenotypic variability in 17beta-hydroxysteroid dehydrogenase-3 deficiency and diagnostic pitfalls. *Clin. Endocrinol.* **2007**, *67*, 20–28. [CrossRef] [PubMed]
44. Adeniji, A.O.; Chen, M.; Penning, T.M. AKR1C3 as a target in castrate resistant prostate cancer. *J. Steroid Biochem. Mol. Biol.* **2013**, *137*, 136–149. [CrossRef] [PubMed]
45. Yazawa, T.; Inaba, H.; Imamichi, Y.; Sekiguchi, T.; Uwada, J.; Islam, M.S.; Orisaka, M.; Mikami, D.; Ida, T.; Sato, T.; et al. Profiles of 5α-Reduced Androgens in Humans and Eels: 5α-Dihydrotestosterone and 11-Ketodihydrotestosterone Are Active Androgens Produced in Eel Gonads. *Front. Endocrinol.* **2021**, *12*, 657360. [CrossRef] [PubMed]
46. Turcu, A.F.; Auchus, R.J. Clinical significance of 11-oxygenated androgens. *Curr. Opin. Endocrinol. Diabetes Obes.* **2017**, *24*, 252–259. [CrossRef]
47. O'Donnell, L.; Whiley, P.A.F.; Loveland, K.L. Activin A and Sertoli Cells: Key to Fetal Testis Steroidogenesis. *Front. Endocrinol.* **2022**, *13*, 898876. [CrossRef] [PubMed]
48. Whiley, P.A.F.; O'Donnell, L.; Moody, S.C.; Handelsman, D.J.; Young, J.C.; Richards, E.A.; Almstrup, K.; Western, P.S.; Loveland, K.L. Activin A Determines Steroid Levels and Composition in the Fetal Testis. *Endocrinology* **2020**, *161*, bqaa058. [CrossRef]
49. Shaw, G.; Fenelon, J.; Sichlau, M.; Auchus, R.J.; Wilson, J.D.; Renfree, M.B. Role of the alternate pathway of dihydrotestosterone formation in virilization of the Wolffian ducts of the tammar wallaby, Macropus eugenii. *Endocrinology* **2006**, *147*, 2368–2373. [CrossRef]
50. Wilson, J.D.; Auchus, R.J.; Leihy, M.W.; Guryev, O.L.; Estabrook, R.W.; Osborn, S.M.; Shaw, G.; Renfree, M.B. 5α-androstane-3α, 17β-diol is formed in tammar wallaby pouch young testes by a pathway involving 5α-pregnane-3α, 17α-diol-20-one as a key intermediate. *Endocrinology* **2003**, *144*, 575–580. [CrossRef]
51. Mahendroo, M.; Wilson, J.D.; Richardson, J.A.; Auchus, R.J. Steroid 5alpha-reductase 1 promotes 5alpha-androstane-3alpha,17beta-diol synthesis in immature mouse testes by two pathways. *Mol. Cell Endocrinol.* **2004**, *222*, 113–120. [CrossRef]
52. Flück, C.E.; Meyer-Böni, M.; Pandey, A.V.; Kempná, P.; Miller, W.L.; Schoenle, E.J.; Biason-Lauber, A. Why boys will be boys: Two pathways of fetal testicular androgen biosynthesis are needed for male sexual differentiation. *Am. J. Hum. Genet.* **2011**, *89*, 201–218. [CrossRef]
53. Dhayat, N.A.; Dick, B.; Frey, B.M.; d'Uscio, C.H.; Vogt, B.; Flück, C.E. Androgen biosynthesis during minipuberty favors the backdoor pathway over the classic pathway: Insights into enzyme activities and steroid fluxes in healthy infants during the first year of life from the urinary steroid metabolome. *J. Steroid Biochem. Mol. Biol.* **2017**, *165*, 312–322. [CrossRef] [PubMed]
54. Biason-Lauber, A.; Miller, W.L.; Pandey, A.V.; Flück, C.E. Of marsupials and men: "Backdoor" dihydrotestosterone synthesis in male sexual differentiation. *Mol. Cell Endocrinol.* **2013**, *371*, 124–132. [CrossRef] [PubMed]
55. Fukami, M.; Homma, K.; Hasegawa, T.; Ogata, T. Backdoor pathway for dihydrotestosterone biosynthesis: Implications for normal and abnormal human sex development. *Dev. Dyn.* **2013**, *242*, 320–329. [CrossRef] [PubMed]
56. O'Shaughnessy, P.J.; Antignac, J.P.; Le Bizec, B.; Morvan, M.-L.; Svechnikov, K.; Söder, O.; Savchuk, I.; Monteiro, A.; Soffientini, U.; Johnston, Z.C. Alternative (backdoor) androgen production and masculinization in the human fetus. *PLoS Biol.* **2019**, *17*, e3000002. [CrossRef] [PubMed]
57. Wilson, J.D.; Griffin, J.E.; Russell, D.W. Steroid 5 alpha-reductase 2 deficiency. *Endocr. Rev.* **1993**, *14*, 577–593. [CrossRef] [PubMed]
58. Luu-The, V.; Tremblay, P.; Labrie, F. Characterization of type 12 17beta-hydroxysteroid dehydrogenase, an isoform of type 3 17beta-hydroxysteroid dehydrogenase responsible for estradiol formation in women. *Mol. Endocrinol.* **2006**, *20*, 437–443. [CrossRef] [PubMed]
59. Sha, J.; Baker, P.; O'Shaughnessy, P.J. Both reductive forms of 17 beta-hydroxysteroid dehydrogenase (types 1 and 3) are expressed during development in the mouse testis. *Biochem. Biophys. Res. Commun.* **1996**, *222*, 90–94. [CrossRef]
60. Saloniemi, T.; Welsh, M.; Lamminen, T.; Saunders, P.; Mäkelä, S.; Streng, T.; Poutanen, M. Human HSD17B1 expression masculinizes transgenic female mice. *Mol. Cell Endocrinol.* **2009**, *301*, 163–168. [CrossRef]
61. Marijanovic, Z.; Laubner, D.; Moller, G.; Gege, C.; Husen, B.; Adamski, J.; Breitling, R. Closing the gap: Identification of human 3-ketosteroid reductase, the last unknown enzyme of mammalian cholesterol biosynthesis. *Mol. Endocrinol.* **2003**, *17*, 1715–1725. [CrossRef]
62. Napoli, J.L. 17beta-Hydroxysteroid dehydrogenase type 9 and other short-chain dehydrogenases/reductases that catalyze retinoid, 17beta- and 3alpha-hydroxysteroid metabolism. *Mol. Cell Endocrinol.* **2001**, *171*, 103–109. [CrossRef]
63. Blanchard, P.G.; Luu-The, V. Differential androgen and estrogen substrates specificity in the mouse and primates type 12 17beta-hydroxysteroid dehydrogenase. *J. Endocrinol.* **2007**, *194*, 449–455. [CrossRef] [PubMed]

64. Shima, Y.; Miyabayashi, K.; Haraguchi, S.; Arakawa, T.; Otake, H.; Baba, T.; Matsuzaki, S.; Shishido, Y.; Akiyama, H.; Tachibana, T.; et al. Contribution of Leydig and Sertoli cells to testosterone production in mouse fetal testes. *Mol. Endocrinol.* **2013**, *27*, 63–73. [CrossRef]
65. Miller, W.L.; Auchus, R.J. The molecular biology, biochemistry, and physiology of human steroidogenesis and its disorders. *Endocr. Rev.* **2011**, *32*, 81–151. [CrossRef] [PubMed]
66. Hakkarainen, J.; Zhang, F.-P.; Jokela, H.; Mayerhofer, A.; Behr, R.; Cisneros-Montalvo, S.; Nurmio, M.; Toppari, J.; Ohlsson, C.; Kotaja, N. Hydroxysteroid (17β) dehydrogenase 1 expressed by Sertoli cells contributes to steroid synthesis and is required for male fertility. *FASEB J.* **2018**, *32*, 3229–3241. [CrossRef] [PubMed]
67. Nokelainen, P.; Puranen, T.; Peltoketo, H.; Orava, M.; Vihko, P.; Vihko, R. Molecular cloning of mouse 17β-Hydroxysteroid Dehydrogenase Type 1 and characterization of enzyme activity. *Eur. J. Biochem.* **1996**, *236*, 482–490. [CrossRef] [PubMed]
68. Byrns, M.C.; Jin, Y.; Penning, T.M. Inhibitors of type 5 17β-hydroxysteroid dehydrogenase (AKR1C3): Overview and structural insights. *J. Steroid Biochem. Mol. Biol.* **2011**, *125*, 95–104. [CrossRef] [PubMed]
69. Pelletier, G.; Luu-The, V.; Tětu, B.; Labrie, F. Immunocytochemical localization of type 5 17 β-hydroxysteroid dehydrogenase in human reproductive tissues. *J. Histochem. Cytochem.* **1999**, *47*, 731–737. [CrossRef]
70. Bellemare, V.; Phaneuf, D.; Luu-The, V. Target deletion of the bifunctional type 12 17β-hydroxysteroid dehydrogenase in mice results in reduction of androgen and estrogen levels in heterozygotes and embryonic lethality in homozygotes. *Horm. Mol. Biol. Clin. Investig.* **2010**, *2*, 311–318. [CrossRef]
71. Suzuki, H.; Ozaki, Y.; Ijiri, S.; Gen, K.; Kazeto, Y. 17β-Hydroxysteroid dehydrogenase type 12a responsible for testicular 11-ketotestosterone synthesis in the Japanese eel, Anguilla japonica. *J. Steroid. Biochem. Mol. Biol.* **2020**, *198*, 105550. [CrossRef]

Received: 4 September 2024 | Revised: 28 October 2024 | Accepted: 1 November 2024

DOI: 10.1096/fj.202402093R

RESEARCH ARTICLE

The FASEB Journal

Compensatory mechanisms that maintain androgen production in mice lacking key androgen biosynthetic enzymes

Ben M. Lawrence[1,2] | **Liza O'Donnell**[3] | **Anne-Louise Gannon**[1] | **Sarah Smith**[1] | **Michael K. Curley**[4] | **Annalucia Darbey**[4] | **Rosa Mackay**[4] | **Peter J. O'Shaughnessy**[5] | **Lee B. Smith**[3] | **Diane Rebourcet**[1,6]

[1]College of Engineering, Science and Environment, The University of Newcastle, Callaghan, New South Wales, Australia

[2]School of BioSciences, The University of Melbourne, Parkville, Victoria, Australia

[3]Office of the Deputy Vice Chancellor (Research), Griffith University, Southport, Queensland, Australia

[4]MRC Centre for Reproductive Health, University of Edinburgh, The Queen's Medical Research Institute, Edinburgh, UK

[5]School of Biodiversity, One Health & Veterinary Medicine, College of Medical, Veterinary and Life Sciences, University of Glasgow, Garscube Campus, Glasgow, UK

[6]Inserm, EHESP, Irset (Institut de recherche en santé, environnement et travail) - UMR_S 1085, Univ Rennes, Rennes, France

Correspondence
Lee B. Smith, Griffith University, 1 Parklands Drive, Southport, QLD 4215, Australia.

Abstract

Testosterone and dihydrotestosterone (DHT) are essential for male development and fertility. In the canonical androgen production pathway, testosterone is produced in the testis by HSD17B3; however, adult male *Hsd17b3* knockout (KO) mice continue to produce androgens and are fertile, indicating compensatory mechanisms exist. A second, alternate pathway produces DHT from precursors other than testosterone via 5α-reductase (SRD5A) activity. We hypothesized that the alternate pathway contributes to androgen bioactivity in *Hsd17b3* KO mice. To investigate contributions arising from and interactions between the canonical and alternate pathways, we pharmacologically inhibited SRD5A and ablated *Srd5a1* (the predominant SRD5A in the testis) on the background of *Hsd17b3* KO mice. Mice with perturbation of either the canonical or both pathways exhibited increased LH, testicular steroidogenic enzyme expression, and normal reproductive tracts and fertility. In the circulation, alternate pathway steroids were increased in the absence of HSD17B3 but were reduced by co-inhibition of SRD5A1. Mice with perturbations of both pathways produced normal basal levels of intratesticular testosterone, suggesting the action of other unidentified hydroxysteroid dehydrogenase(s). Strikingly, testicular expression of another SRD5A enzyme, *Srd5a2*, was markedly increased in the absence of *Hsd17b3*, suggesting a compensatory increase in SRD5A2 to maintain androgen bioactivity during

Abbreviations: 11K, 11-keto; 11OH, 11-hydroxy; 17OH, 17-hydroxy; 17OH-DHP, 17-hydroxy-5α-dihydroprogesterone; 3α-Diol, 5α-androstane- 3α, 17β-diol; 3β-diol, 5α-androstane-3β, 17β-diol; 5α-DHP, 5α-dihydroprogesterone; AGD, anogenital distance; AKR1C, aldo-keto reductase family 1 member C; AR, androgen receptor; CYP11A1, cytochrome P450 11A1, cholesterol side-chain cleavage enzyme; CYP17A1, cytochrome P450 17A1; CYP19A1, cytochrome P450 family 19 subfamily A member 1; DHEA, dehydroepiandrosterone; dHet, double heterozygous; DHT, dihydrotestosterone; dKO, double knockout; hCG, human chorionic gonadotrophin; HSD17B, hydroxysteroid-dehydrogenase-17-beta; HSD3B, hydroxysteroid-dehydrogenase-3-beta; KO, knockout; LH, luteinizing hormone; LHCGR, luteinizing hormone/choriogonadotropin receptor; SRD5A, steroid 5α-reductase; WT, wild-type.

Lee B. Smith and Diane Rebourcet joint senior authors.

Email: lee.smith@griffith.edu.au

Funding information
DHAC | National Health and Medical Research Council (NHMRC), Grant/Award Number: APP1158344; UKRI | Medical Research Council (MRC), Grant/Award Number: MR/N002970/1

HSD17B3 deficiency. Finally, we observed elevated circulating concentrations of the 11-keto-derivative of DHT, suggesting compensatory extra-gonadal induction of bioactive 11-keto androgen production. Taken together, we conclude that, in the absence of the canonical pathway of androgen production, multiple intra- and extra-gonadal mechanisms cooperate to maintain testosterone and DHT production, supporting male development and fertility.

KEYWORDS
androgens, dihydrotestosterone, male fertility, steroids, testis, testosterone

1 | INTRODUCTION

Male development, fertility, lifelong health, and well-being are androgen-dependent. Perturbed androgen action in men is linked with infertility/low sperm counts[1] and an increased risk of developing chronic and age-related conditions, including cardiovascular disease, diabetes, obesity, and metabolic syndrome.[2,3] The androgen testosterone and its 5α-reduced derivative dihydrotestosterone (DHT) are key drivers of male sexual development and function. In males, testosterone is predominantly synthesized by Leydig cells in the testes via a single testis-specific 17-ketosteroid reductase enzyme, HSD17B3. Testosterone and DHT both act through the androgen receptor (AR) to promote androgen-dependent gene transcription; however, DHT has a higher affinity for and dissociates more slowly from the AR and thus is a more potent androgen than testosterone.[4]

Androgen biosynthesis occurs via multiple pathways (Figure 1). The canonical pathway involves the synthesis of testosterone from androstenedione, which can then be converted to DHT by steroid 5α-reductase (SRD5A) enzymes.[5–7] In contrast, the alternate pathway utilizes steroid precursors other than testosterone to produce DHT.[5,7,8] This pathway was first discovered in the tammar wallaby[9,10] and has since been confirmed in many species, including mice and humans.[7,11–14] The alternate pathway entry point utilizes SRD5A to convert the precursors progesterone, 17OH-progesterone, and androstenedione from the canonical pathway into the alternate pathway, producing 5α-dihydroprogesterone, 17OH-dihydroprogesterone, and androstanedione, respectively (Figure 1[14]). The aldo-keto reductase family 1 member C enzymes (AKR1C1–4), the CYP17A1 enzyme, and HSD17B6 then convert alternate pathway precursors into DHT (Figure 1).

The physiological relevance of the canonical and alternate pathways to male reproductive development have been independently explored in humans.[12,14] Loss of function mutations in enzymes specific to the canonical pathway lead to disordered sexual development in humans.[12,15–17] Loss of function mutations in AKR1C2 and AKR1C4 (specific to the alternate pathway) also result in disordered sexual development due to under-masculinization.[12] Therefore, normal activity in both pathways appears to be essential for masculinization in human males.[12,14]

Loss of function mutations to *HSD17B3* and disruption of the canonical pathway is the most common disorder of androgen synthesis, leading to disordered sexual development and male infertility.[17] HSD17B3 deficiency is characterized by a high androstenedione to testosterone ratio[18] due to an inability to reduce androstenedione into testosterone.[16,19,20] 46,XY HSD17B3-deficient individuals can undergo late-onset masculinization during puberty, where male characteristics can develop.[19,21] In contrast to humans, in two independently generated *Hsd17b3* knockout (KO) mouse lines, male mice were phenotypically normal at birth, and the adults were fertile with normal levels of intratesticular testosterone[20,22] and DHT.[22]

Thus, *Hsd17b3* KO male mice maintain sufficient androgen action for sexual development and testis function. These observations point to the existence of compensatory mechanisms in mice to maintain androgen biosynthesis pathways independent of HSD17B3, and increased activity through the alternate pathway could be one such mechanism. It is also possible that 11-keto androgens could contribute to androgen bioactivity in these mice. 11-keto androgens are bioactive androgens synthesized from adrenal-derived 11-oxygenated steroids and are likely to be important in females but are present at much lower levels in males.[23] 11-keto androgens are the predominant bioactive androgens in fish[24] and are present in the circulation of humans[24,25] and the testes of mice.[26,27] 11-keto androgens have been suggested to be potent activators of the AR[24] although in vitro they have a considerably lower potency in terms of AR activation than their native androgens.[28] In fetal mouse testes, a decreased ability to convert androstenedione to testosterone is associated with increased 11-keto-testosterone levels, suggesting increased keto-androgen biosynthesis could be a compensatory response to reduced androgen biosynthesis during fetal testis development.[27] However, the role of 11-keto androgens in adult male mice is not known.

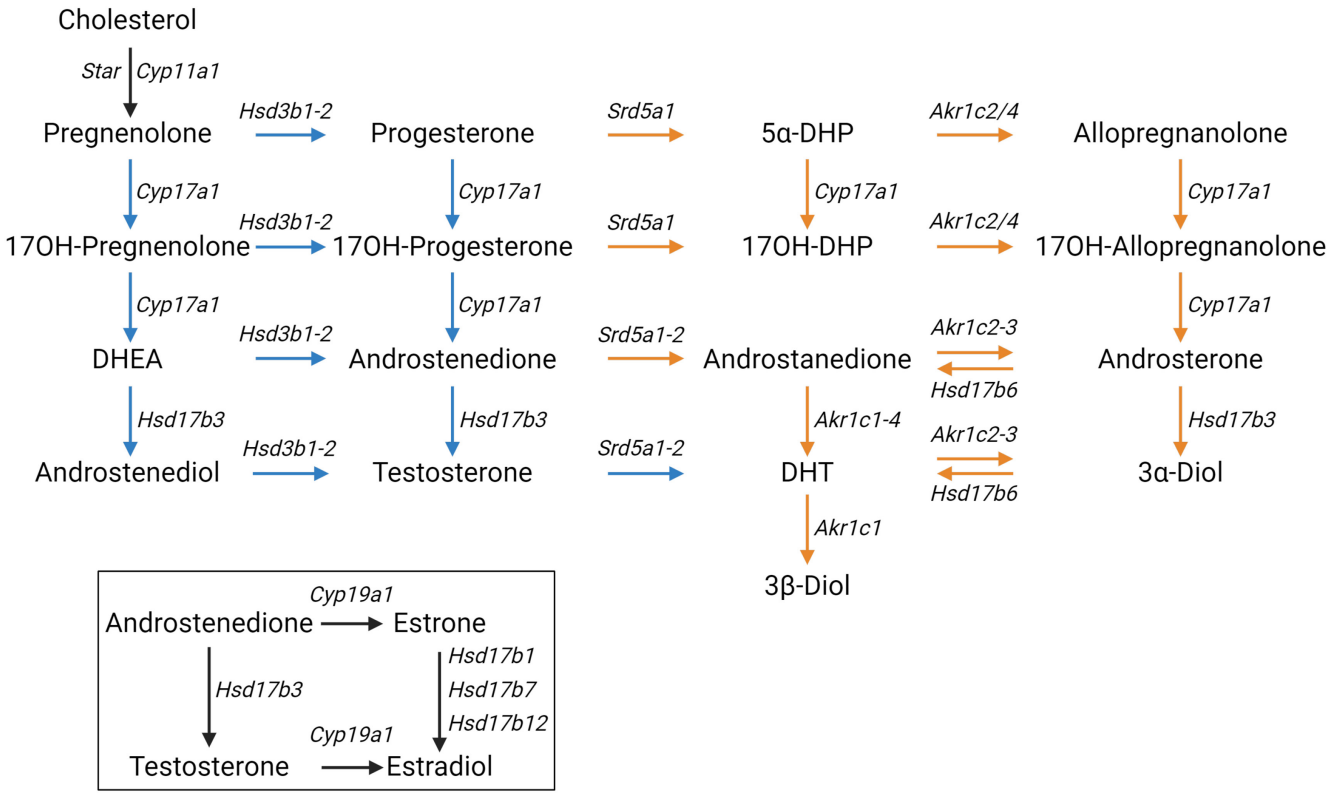

FIGURE 1 The canonical and alternate pathways of androgen biosynthesis. All androgens originate from cholesterol and are converted by multiple enzymes to produce the active androgens testosterone and dihydrotestosterone (DHT). The canonical pathway (blue arrows) produces testosterone, which can act directly on the androgen receptor or be used as a precursor to DHT. The alternate pathway (orange arrows) can synthesize DHT without the need for testosterone synthesis. The mouse gene symbols for the enzymes responsible for each reaction are shown in italics. The dashed box indicates that androstenedione and testosterone can also be converted to estrogens via CYP19A1 and are aromatized to estrone and estradiol, respectively. 17OH, 17-hydroxy; 17OH-DHP, 17-hydroxy-5α-dihydroprogesterone; 3α-Diol, 5α-androstane-3α, 17β-diol; 3β-Diol, 5α-androstane-3β, 17β-diol; 5α-DHP, 5α-dihydroprogesterone; DHEA, dehydroepiandrosterone; DHT, dihydrotestosterone.

The current study investigates the hypothesis that ablation of the canonical pathway in mice induces compensatory mechanisms to maintain androgen bioactivity. We hypothesized that the canonical and alternate pathways cooperate to maintain male sexual development and adult testis function and fertility in mice. To investigate this, we created mice lacking both HSD17B3 and SRD5A1. SRD5A1 is the predominant SRD5A in the rodent pubertal and adult testis[13,29] and is likely, therefore, to be an essential gateway entry point into the alternate pathway (Figure 1). We examined whether SRD5A1 and the alternate pathway of androgen biosynthesis maintain DHT production and preserve testis development and fertility in *Hsd17b3* KO male mice.

2 | MATERIALS AND METHODS

2.1 | Transgenic mice

The *Hsd17b3* KO mice used for the dutasteride study were generated as previously described,[20] and experiments were performed at the University of Edinburgh under the UK Animal Scientific Procedures Act, Home Office License number PPL 70/8804.

Both *Hsd17b3* and *Srd5a1* are expressed as early as embryonic day 13.5 in the fetal mouse testis.[26] *Hsd17b3 and Srd5a1* double knockout (dKO) mice were generated by the MEGA Genome Engineering Facility at the Garvin Institute of Medical Research, Darlinghurst, NSW. Crispr/Cas9 was used to generate a 7-base pair deletion at the end of exon 1 in both genes, which caused a frameshift mutation. For general colony management, $Hsd17b3^{+/-}$; $Srd5a1^{+/-}$ males and females were bred together. Due to the low percentage of recombination occurring between the *Hsd17b3* and *Srd5a1* genes on chromosome 13, mice with a mixed genotype were used to generate more of that specific genotype. The following genotypes were used in this study: $Hsd17b3^{+/+}$; $Srd5a1^{+/+}$ (wild type, WT), $Hsd17b3^{+/-}$; $Srd5a1^{+/+}$ (*Hsd17b3* Het, *Srd5a1* WT), $Hsd17b3^{+/-}$; $Srd5a1^{+/-}$ (double heterozygous, dHet), $Hsd17b3^{-/-}$; $Srd5a1^{+/-}$ (*Hsd17b3* KO), and $Hsd17b3^{-/-}$; $Srd5a1^{-/-}$ (double KO, dKO). Mice were

exposed to a 12-h day/night cycle and had access to soy-free chow to prevent potential estrogenic effects and to fresh drinking water ad libitum. All procedures were approved by the University of Newcastle's Animal Care and Ethics Committee (ACEC; approval #A-2018-820). All animal experiments were performed in accordance with the Australian code of practice for the care and use of animals for scientific purposes by the National Health and Medical Research Council of Australia.

2.2 | In vivo treatments

Dutasteride (Sigma-Aldrich, Gillingham, United Kingdom) was used to inhibit 5α-reductase enzymes. Wild type, heterozygous (together referred to as controls), and *Hsd17b3* KO mice were treated daily with either a vehicle or 1.8 mg/kg/d dutasteride[30] in their diet from day 50, and tissues were collected 30 days later. Adult mice received a single 20 IU intraperitoneal injection of human chorionic gonadotrophin (hCG) (Sigma-Aldrich, Australia) as previously described.[20] Tissues/serum were collected 16 h post injection.

2.3 | Tissue collection

Adult mice were killed by inhalation of CO_2, whereas day 0 mice were killed by decapitation. Blood was collected by cardiac puncture and serum obtained by centrifugation at 4°C for 10 min and then snap frozen and stored at −80°C. Anogenital distance (AGD) was measured using digital calipers. Tissues were collected aseptically, weighed, and either fixed in Bouin's solution (2 h for neonatal tissues, 6 h for adult tissues) for histological analysis or snap frozen and stored at −80°C for RNA, sperm quantification, or steroid analysis.

2.4 | Genotyping

Genotyping was performed on ear biopsies after weaning and a second time on tail clips to verify the genotype postmortem. Genomic DNA (gDNA) was digested in Tris-EDTA-Tween, pH 8, and Proteinase K (20 μg per ear biopsy or 40 μg per tail clip) for 1 h at 55°C, followed by 7 min at 95°C to denature remaining Proteinase K. Digested samples were diluted 1:10 in DEPC-treated DNase- and RNase-free sterile water.

The genotype of transgenic mice was identified by transgene-specific PCR assays. PCR was performed on gDNA extracts using a Type-it Mutation Detect PCR Kit (QIAGEN, VIC, Australia). Details of genotyping PCR assays are included in Supplemental Information (Tables S1 and S2). PCR products were analyzed on the QIAxcel Advanced System using QIAxcel ScreenGel Software (QIAGEN, VIC, Australia). The amplified DNA was detected by a QIAxcel DNA high resolution kit (QIAGEN, VIC, Australia), and PCR product sizes were recorded.

2.5 | Epididymal sperm reserve evaluation

Epididymal sperm were quantified from frozen epididymal samples. Epididymides were thawed on ice, and the cauda epididymis was removed and homogenized in 0.9% NaCl and 0.5% Triton X-100 using an Eppendorf micropestle (Eppendorf, Macquarie Park, NSW, Australia). Elongated spermatids were counted in a Neubauer hemocytometer cell counting chamber (Adelab Scientific, Thebarton, SA) by a blinded observer.

2.6 | Quantitative RT-PCR

RNA was extracted using the RNeasy Mini kit (QIAGEN, VIC, Australia) as per manufacturer's instructions, including RNase-free DNase on-column digestion (QIAGEN, VIC, Australia). For RNA extraction of adult mouse tissue, an external Luciferase RNA control (Promega, Alexandria, NSW, Australia) was added at 1 ng/20 mg tissue to the homogenized tissue. RNA concentration was measured using a NanoDrop Lite Spectrophotometer (Thermo Fisher Scientific, VIC, Australia). Extracted RNA was reverse transcribed to synthesize cDNA using the SuperScipt VILO cDNA Synthesis Kit (Thermo Fisher Scientific, VIC, Australia) as per manufacturer's instructions. A reverse transcriptase negative (−RT) control and a water (no template) control were included in all reverse transcriptions.

For qRT-PCR, target-specific primers and corresponding specific probes were identified and selected using the online Roche Universal Probe Library (UPL) Assay Design Centre. qRT-PCR was performed on the LightCycler 96 system (Millenium Science, Mulgrave, VIC, Australia). Concentrations of reagents and details of primers and UPL probes are listed in Supplementary Information (Tables S3 and S4). Quantification of mRNA expression was calculated using the $2^{-\Delta\Delta Ct}$ method. Gene expression was determined relative to *Beta-actin* in neonatal tissues (Universal ProbeLibrary mouse *Beta-actin* gene assay, Sigma-Aldrich, Australia) and relative to the external housekeeping Luciferase gene in adult tissues (Roche, AU). As each sample was run in triplicate, an average of the Ct value was taken.

2.7 | Hormone analysis

Serum LH levels in mice were measured using a commercially validated sandwich LH (Rodent) enzyme-linked immunosorbent assay (ELISA) kit, #KA2332 (Abnova, Taiwan). Steroids were quantified in serum and testis homogenates from mice to determine circulating and intratesticular hormone levels, respectively. Samples were thawed and kept cold on ice prior to analysis. Fragments of adult testes (20–40 mg) and whole neonatal testes were weighed and homogenized in 50 mM Tris pH 7.4, 1% deoxycholate, 0.01% SDS, containing PhosSTOP (Sigma-Aldrich, Australia) and cOmplete Mini Protease Inhibitor Cocktail (Sigma-Aldrich, Australia) at a concentration of 20 μL/mg of adult testis tissue or 100 μL/mg for neonatal testis tissue. Samples were homogenized for 4 × 30 s increments at 25 Hz, with 1 min on ice between each interval to ensure samples did not overheat. Samples were stored at −80°C until analysis. Mass spectrometry steroid analysis was performed at the ANZAC Research Institute in Concord West, NSW. Details of steroids analyzed and detection limits are listed in Supplemental Information (Table S5).

2.8 | Tissue histology

Fixed tissues were processed, paraffin-embedded, and 5 μm sections were prepared. Sections were dewaxed in xylene (Sigma-Aldrich, Australia) and rehydrated through a series of decreasing ethanol gradients. Tissue sections were stained with hematoxylin and eosin (Sigma-Aldrich, Australia).

2.9 | Microscopy

Testis and epididymis of day 0 newborn neonates were imaged using a ZEISS SteREO Discovery.V12 Microscope (Carl Zeiss AG, Germany). Light microscopy images of adult tissue sections were captured using a Zeiss AXIO Imager A1 microscope (Carl Zeiss AG, Germany). Images were accessed through ZEN imaging software (Carl Zeiss AG, Germany).

2.10 | Statistical Analysis

Statistical analyses were performed using GraphPad Prism 8.4.3 software (GraphPad Software, San Diego, CA, USA). The Gaussian distribution of datasets was assessed by the Shapiro–Wilk normality test to determine if parametric or nonparametric statistical testing would be most appropriate. Datasets that passed the normality test underwent parametric tests, including one-way ANOVA with Tukey's post hoc test and two-way ANOVA with Tukey's post hoc test when two independent variables were present. Nonparametric statistical testing was applied to datasets that did not pass the normality test, and statistical significance was determined using a Kruskal–Wallis test and Dunn's multiple comparisons posthoc analysis. Data were considered significantly different when the p-value was ≤0.05. Data are presented as the mean with the standard error of the mean (SEM). Power calculations were performed by GraphPad StatMateTM 2.00 software to identify an appropriate group size required for hormone analysis.

3 | RESULTS

3.1 | Dutasteride, an inhibitor of 5α-reductase enzyme activity, does not alter testis size or morphology in adult male mice lacking HSD17B3

To establish whether SRD5A and the alternate pathway of androgen biosynthesis contribute to the preserved androgen action in adult *Hsd17b3* KO mice, we first used a well-established pharmacological inhibitor of SRD5A activity, dutasteride, which is a competitive inhibitor of both SRD5A type 1 and 2 enzymes (SRD5A1 and SRD5A2). Wild-type and *Hsd17b3* KO mice (50 days old) were exposed to either dutasteride or vehicle treatment in their diet for 30 days, with tissue collected at day 80.

Seminal vesicle weight is highly dependent on DHT, and a reduction in seminal vesicle weight is observed after the administration of SRD5A inhibitors[31,32]; thus, we assessed impacts on this organ. Dutasteride caused a significant reduction in seminal vesicle weight in both wild-type and *Hsd17b3* KO mice (Figure 2F); however, anogenital distance (AGD) did not change, and there were no changes in body, testis, or epididymis weights after dutasteride treatment (Figure 2B–E). The gross morphology of the testis of wild-type and *Hsd17b3* KO mice was also unaffected by dutasteride treatment (Figure 2G). These results suggest that SRD5A inhibition in adult *Hsd17b3* KO mice does not affect testis weight or gross histology.

3.2 | Circulating steroid analysis in dutasteride-treated mice reveals that the canonical and alternate pathways of androgen biosynthesis co-operate to maintain androgen production

Key steroids from the canonical and alternate androgen pathways were quantified in the circulation of

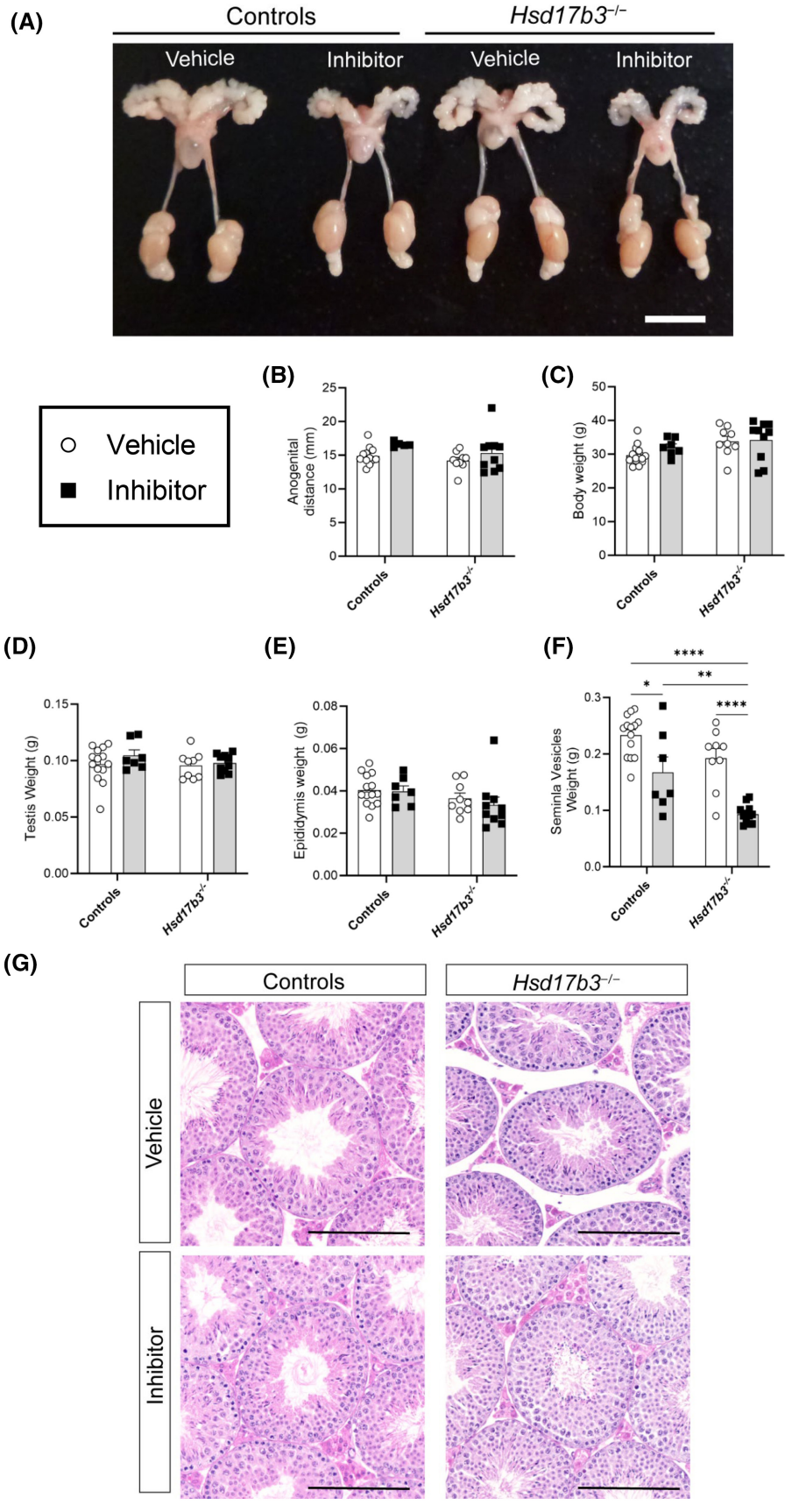

FIGURE 2 Competitive inhibition of 5α-reductase enzymes (SRD5A1 and SRD5A2) by dutasteride. (A) Representative images of the male reproductive tract of adult control and *Hsd17b3*$^{-/-}$ (*Hsd17b3* knockout [KO]) mice following 30 days of vehicle or dutasteride (inhibitor) treatment. Scale bar: 10 mm. (B) Anogenital distance and (C) total body weight of controls and *Hsd17b3* KO post-treatment of vehicle or inhibitor. Reproductive tissue weights of the (D) testis, (E) epididymis, and (F) seminal vesicles in control and *Hsd17b3* KO mice post vehicle or inhibitor treatment. Two-way ANOVA, Tukey's test, where $p \leq .05$, data shown as mean ± SEM with $n = 7$–14 per group. Significant differences between groups are indicated as *$p \leq .05$, **$p \leq .01$, ****$p \leq .0001$. (G) Representative images of hematoxylin and eosin (H&E) staining of controls and *Hsd17b3*$^{-/-}$ (*Hsd17b3* knockout) mouse testes after vehicle or dutasteride (inhibitor) treatment. Scale bar: 200 μm.

mice treated with dutasteride. Androstenedione levels were significantly increased in *Hsd17b3* KO mice compared to controls (Figure 3A), due to a reduced ability to convert androstenedione to testosterone as previously described.[15,18] Dutasteride treatment caused a further increase in androstenedione levels in *Hsd17b3*

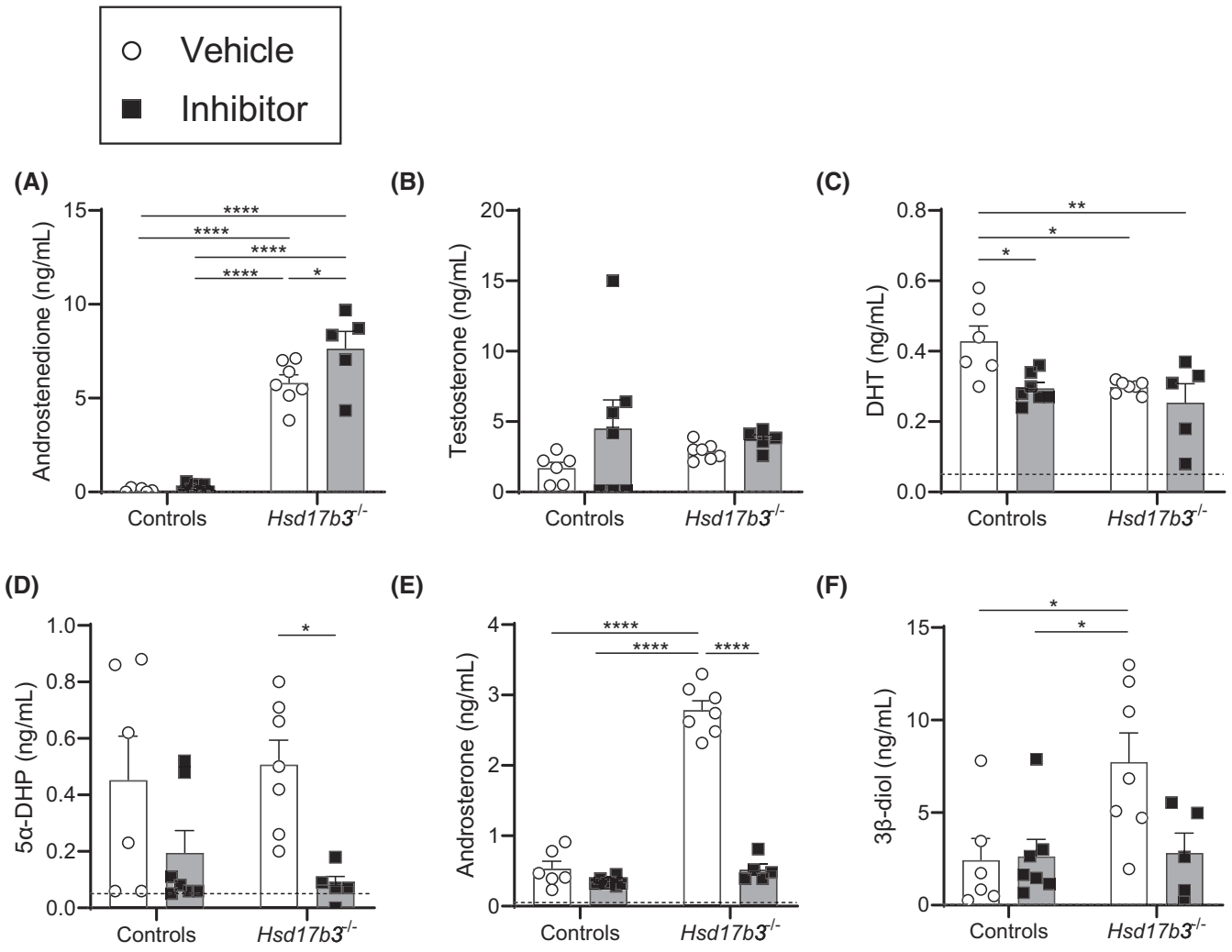

FIGURE 3 Alternate pathway androgen precursors were elevated in mouse serum in the absence of *Hsd17b3* yet were abrogated by the addition of a 5α-reductase inhibitor. Control or *Hsd17b3*$^{-/-}$ (*Hsd17b3* knockout [KO]) mice were treated with either vehicle or dutasteride (5α-reductase inhibitor) in the diet for 30 days and were collected on day 80. (A) Steroids assessed in serum include androstenedione, (B) testosterone, (C) dihydrotestosterone (DHT), (D) 5α-dihydroprogesterone (5α-DHP), (E) androsterone, and (F) 5α-androstane-3*β*,17β-diol (3β-diol). Biological replicates that were below the limit of detection were recorded as 0 ng/mL. The limit of detection ranged from 0.01 ng/mL to 0.05 ng/mL depending on the analyte and is indicated by a dotted black line on the *y*-axis. Two-way ANOVA, Tukey's test where $p \leq .05$, data shown as mean ± SEM with individual values for $n = 5–7$ biological replicates per group. Significant differences between groups are indicated as *$p \leq .05$, **$p \leq .01$, ****$p \leq .0001$.

KO mice compared to vehicle-treated *Hsd17b3* KO mice (Figure 3A), suggesting an accumulation of substrate steroids due to the reduced ability for these to be converted to other steroid products via the alternate pathway. Testosterone levels were unchanged across the different groups (Figure 3B). DHT levels in circulation were significantly decreased in dutasteride-treated control mice compared to vehicle-treated controls (Figure 3C). DHT levels were also reduced in vehicle-treated and dutasteride-treated *Hsd17b3* KO mice compared to vehicle-treated controls; however, no significant difference was observed between these two groups (Figure 3C). Taken together, these results demonstrate that dutasteride in control mice reduced serum DHT to a level similar to *Hsd17b3* KO mice; however, dutasteride was unable to further reduce DHT in *Hsd17b3* KO mice, suggesting the observed reductions in DHT arising from treatment or genotype were not additive.

To investigate the impact of dutasteride on the alternate pathway of androgen biosynthesis, precursor androgens in the alternate pathway, including 5α-DHP, androsterone, and 5α-androstane-3β, 17β-diol (androstanediol, or 3β-diol), were investigated (Figure 3D–F). Androsterone and androstanediol (3β-diol) were significantly increased in vehicle-treated *Hsd17b3* KO mice compared to control mice (Figure 3E,F), suggesting that blockade of the HSD17B3-dependent canonical pathway

increased the synthesis of alternate pathway steroids. Importantly, dutasteride-treatment in *Hsd17b3* KO mice significantly decreased 5α-DHP and androsterone compared to vehicle-treated KO mice (Figure 3D,E), indicating that suppression of SRD5A by dutasteride can decrease the alternate pathway of androgen biosynthesis in *Hsd17b3* KO mice.

These results suggest that the canonical and alternate pathways of androgen biosynthesis cooperate to maintain androgen bioactivity in adult male mice, however whether this is also the case during pre- and postnatal development is unknown.

3.3 | Development and validation of a *Hsd17b3* and *Srd5a1* double knockout mouse model

To investigate the contribution of SRD5A and the alternate pathway of androgen biosynthesis in *Hsd17b3* KO mice during development, where dutasteride treatment presents significant challenges, a double KO mouse model of both *Hsd17b3* and *Srd5a1* was generated. SRD5A1 was chosen because it is the predominant SRD5A operating in the testis and a gateway enzyme into the alternate pathway[7,21] (Figure 1).

Hsd17b3 and *Srd5a1* genes are in close proximity on chromosome 13 in the mouse, with *Hsd17b3* located at site 33.26 cM and *Srd5a1* at site 35.55 cM, as per the National Center for Biotechnology Information [NCBI], thus separated on the chromosome by just 2.29 cM (Figure S1A). Due to this proximity, it was rare for a recombination to occur between the two genes, making it impractical to generate double KOs from cross-breeding individual KOs. Instead, Crispr/Cas technology was used to simultaneously generate independent 7 bp deletions at the end of exon 1 in both genes to trigger frameshift mutations (Figure S1B).

Conversely, once generated, the reduced frequency of recombination between targeted alleles of the two genes presented challenges in collecting all possible genotypes at numbers sufficient to power downstream studies. For studies in adult mice, we were able to collect the appropriate numbers of the informative genotypes of wild type (*Hsd17b3*$^{+/+}$; *Srd5a1*$^{+/+}$), double heterozygous (dHet *Hsd17b3*$^{+/-}$; *Srd5a1*$^{+/-}$), *Hsd17b3* KO (*Hsd17b3*$^{-/-}$; *Srd5a1*$^{+/-}$) and double KO (dKO, *Hsd17b3*$^{-/-}$; *Srd5a1*$^{-/-}$). Studies in newborn mice required retrospective genotyping, and, by chance, no *Hsd17b3* KO males were collected from this cohort; thus, we were only able to collect appropriate numbers of wild-type, dHet, and dKO mice. We have thus restricted our analyses and conclusions to those that can reliably be made from the available data.

However, a previous study has shown that *Hsd17b3* KO have normal AGD and normal levels of testicular androstenedione and testosterone at birth.[33] Also, it has previously been demonstrated that male mice heterozygous for the *Hsd17b3* knockout alleles are indistinguishable from wild types[20] and that male mice heterozygous for the *Srd5a1* knockout allele are able to breed normally.[34] In our study, mice that had a recombination resulting in a *Srd5a1* single KO were all female at birth. As *Srd5a1* KO in female mice results in a parturition defect,[35] these mice were unable to be used to generate male *Srd5a1* single KO offspring. However, it has previously been shown that male homozygous *Srd5a1* KO mice develop normally and sire normal numbers of offspring.[35]

The genotypes were identified from ear or tail DNA using standard PCR (Figure S1C). Successful disruption to both pathways was confirmed by hormone analysis. Ablation of HSD17B3 was confirmed by a low intratesticular testosterone to androstenedione ratio in *Hsd17b3* KO and dKO mice (Figure S1D). *Hsd17b3* KO mice also exhibited a significantly higher ratio of circulating androsterone to androstenedione compared to WT, *Hsd17b3*$^{+/-}$; *Srd5a1*$^{+/+}$, and dHet controls (Figure S1E), indicative of increased alternate pathway steroids in the absence of *Hsd17b3*, consistent with observations in the dutasteride study (Figure 3E,F). The decreased ratio of circulating androsterone to androstenedione in dKO compared to *Hsd17b3* KO mice (Figure S1E) is consistent with decreased SRD5A activity and a decrease in the alternate pathway of androgen biosynthesis. Together, these data confirm the successful production of a mouse model lacking both HSD17B3 and SRD5A1.

3.4 | Fetal development of male mice is not impacted by the loss of HSD17B3 and SRD5A1

Loss of function mutations in alternate pathway enzymes result in disorders of sexual development in humans[12,15,36]; however, whether the alternate pathway has a role during mouse fetal development is not clear. We therefore investigated the impact of manipulating both the canonical and alternate pathways of androgen biosynthesis on fetal development of the male reproductive tract. Neonatal pups were collected on the day of birth (day 0). As mentioned above, *Hsd17b3* KO mice at day 0 have normal levels of testicular androstenedione and testosterone and a normal AGD, due to the ability of HSD17B1 to compensate for the lack of HSD17B3 during fetal development.[33]

There were no gross changes in the phenotype of the dKO testes or epididymides compared to WT or dHet mice at day 0 (Figure S2A). Epididymal coiling, known

to be androgen-dependent, was noted in all genotypes. The cell composition of the day 0 testis was normal, with seminiferous tubule and interstitial cell histology similar across all genotypes (Figure S2D). No significant differences were detected in male body weight (Figure S2C), nor in male or female AGD (Figure S2B). Previous studies have shown that AGD in neonatal male mice lacking *Hsd17b3* is also normal; however, the AGD of male mice lacking both *Hsd17b1* and *Hsd17b3* is similar to females,[33] highlighting that HSD17B1 and HSD17B3 can compensate for each other during fetal development.[33]

Thus, there were no observable gross differences in the sexual development of dKO males compared to controls, pointing to the existence of compensatory mechanisms to maintain androgen production during fetal life.

3.5 | Androgen biosynthesis in neonatal *Hsd17b3* and *Srd5a1* double knockout mice indicates the existence of compensatory mechanisms to maintain the canonical and alternate pathways

We next investigated the effects of combined deletion of *Hsd17b3* and *Srd5a1* on androgen biosynthesis at birth (day 0). First, we assessed the testicular expression of key enzymes involved in androgen production (Figure 4). The expression of the cholesterol side-chain cleavage enzyme cytochrome P450 family 11 subfamily A member (*Cyp11a1*) and the enzyme cytochrome P450 family 17 subfamily A member (*Cyp17a1*), both specifically expressed in Leydig cells, were significantly increased in the testis of dKO mice compared to WT and dHet animals (Figure 4A,B). The expression of *Hsd17b1*, an enzyme that has previously been shown to contribute to testosterone production during mouse fetal development,[33] was unchanged in the dKO testis (Figure 4C). Importantly, the expression of the type 2 5α-reductase enzyme, *Srd5a2*, was significantly increased in the dKO mouse testis (Figure 4D), suggesting that increased SRD5A2 could be a compensatory response to the loss of *Hsd17b3* and *Srd5a1* in the fetal testis.

Circulating steroids in day 0 neonatal pups were measured by mass spectrometry (Figure 5). Androstenedione was the only analyte to be detected consistently in any cohort, with the other steroids, including testosterone, androsterone, and DHT, below the limits of detection. Circulating androstenedione levels were predominantly undetectable in WT and dHet mice but were detected in all dKO mice (Figure 5). This data suggests that neonatal dKO mice have significantly increased androstenedione levels compared to WT and dHet animals due to an inability to efficiently convert androstenedione into testosterone or other androgen precursors, as previously observed in adult *Hsd17b3* KO mice.[20]

Next, we measured intratesticular steroid levels in neonatal day 0 mice by mass spectrometry to assess steroidogenesis in the context of disruption of both the canonical and

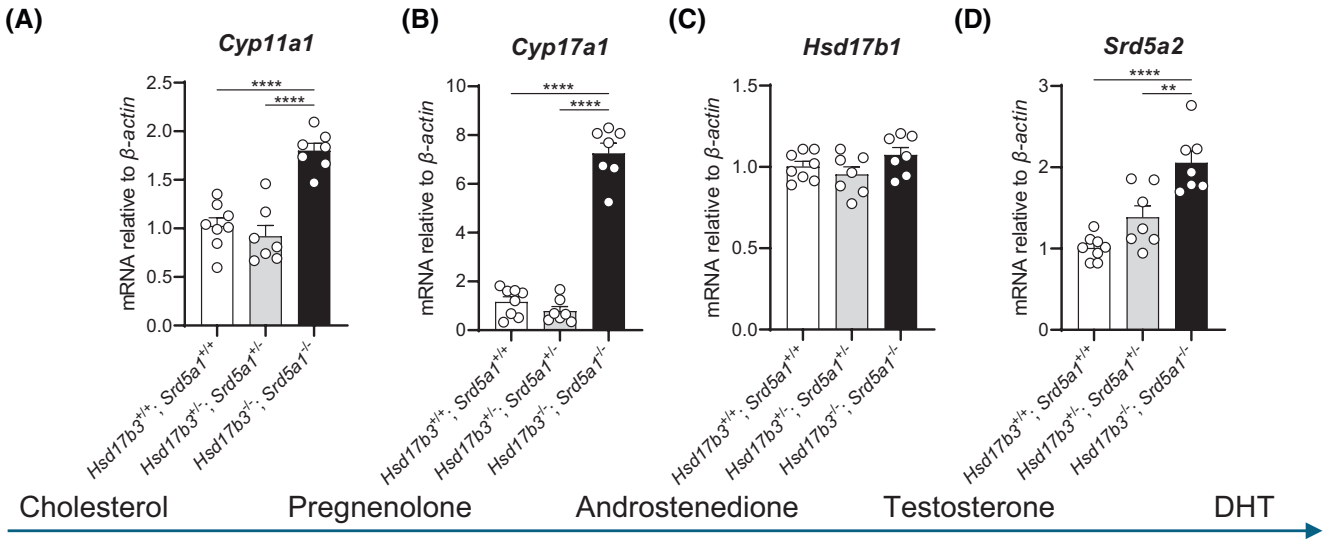

FIGURE 4 Analysis of testicular mRNA expression of steroidogenic enzymes involved in androgen biosynthesis in the neonatal *Hsd17b3*$^{-/-}$ and *Srd5a1*$^{-/-}$ (double knockout, dKO) mouse testis (day 0). (A) mRNA transcript levels of cholesterol side-chain cleavage enzyme (*Cyp11a1*), (B) cytochrome P450 family 17 subfamily A member (*Cyp17a1*), (C) 17β-hydroxysteroid dehydrogenase type 1 (*Hsd17b1*), and (D) steroid 5α-reductase type 2 (*Srd5a2*) in the testis of mice on the day of birth (day 0). One-way ANOVA, Tukey's test where $p \leq .05$, data shown as mean ± SEM with $n = 7–8$ per group. Significant differences between groups are indicated as $^{**}p \leq .01$, $^{****}p \leq .0001$. mRNA transcripts of enzymes (A–D) are shown according to the steroids produced at certain steps of the androgen production pathway (blue arrow).

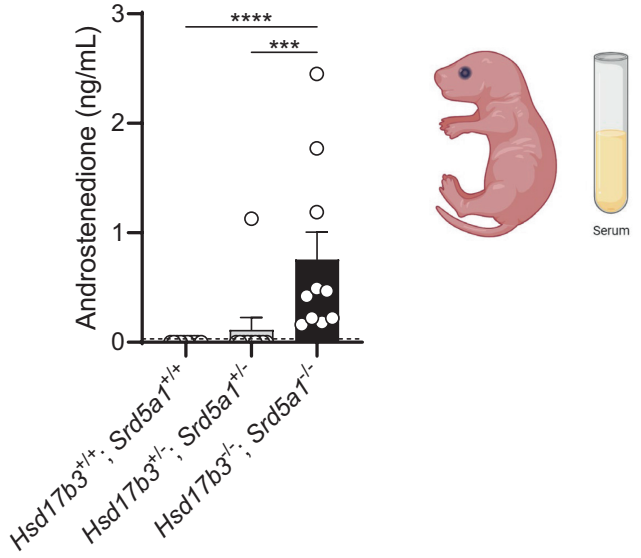

FIGURE 5 Circulating levels of androstenedione are elevated in neonatal *Hsd17b3*$^{-/-}$ and *Srd5a1*$^{-/-}$ double knockout (dKO) mice. Androstenedione levels in the serum of *Hsd17b3*$^{+/+}$; *Srd5a1*$^{+/+}$ (wild type), *Hsd17b3*$^{+/-}$; *Srd5a1*$^{+/-}$ (double heterozygous), and *Hsd17b3*$^{-/-}$; *Srd5a1*$^{-/-}$ (dKO) males on the day of birth. Samples where androstenedione was below the limit of detection were recorded as 0 ng/mL. Limit of detection: 0.03 ng/mL, indicated by dotted black line. One-way ANOVA, Kruskal–Wallis test where $p \leq .05$, data shown as mean ± SEM with $n = 10$ per group. Significant differences between groups are indicated as ***$p \leq .001$, ****$p \leq .0001$.

alternate pathways (Figure 6). No changes were observed between any genotype in pregnenolone, 17-OH pregnenolone, or 17-OH progesterone, which are all precursors in the canonical androgen pathway (Figure 6A,D,E), however, there was a significant increase in progesterone levels in the dKO testis compared to dHet mice (Figure 6B). DHEA and androstenediol, which are synthesized via the Δ5 route of the canonical pathway, were below the limit of detection (Figure 6G,K) likely because mice favor the Δ4 route, where *Cyp17a1* can more efficiently convert 17-OH progesterone into androstenedione as opposed to converting 17-OH pregnenolone into DHEA.

Intratesticular androstenedione was significantly increased in dKO mice compared to WT and dHet animals (Figure 6H); however, no changes were previously observed in neonatal *Hsd17b3* KO mice.[33] These observations suggest an accumulation of precursor steroids due to the inability of the dKO testes to efficiently convert androstenedione via the canonical and alternate pathways. Previous studies have shown that intratesticular testosterone levels were normal in *Hsd17b3* KO mice at day 0[33]; however, in neonatal dKO mice, intratesticular testosterone levels were significantly increased compared to WT and dHet animals (Figure 6L). Taken together, these observations suggest that, in neonatal dKO mice, elevated levels of androstenedione precursor are due to the deletion of both *Hsd17b3* and *Srd5a1* preventing androstenedione metabolism via the canonical and alternate pathways, and that testosterone continues to be converted from androstenedione via neonatal expression of HSD17B1 (Figure 4C[33]) and potentially other, as yet unidentified, hydroxysteroid dehydrogenases.[20,33]

There were no significant differences in alternate pathway androgen precursors including 5α-DHP, allopregnanolone, androsterone, 5α-androstane-3α,17β-diol (3α-diol), and 5α-androstane-3β,17β-diol (3β-diol) between any genotype collected (Figure 6C,F,I,J,N). Similarly, intratesticular DHT levels were unaffected in dKO mice (Figure 6M). These data suggest that the alternate androgen production pathway is maintained at birth in the testes of dKO mice, likely due to testicular expression of *Srd5a2* (Figure 4D).

Finally, we investigated estrogenic steroids that are produced via the aromatase enzyme (CYP19A1) and can be converted via androstenedione or testosterone into the weak estrogen, estrone (E1), and the potent estrogen, estradiol (E2), respectively (Figure 1). Whilst estrone levels were below the limit of detection (data not shown), intratesticular estradiol was detected in all samples but showed no significant changes between WT, dHet, and dKO mice (Figure 6O). This data suggests that the disruption to the canonical and alternate androgen pathways of biosynthesis does not impact estrogen production at birth.

FIGURE 6 Analysis of intratesticular steroids in the mouse testis on the day of birth. Steroids were measured in testes from *Hsd17b3*$^{+/+}$; *Srd5a1*$^{+/+}$ (wild type), *Hsd17b3*$^{+/-}$; *Srd5a1*$^{+/-}$ (double heterozygous), and *Hsd17b3*$^{-/-}$ and *Srd5a1*$^{-/-}$ (double knockout, dKO) mice. (A–M) Quantitation of intratesticular androgen precursors and active androgens involved in the canonical and alternate androgen production pathways. Steroids measured include (A) pregnenolone, (B) progesterone, (C) 5α-dihydroprogesterone (5α-DHP), (D) 17-OH pregnenolone, (E) 17-OH progesterone, (F) allopregnanolone, (G) dehydroepiandrosterone (DHEA), (H) androstenedione, (I) androsterone, (J) 5α-androstane-3α, 17β-diol (3α-diol), (K) androstenediol, (L) testosterone, (M) dihydrotestosterone (DHT), (N) 5α-androstane-3β, 17β-diol (3β-diol) and (O) estradiol. Blue arrows indicate the direction of the canonical androgen production pathway. Orange arrows indicate conversion occurring in the alternate androgen production pathway. Dotted arrows indicate an indirect conversion. Biological replicates that were below the limit of detection were recorded as 0 ng/mL. The limit of detection ranged from 2.5 pg/mL to 0.05 ng/mL depending on the analyte and is indicated by a dotted black line. One-way ANOVA, Tukey's test (for parametric data) or Kruskal–Wallis test (for nonparametric data), where $p \leq .05$, data shown as mean ± SEM with $n = 9$–10 per group. Significant differences between groups are indicated as *$p \leq .05$, **$p \leq .01$, ***$p \leq .001$.

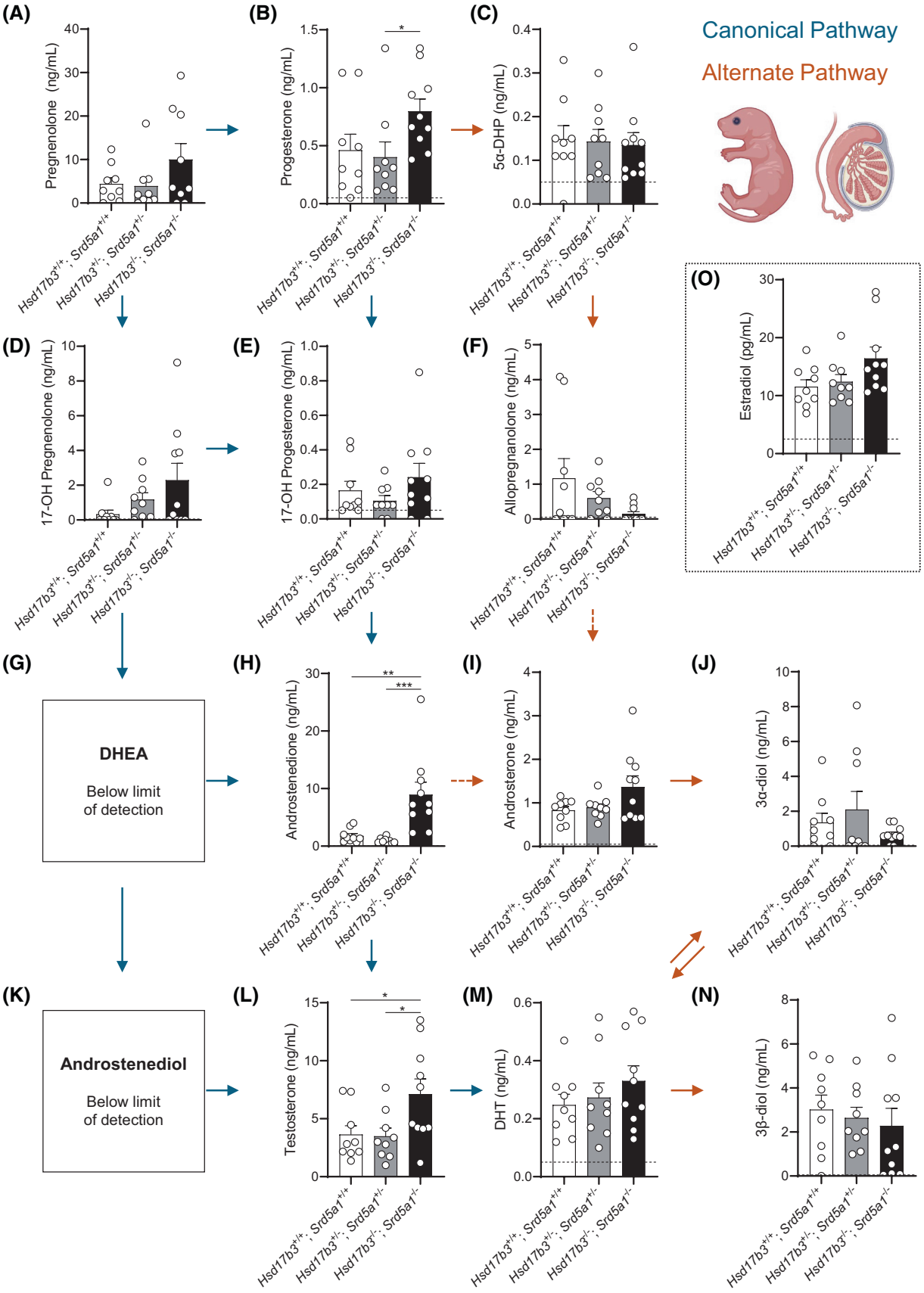

Taken together, the above data suggest that, when *Hsd17b3* and *Srd5a1* are deleted during fetal development, the canonical and alternate pathways of androgen biosynthesis in the testis are preserved via compensatory action of other enzymes, including HSD17B1 and SRD5A2.

3.6 | The ablation of *Hsd17b3* and *Srd5a1* does not impact the postnatal development of the adult male reproductive system

To examine the postnatal impact of the loss of *Hsd17b3* and *Srd5a1* on adult male mice, the gross morphology of the reproductive system in adult (day 80) dKO animals was analyzed. These mice were compared to mice lacking *Hsd17b3* alone. The results showed that male reproductive organs were grossly normal, including the seminal vesicles, prostate, vas deferens, epididymides, and testes in both adult *Hsd17b3* KO and dKO (Figure S3A). Although the AGD was not changed in dKO mice at birth (Figure S2B), it was decreased in adult *Hsd17b3* KO and dKO mice compared to all other groups (Figure S3B), suggesting perturbed androgen action during postnatal development such that the prenatally-programmed maximum AGD could not be reached.[37] The AGD of dKO mice was not reduced compared to *Hsd17b3* KO mice, indicating that the removal of *Srd5a1* does not further influence the AGD (Figure S3B). Body weights were consistent amongst all genotypes with the exception of *Hsd17b3* KO mice, which showed a slight but significant decrease compared to WT controls and dKO mice (Figure S3C); however, this has not previously been observed in the *Hsd17b3* single KO studies.[20,22] There were no differences in testis, epididymis, or seminal vesicle weights between genotypes, which are biomarkers of intratesticular and circulating androgens (Figure S3D–F). A reduction in kidney weight was observed in *Hsd17b3* KO mice compared to WT animals, however no other changes were seen among any other genotype (Figure S3G). Finally, the weight of gonadal fat in dKO mice was increased compared to dHet animals only, suggesting possible changes in peripheral testosterone or estrogen levels (Figure S3H). As no difference was observed in any of these endpoints between $Hsd17b3^{+/+}$; $Srd5a1^{+/+}$ and $Hsd17b3^{+/-}$; $Srd5a1^{+/+}$ mice, these groups were combined for all further analyses on adult mice and are referred to as "controls."

3.7 | Ablation of *Hsd17b3* and *Srd5a1* does not alter fertility in adult male mice

In the testis, the gross morphology of the seminiferous tubules and interstitial cells was normal across all groups (Figure 7A). Relative quantification of the mRNA transcript levels of *Hsd3b6*, a Leydig cell maturation marker, revealed a significant decrease in *Hsd17b3* KO and dKO mice compared to controls and dHet mice (Figure 7C). The cauda epididymis had grossly normal morphology, and the lumen contained mature sperm (Figure 7B). There were no significant differences in the number of epididymal sperm (Figure 7D). Fertility in adult dKO male mice appeared normal, as dKO male mice were able to sire litters ($n = 5$ mice). dKO males sired normal-sized litters, for example, an average 6.4 ± 2.5 pups per litter ($n = 11$ L) compared to dHet-sired litters 5.6 ± 1.9 pups per litter ($n = 42$ L). The above data suggests that, like in *Hsd17b3* KO males, postnatal male reproductive tract development is maintained and fertility is unaffected in dKO males.

3.8 | Testicular androgen biosynthesis is maintained in *Hsd17b3* and *Srd5a1* double knockout mice

Previous studies have demonstrated that testicular testosterone production is maintained in *Hsd17b3* KO mice[22] and therefore we analyzed testicular steroids in both *Hsd17b3* KO and dKO mice. Pregnenolone, progesterone, 17-OH pregnenolone, 17-OH progesterone, and androstenedione were all significantly increased in the testis of *Hsd17b3* KO and dKO males (Figure 8A,B,D,E,H). Importantly, pregnenolone and androstenedione were further increased in the dKO testis compared to *Hsd17b3* KO (Figure 8A,H). This data suggests that steroid precursors accumulate when the canonical pathway is impaired in *Hsd17b3* KO and that there is a further accumulation of steroid precursors when both the canonical and alternate pathways are impaired in the testes of dKO mice.

As previously demonstrated, *Hsd17b3* KO mice continued to synthesize normal basal levels of testosterone and DHT (Figure 8L,M).[15,18] Normal intratesticular testosterone levels were also observed in dKO testes (Figure 8L) and, surprisingly, intratesticular DHT levels were also normal in the absence of SRD5A1 (Figure 8M).

Analysis of alternate pathway steroids revealed that 5α-DHP levels were mostly below the limit of detection in the testis of all genotypes (Figure 8C) and allopregnanolone was not detectable (Figure 8F). In *Hsd17b3* KO testes, there were no significant changes in alternate pathway steroids compared to controls, suggesting that this pathway in the testis is largely unaffected by the loss of HSD17B3. Levels of the alternate pathway steroid androsterone were < 1 ng/mL in WT and dHet testes, but some *Hsd17b3* KO and dKO mice exhibited high levels (Figure 8I), perhaps consistent with increased alternate pathway activity in terms of androsterone production; however, the reason for the variation is not clear. Strikingly, alternate pathway steroids that require SRD5A, including androsterone, 3α-diol

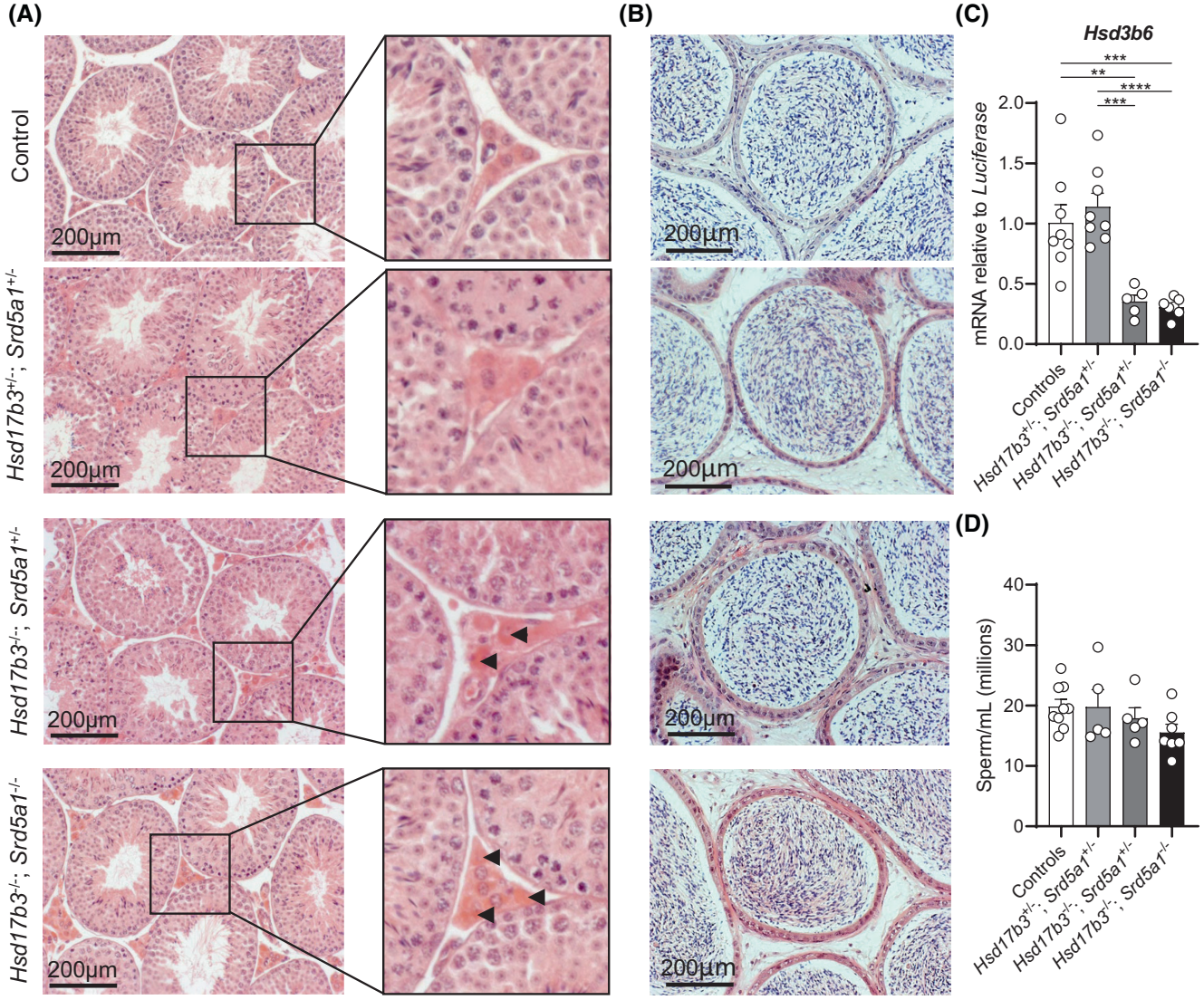

FIGURE 7 Normal sperm production in adult *Hsd17b3* and *Srd5a1* double knockout (dKO) mice. (A) Hematoxylin and eosin (H&E) staining of day 80 adult testis from control (*Hsd17b3*$^{+/+}$; *Srd5a1*$^{+/+}$ [wild type]), *Hsd17b3*$^{+/-}$; *Srd5a1*$^{+/-}$ (double heterozygous [dHet]), *Hsd17b3*$^{-/-}$; *Srd5a1*$^{+/-}$ (*Hsd17b3* knockout [KO]) and *Hsd17b3*$^{-/-}$; *Srd5a1*$^{-/-}$ (dKO) mice. The black box indicates the further magnified section of the image. Black arrowheads indicate Leydig cells. Scale bar: 200 µm. (B) Representative H&E staining images of day 80 adult cauda epididymis from control, dHet, *Hsd17b3* KO, and dKO mice. Scale bar: 200 µm. (C) mRNA transcript levels relative to a luciferase external control of 3β-hydroxysteroid dehydrogenase type 6 (*Hsd3b6*) in adult testis tissue. One-way ANOVA, Tukey's test where $p \leq .05$, data shown as mean ± SEM with $n = 5–8$ per group. Significant differences between groups are indicated as $^{**}p \leq .01$, $^{***}p \leq .001$, $^{****}p \leq .0001$. (D) Epididymal sperm counts from the cauda epididymis. One-way ANOVA, Tukey's test where $p \leq .05$, data shown as mean ± SEM with $n = 5–9$ per group.

and 3β-diol, were not significantly altered by the loss of SRD5A1 in dKO mice (Figure 8I,J,N).

Taken together, the above data suggest that the production of DHT and other steroids in the alternate pathway of androgen synthesis in the testis is preserved in the absence of SRD5A1 in dKO mice.

Finally, to investigate whether the levels of androstenedione and testosterone were influenced by conversion into estrogens via the aromatase enzyme, testicular estrone and estradiol were measured. Intratesticular estrone levels were below the limit of detection (data not shown), and estradiol concentrations remained normal across the different genotypes (Figure 8O), suggesting that testicular aromatase activity is not altered in these mice.

3.9 | The ablation of *Hsd17b3* and *Srd5a1* increases the expression of key steroidogenic genes in adult testes

The above data suggests that steroidogenesis is preserved in both *Hsd17b3* KO and *Hsd17b3* and *Srd5a1* dKO mice,

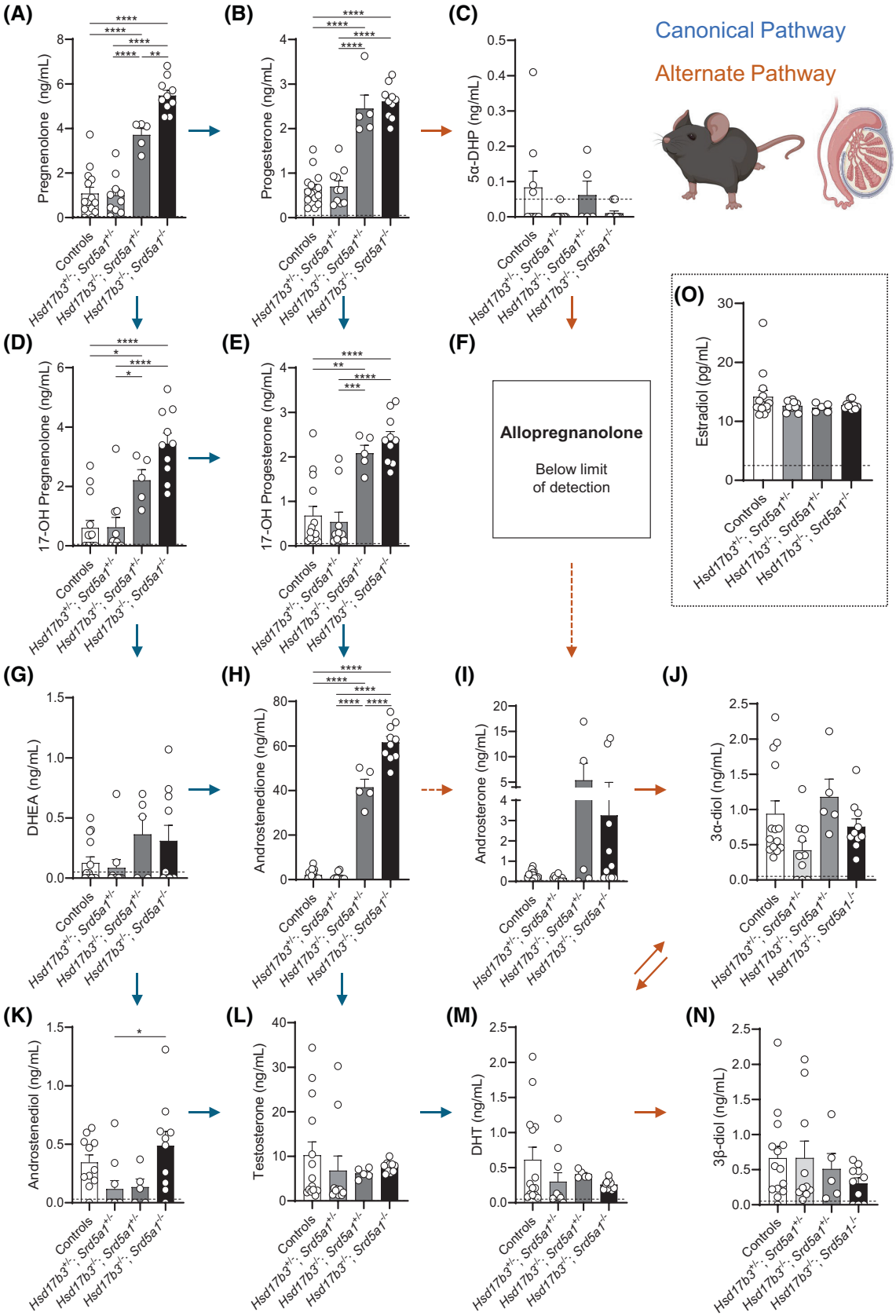

and thus we next investigated the testicular expression of steroidogenic enzymes. As previously observed in mice lacking *Hsd17b3*,[20,22] the Leydig cells of both *Hsd17b3* KO and *Hsd17b3* and *Srd5a1* dKO adult mice exhibited a phenotype of increased LH responsiveness and increased production of key steroidogenic enzymes, consistent

FIGURE 8 Analysis of intratesticular steroids in *Hsd17b3*$^{-/-}$ knockout (KO) and *Hsd17b3*$^{-/-}$; *Srd5a1*$^{-/-}$ double knockout (dKO) adult (day 80) males. (A–N) Steroid quantification of testicular androgen precursors and active androgens involved in the canonical and alternate androgen production pathways. Steroids measured include (A) pregnenolone, (B) progesterone, (C) 5α-dihydroprogesterone (5α-DHP), (D) 17-OH pregnenolone, (E) 17-OH progesterone (F) allopregnanolone, (G) dehydroepiandrosterone (DHEA), (H) androstenedione, (I) androsterone, (J) 5α-androstane-3α, 17β-diol (3α-diol), (K) androstenediol, (L) testosterone, (M) dihydrotestosterone (DHT), (N) 5α-androstane-3β, 17β-diol (3β-diol), and (O) estradiol. Blue arrows indicate the direction of the canonical androgen production pathway. Orange arrows indicate conversion occurring in the alternate androgen production pathway. Dotted arrows indicate an indirect conversion. Biological replicates that were below the limit of detection were recorded as 0 ng/mL. The limit of detection ranged from 2.5 pg/mL to 0.05 ng/mL depending on the analyte and is indicated by a dotted black line on the *y*-axis. One-way ANOVA, Tukey's test, where $p \leq .05$, data shown as mean ± SEM with $n = 5–14$ per group. Significant differences between groups are indicated as *$p \leq .05$, **$p \leq .01$, ***$p \leq .001$, ****$p \leq .0001$.

with a phenotype of steroidogenic compensation.[20] *Hsd17b3* KO and dKO testes exhibited elevated expression of luteinizing hormone/choriogonadotropin receptor (*Lhcgr*) and steroid biosynthetic enzymes, including *StAR*, *Cyp11a1*, and *Cyp17a1* (Figure 9A–CE). Of note, *Cyp17a1* is involved in both the canonical and alternate pathways of androgen biosynthesis (Figure 1). There were no differences between genotypes in testicular expression of *Hsd3b1* (Figure 9D), as previously observed in *Hsd17b3* KO mice.[20,22] *Hsd17b6*, a steroidogenic enzyme involved in the alternate pathway, showed no changes in transcript levels between any of the groups (Figure 9F). *Hsd17b5*, another enzyme involved in the alternate androgen pathway and known to produce testosterone, was also assessed; however, transcript levels were undetectable in all genotypes.

As mRNA expression of steroidogenic enzymes was increased in *Hsd17b3* KO and dKO male mice (Figure 9A–CE), AR expression was also assessed to see if it was altered. However, testicular mRNA expression of the AR was unchanged across all genotypes (Figure 9G).

Strikingly, mRNA expression of the other steroid SRD5A enzyme, *Srd5a2*, was very low in the testes from control and dHet mice but was markedly and significantly increased >40-fold in both *Hsd17b3* KO and dKO mouse testes (Figure 9H). This data suggests that *Srd5a2* is switched on in both *Hsd17b3* KO and dKO testes and therefore could maintain production of DHT in the adult testis to compensate for impaired androgen production in these models.

In summary, this data demonstrates that, as in *Hsd17b3* KO testes, dKO also exhibits a phenotype of steroidogenic compensation. The demonstration that testicular *Srd5a2* is switched on in both *Hsd17b3* KO and dKO mice suggests that increased SRD5A2 is a compensatory response to ablation of the canonical pathway in the testis and is likely to be responsible for continued testicular production of the potent androgen DHT.

3.10 | The testes of both *Hsd17b3* KO and dKO mice produce basal levels of testosterone and DHT that are not responsive to hCG

The above studies were performed in mice with endogenous LHCGR activation in Leydig cells via the natural ligand, LH; however, it is known that *Hsd17b3* KO mice show reduced responsiveness to the LHCGR agonist human chorionic gonadotrophin (hCG) and are unable to increase testosterone production in response to hCG.[20] Therefore, we also investigated testicular steroidogenesis under the conditions of maximal LHCGR stimulation using exogenous hCG. hCG treatment tests the maximal ability of the Leydig cells to produce androgens and also reduces natural variation in testosterone and the impact that alpha males may have in a cage of mice.[38]

After hCG stimulation, no differences were observed in canonical pathway steroids pregnenolone, 17-OH progesterone, and DHEA between *Hsd17b3* KO or dKO mice and controls (Figure 10A,E,G). Testicular progesterone was not different between *Hsd17b3* KO mice and controls but was significantly increased in dKO mice (Figure 10B). hCG-stimulated levels of 17-OH pregnenolone and androstenedione were significantly increased in both *Hsd17b3* KO and dKO mice compared to controls and dHet mice (Figure 10D,H). These results are consistent with an upregulation of *Cyp17a1* enzyme expression in the testis (Figure 9E), as previously observed, and a reduced ability to convert androstenedione to testosterone in the absence of *Hsd17b3*.[20,22]

Stimulation with hCG significantly increased testicular testosterone and DHT levels in control and dHet testes, but the levels were low in *Hsd17b3* KO and dKO mice (Figure 10L,M). This data supports previous observations in *Hsd17b3* KO mice where hCG hyperstimulation is unable to increase testosterone production, consistent with a phenotype of steroidogenic compensation, the fact that HSD17B3 is a rate-limiting step for testosterone production, and the

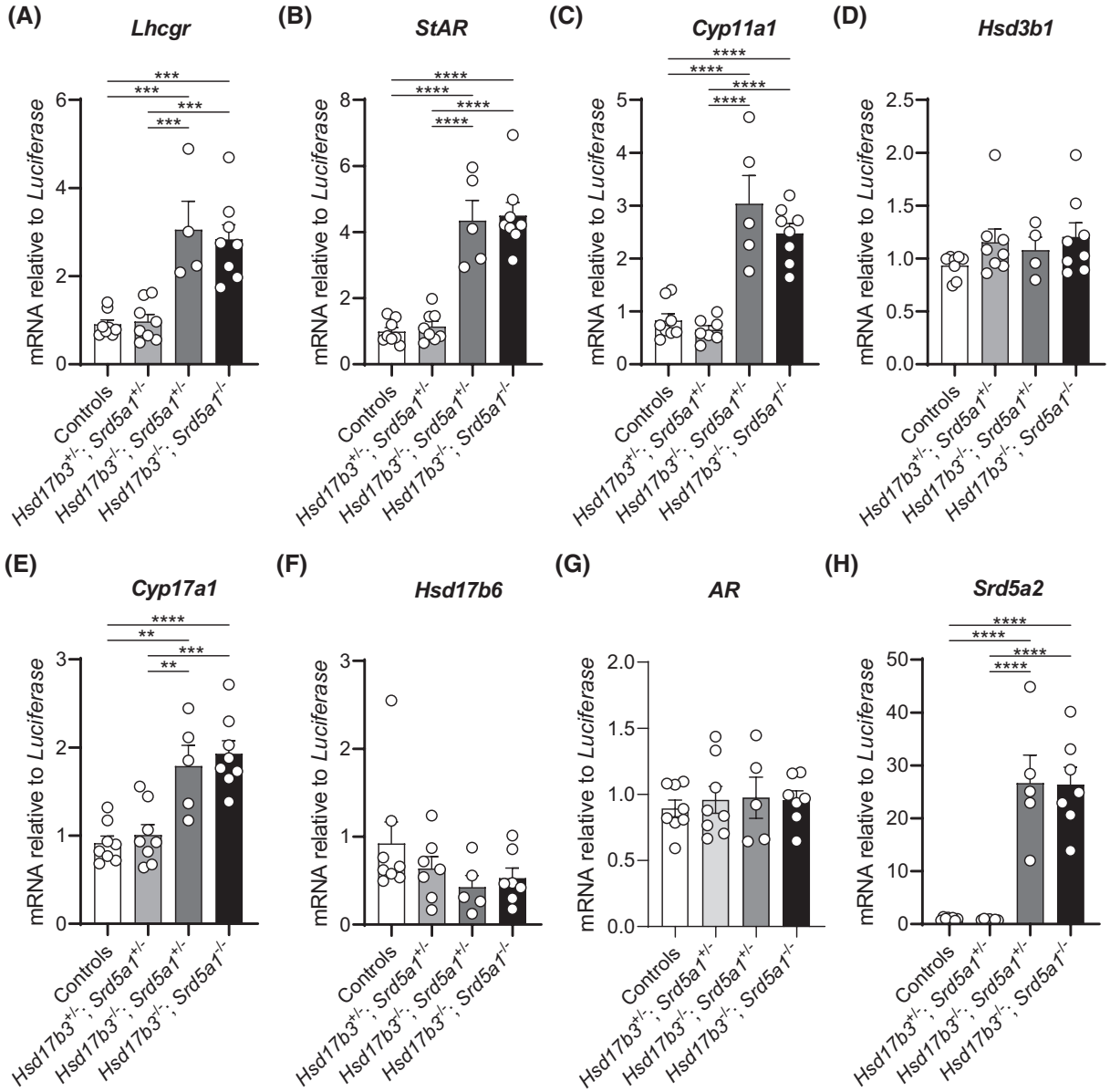

FIGURE 9 Elevated expression of key steroidogenic enzymes in the adult testes of *Hsd17b3* KO and *Hsd17b3* and *Srd5a1* double knockout (dKO) mice. mRNA transcript levels in the adult testis relative to a luciferase external control. Transcripts quantified include (A) Luteinizing hormone/choriogonadotropin receptor (*Lhcgr*), (B) steroidogenic acute regulatory protein (*StAR*), (C) cholesterol side-chain cleavage enzyme (*Cyp11a1*), (D) 3β-hydroxysteroid dehydrogenase type 1 (*Hsd3b1*), (E) cytochrome P450 family 17 subfamily A member (*Cyp17a1*), (F) 17β-hydroxysteroid dehydrogenase type 6 (*Hsd17b6*), (G) androgen receptor (*AR*), and (H) steroid 5α-reductase type 2 (*Srd5a2*). One-way ANOVA, Tukey's test where $p \leq .05$, data shown as mean ± SEM with $n = 5–8$ per group. Significant differences between groups are indicated as $^{**}p \leq .01$, $^{***}p \leq .001$, $^{****}p \leq .0001$.

FIGURE 10 Intratesticular steroid analysis of *Hsd17b3*$^{-/-}$ knockout (KO) and *Hsd17b3*$^{-/-}$; *Srd5a1*$^{-/-}$ double knockout (dKO) mice following luteinizing hormone/chorionic gonadotrophin receptor (LHCGR) activation. LHCGR signaling was activated by hCG administration, and androgen precursors and active androgens in the canonical and alternate androgen production pathways were measured in the testes of day 80 adults. Steroids quantified include (A) pregnenolone, (B) progesterone, (C) 5α-dihydroprogesterone (5α-DHP), (D) 17-OH pregnenolone, (E) 17-OH progesterone, (F) allopregnanolone, (G) dehydroepiandrosterone (DHEA), (H) androstenedione, (I) androsterone, (J) 5α-androstane-3α, 17β-diol (3α-diol), (K) androstenediol, (L) testosterone, (M) dihydrotestosterone (DHT), and (N) 5α-androstane-3β, 17β-diol (3β-diol). Blue arrows indicate the direction of the canonical androgen production pathway. Orange arrows indicate the alternate androgen production pathway. Dotted arrows indicate an indirect conversion. Biological replicates that were below the limit of detection were recorded as 0 ng/mL. The limit of detection ranged from 0.01 ng/mL to 0.05 ng/mL depending on the analyte and is indicated by a dotted black line on the *y*-axis. One-way ANOVA, Tukey's test, where $p \leq .05$, data shown as mean ± SEM with $n = 3–12$ per group. Significant differences between groups are indicated as $^{*}p \leq .05$, $^{**}p \leq .01$, $^{***}p \leq .001$, $^{****}p \leq .0001$.

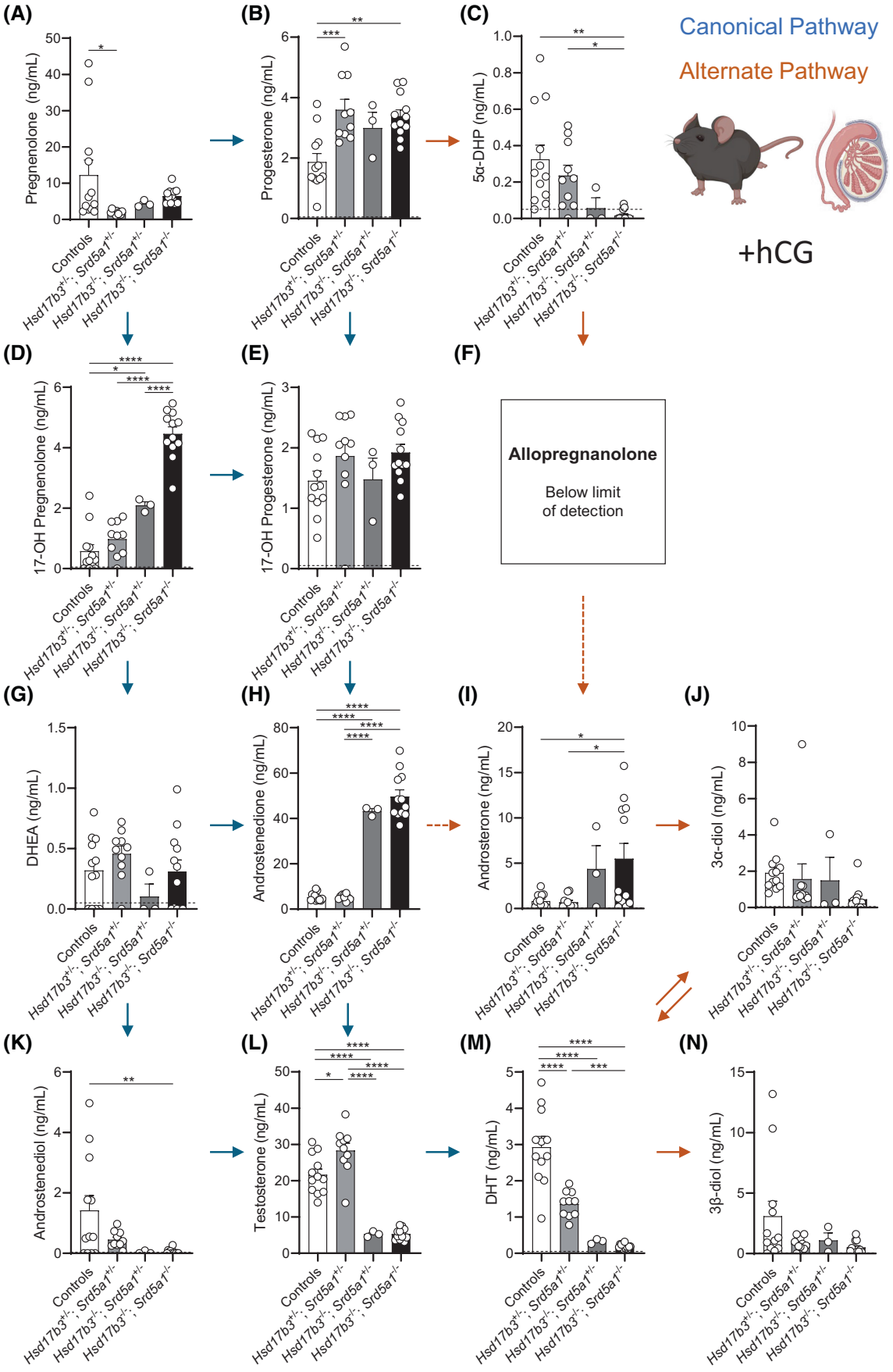

ability of KO Leydig cells to maintain testosterone via other, as yet unidentified, hydroxysteroid dehydrogenases.[20]

An investigation of alternate androgen pathway precursors following hCG treatment revealed that 5α-DHP levels were significantly decreased in dKO mice compared to control and dHet mice, and the majority of 5α-DHP measurements were below the limit of detection in dKO testes (Figure 10C). These data are consistent with a role for SRD5A1, but not SRD5A2, in 5α-DHP synthesis in the testis (Figure 1). Intratesticular levels of androsterone were significantly increased in dKO mice compared to controls and dHet animals (Figure 10I), likely reflecting increased *Srd5a2* (Figure 9H), which can act via the alternate pathway (Figure 1); however, there were no significant differences among the genotypes in 3α-diol and 3β-diol (Figure 10J,N).

In summary, these data suggest that, in the absence of *Hsd17b3* and *Srd5a1*, hCG-treated Leydig cells continue to produce abundant levels of androstenedione yet basal levels of testosterone that are likely produced by other, hitherto unidentified, hydroxysteroid dehydrogenases, similar to *Hsd17b3* KO mice.[20] Basal production of DHT continues (Figure 8M), likely via the increased testicular expression of *Srd5a2* (Figure 9H), and thus is able to contribute to sustained androgen action in dKO testes.

3.11 | Both *Hsd17b3* KO and dKO mice exhibit a phenotype of steroidogenic compensation

The data above details testicular steroid levels during either basal (unstimulated) conditions (Figure 8) or stimulation of Leydig cell LHCGR by hCG (Figure 10). We next investigated the hCG-responsiveness of Leydig cell steroidogenesis in each genotype by comparing steroid levels between basal and hCG-stimulated testis samples (Figure S4).

In control mice, hCG treatment significantly increased pregnenolone, progesterone, and 17-OH progesterone (Figure S4A,C,D), consistent with hCG activation of Leydig cell LHCGR stimulating steroidogenesis; however, hCG stimulation of pregnenolone and 17-OH progesterone was not observed in *Hsd17b3* KO and dKO mice (Figure 4A,D). In terms of testicular androgens, hCG treatment significantly increased testicular testosterone and DHT levels in control and dHet mice but not in *Hsd17b3* KO or dKO mice (Figure S4F,K), consistent with a loss of responsiveness to LHCGR activation, as previously demonstrated in *Hsd17b3* KO mice.[20] Curiously, hCG stimulation in dKO mice led to a small but significant increase in 17-OH pregnenolone and progesterone and a small but significant reduction in androstenedione compared to basal levels; however, this was not observed in *Hsd17b3* KO mice (Figure S4B,C,E), suggesting these changes could be unique to impairment of the alternate pathway.

Alternate pathway androgen precursors were also compared to determine the hCG-responsiveness of the alternate pathway of androgen production. Both 5α-DHP and 3β-diol were increased by hCG in control testes (Figure S4G,J), suggesting that the alternate pathway can respond to hCG stimulation in wild-type mice; however, the levels in *Hsd17b3* KO and dKO mice remained unchanged (Figure S4G,J), consistent with reduced responsiveness to hCG.

Overall, the data are consistent with a phenotype of compensated steroidogenesis in both *Hsd17b3* KO and dKO mice, whereby steroidogenesis is operating at a near-maximal level of LHCGR stimulation to drive both the canonical and alternate pathways of androgen biosynthesis, and thus hCG treatment cannot induce further increases.

3.12 | Analysis of steroids in the circulation reveals an increase in alternate pathway steroids in the absence of *Hsd17b3*, and that ablation of *Srd5a1* reduces alternate androgen biosynthesis

The above data suggests that testicular SRD5A activity is preserved in *Hsd17b3* and *Srd5a1* dKO testes, likely because of a marked up-regulation of testicular *Srd5a2* expression. To investigate the impact of the loss of both *Hsd17b3* and *Srd5a1* on hormones in the circulation, we

FIGURE 11 Circulating hormone analysis of adult (day 80) male $Hsd17b3^{-/-}$ knockout (KO) and $Hsd17b3^{-/-}$; $Srd5a1^{-/-}$ double knockout (dKO) mice. (A) The gonadotrophin luteinizing hormone (LH) was measured in the serum of adult mice. (B–O) Quantification of steroids involved in the canonical and alternate androgen biosynthesis pathways. Androgens and androgen precursors quantified by mass spectrometry include (B) pregnenolone, (C) progesterone, (D) 5α-dihydroprogesterone (5α-DHP), (E) 17-OH pregnenolone, (F) 17-OH progesterone (G) allopregnanolone, (H) dehydroepiandrosterone (DHEA), (I) androstenedione, (J) androsterone, (K) 5α-androstane-3α, 17β-diol (3α-diol), (L) androstenediol, (M) testosterone, (N) dihydrotestosterone (DHT), and (O) 5α-androstane-3β, 17β-diol (3β-diol). Blue arrows indicate the direction of the canonical androgen production pathway. Orange arrows indicate conversion occurring in the alternate androgen production pathway. Dotted arrows indicate an indirect conversion. Biological replicates that were below the limit of detection were recorded as 0 ng/mL. The limit of detection ranged from 0.01 ng/mL to 0.05 ng/mL depending on the analyte and is indicated by a dotted black line on the *y*-axis. One-way ANOVA, Tukey's test, where $p \leq .05$, data shown as mean ± SEM with $n = 5–14$ per group. Significant differences between groups are indicated as *$p \leq .05$, **$p \leq .01$, ***$p \leq .001$, ****$p \leq .0001$.

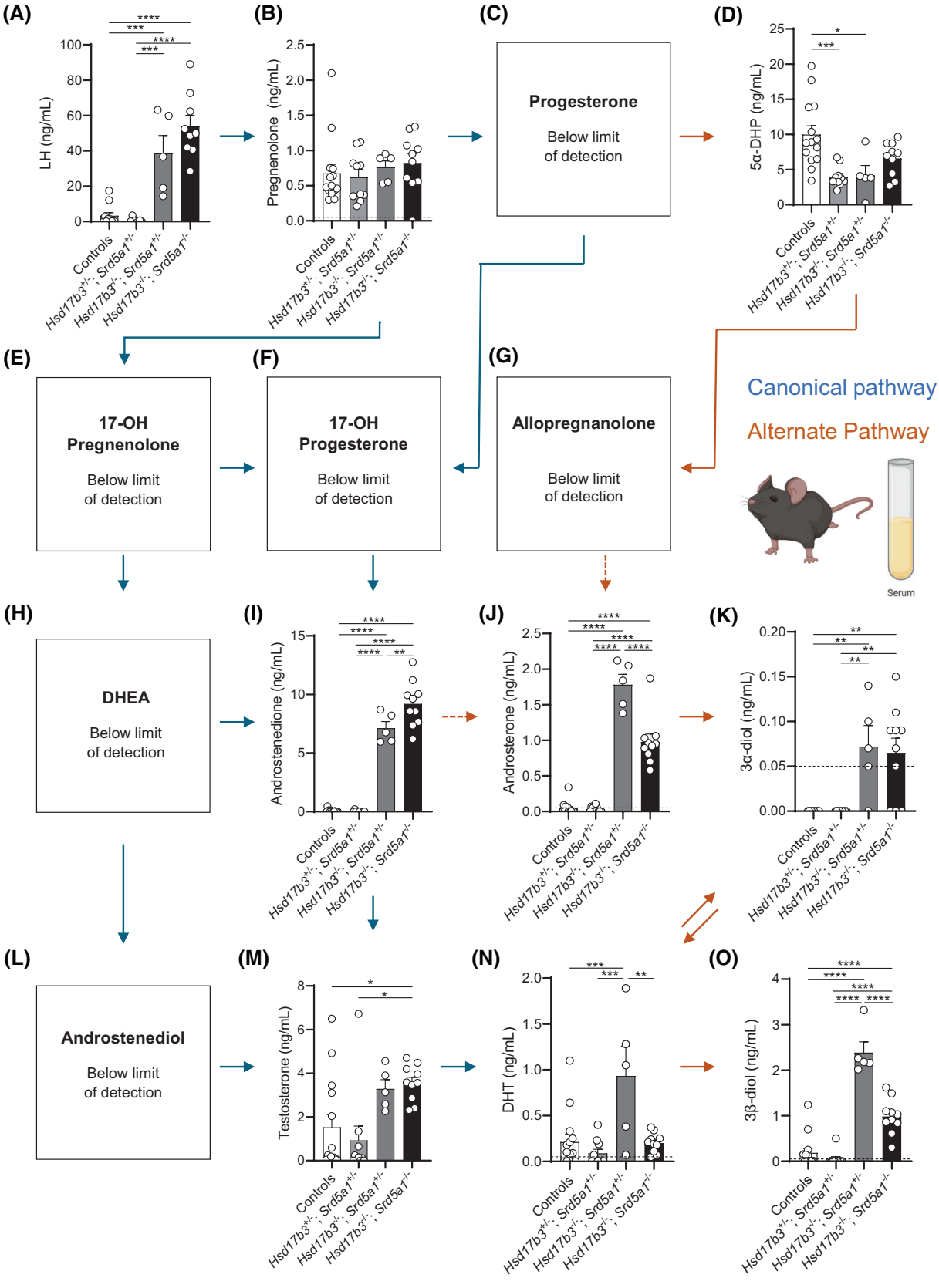

measured LH and steroids in the canonical and alternate pathways of androgen biosynthesis in the serum, with the latter determined using the same mass spectrometry method used to measure testicular steroidogenesis.

Circulating LH was significantly increased in *Hsd17b3* KO, as previously described,[20,22] and was also increased in dKO mice compared to control and dHet males (Figure 11A). The elevated serum LH, along with

increased testicular steroidogenesis, further confirms that, like *Hsd17b3* KO mice,[20,22] dKO mice show a phenotype of steroidogenic compensation, whereby mice exhibit elevated levels of LH, increased LH receptor expression (Figure 9A), and increased testicular steroidogenic enzyme expression (Figure 9B,C,E).

In terms of steroid precursors, circulating pregnenolone was not changed between genotypes (Figure 11B), and other precursor steroids prior to androstenedione formation were not detectable (Figure 11). Circulating androstenedione was significantly increased in *Hsd17b3* KO mice (Figure 11I), as observed previously.[15,18] Androstenedione levels were further increased in dKO mice compared to *Hsd17b3* KO (Figure 11I), consistent with a further accumulation of this androgen precursor when both the canonical and alternate androgen biosynthesis pathways are disrupted. No significant differences were detected in serum testosterone levels between control and *Hsd17b3* KO mice; however, there was considerable variation in the control cohort (Figure 11M), and previous studies have shown increased serum testosterone in this model.[20,22] Serum testosterone was significantly increased in dKO mice compared to controls (Figure 11M). Estrone and estradiol were not detected in the adult male circulation in all genotypes (data not shown).

In the alternate pathway, the androgen precursors androsterone, 3α-diol, and 3β-diol in serum were all significantly increased in *Hsd17b3* KO mice compared to controls (Figure 11J,K,O), as was serum DHT (Figure 11N). These data suggest that the loss of HSD17B3 is associated with an increase in androgen synthesis via the alternate pathway in peripheral tissues. Importantly, the loss of *Srd5a1* in dKO mice caused a marked reduction in serum androsterone, 3β-diol, and DHT compared to *Hsd17b3* KO mice (Figure 11J,N,O). These data confirm that the ablation of *Srd5a1* in *Hsd17b3* KO mice reduces androgen biosynthesis via the alternate pathway in peripheral tissues but suggest that the alternate pathway is maintained in the testes, likely due to the compensatory increase in testicular *Srd5a2* expression.

3.13 | Production of the androgen 11-keto-dihydrotestosterone (11K-DHT) is increased in the circulation of *Hsd17b3* KO and dKO mice

The phenotypes of both *Hsd17b3* KO and dKO mice suggest the existence of multiple mechanisms of compensation when the canonical and alternate pathways of androgen biosynthesis are reduced by the ablation of the major androgen biosynthetic enzymes. Therefore, we next considered whether the production of 11-keto androgens could be altered in these mice. This was deemed particularly relevant because observations in fetal mice with reduced testicular expression of *Hsd17b1* and *Hsd17b3* showed elevated testicular 11-keto androstenedione and testosterone, suggesting that increased 11-keto-androgen production could be a compensatory response to reduced hydroxysteroid dehydrogenase activity.[27]

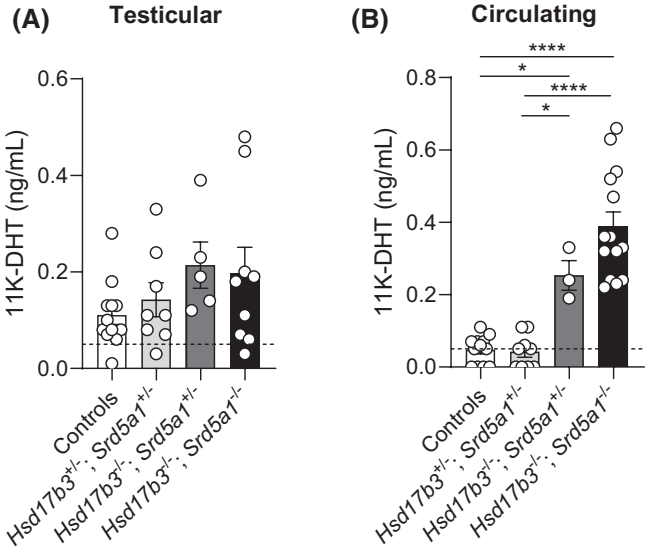

FIGURE 12 (A) Intratesticular and (B) circulating levels of 11-keto-dihydrotestosterone (11K-DHT) in adult (day 80) male *Hsd17b3*$^{-/-}$ knockout (KO) and *Hsd17b3*$^{-/-}$; *Srd5a1*$^{-/-}$ double knockout (dKO) mice. The limit of detection was 0.05 ng/mL and is indicated by a dotted black line on the *y*-axis. One-way ANOVA, Tukey's test, where $p \leq .05$, data shown as mean ± SEM with $n = 5$–14 per group. Significant differences between groups are indicated as *$p \leq .05$, ****$p \leq .0001$.

We therefore measured testicular and circulating levels of 11-oxyandrogens and 11-keto androgens in adult *Hsd17b3* KO and dKO mice. 11OH-androstenedione, 11OH-testosterone, 11K-androstenedione, and 11K-testosterone (11K-T) were not detected in any testis or serum samples. 11K-DHT was detectable in the testis but did not differ between genotypes (Figure 12A); however, circulating 11K-DHT levels were significantly increased in *Hsd17b3* KO and dKO mice (Figure 12B). The concentration of 11K-DHT in serum was similar to, and in some cases higher than, serum DHT levels (Figure 11M). These data suggest increased extra-gonadal synthesis of 11K-DHT when *Hsd17b3* is ablated prior to birth, suggesting that 11-keto androgen production could be operating as another compensatory mechanism to preserve androgen bioactivity when the major androgen biosynthetic enzymes are ablated.

4 | DISCUSSION

The canonical pathway of androgen biosynthesis involves the production of testosterone via HSD17B3 and

the conversion of testosterone to DHT via the SRD5A enzymes, and the alternate pathway involves the production of DHT via SRD5A independent of testosterone production (Figure 1).[5,8,12,14,15] Both the canonical and alternate pathways are essential for normal human male sexual development.[11–15,36] However, whether and how these pathways cooperate to regulate androgen bioactivity in mice is not understood. In mice, deletion of *Hsd17b3* or loss of function mutations in SRD5A enzymes do not affect male sexual development and fertility,[20,22,31] suggesting compensatory mechanisms maintain androgen production when 17-ketosteroid or SRD5A enzymes are ablated. The current study utilized mice lacking both *Hsd17b3* and *Srd5a1*, the primary SRD5A enzyme acting in the testis, to address the hypothesis that the alternate pathway of androgen biosynthesis contributes to the maintenance of male sexual development and fertility in the absence of *Hsd17b3*. The results reveal multiple mechanisms of compensation in male mice to maintain androgen bioactivity.

The impact of the alternate pathway of androgen biosynthesis in adult *Hsd17b3* KO mice was first investigated using dutasteride, a competitive inhibitor for the SRD5A1 and SRD5A2 enzymes. In *Hsd17b3* KO mice, alternate pathway precursors androsterone and 3β-diol were significantly increased in circulation, suggesting that, when the canonical pathway is impaired, the alternate pathway is up-regulated to preserve androgen production. The up-regulation of alternate pathway precursors in *Hsd17b3* KO mice was reduced by dutasteride treatment, confirming that suppression of SRD5A reduces the entry of steroids into the alternate pathway. While dutasteride reduced circulating DHT in wild-type mice, the levels were unaffected in *Hsd17b3* KO mice, yet seminal vesicle weights were reduced, likely reflecting a local reduction in DHT production in target tissues.[39] No changes in testis weight or histology were seen, suggesting testicular testosterone acts directly to maintain androgen activity in the testis and/or an inability of dutasteride to compete with the high levels of testosterone for the SRD5A catalytic site. Nevertheless, this experiment revealed that alternate pathway precursors are increased in *Hsd17b3* KO mice, pointing to cross-talk between the canonical and alternate pathways. These findings suggest that ablation of SRD5A in *Hsd17b3* KO mice may be a useful model to investigate the contribution of the alternate pathway to androgen production in the absence of HSD17B3.

Thus, we developed mice in which both the canonical and alternate androgen production pathways were impaired by deletion of *Hsd17b3* and *Srd5a1*. We deleted SRD5A1 because it is a key gateway enzyme into the alternate pathway of steroid biosynthesis (Figure 1) and the predominant SRD5A contributing to DHT production in the adult rodent testis.[29] The phenotype of the *Hsd17b3* KO (*Hsd17b3*$^{-/-}$; *Srd5a1*$^{+/-}$) line generated in this study was entirely consistent with the phenotype of *Hsd17b3* KO mouse lines generated by us[20] and others.[22] In both *Hsd17b3* KO and *Hsd17b3* and *Srd5a1* (dKO) mice, the ablation of HSD17B3 was functionally confirmed by a decreased AGD, increased serum androstenedione levels, and a reduced ratio of testicular testosterone to androstenedione, which are hallmarks of HSD17B3 deficiency in humans[13] and mice.[15,18] dKO mice showed a similar phenotype of steroidogenic compensation as *Hsd17b3* KO mice[20,22] and the knockout of the *Srd5a1* allele was functionally validated by significant reductions in the ratio of circulating androsterone to androstenedione and in circulating alternate androgen pathway precursors and DHT compared to *Hsd17b3* KO mice. The creation of dKO mice provides an opportunity to examine the contribution of the alternate pathway to the maintenance of androgen bioactivity in *Hsd17b3* KO mice.

The role of the alternate androgen production pathway in male prenatal sexual development was investigated by assessing dKO mice on the day of birth. Sexual development appeared normal, and steroid analyses suggested this pathway remained functional in the testes. Importantly, the expression of another SRD5A enzyme, *Srd5a2*, was significantly increased in the testes of neonatal dKO mice, suggesting it is up-regulated to compensate for the loss of *Hsd17b3* and/or *Srd5a1*. *Srd5a2* is not up-regulated in the absence of *Srd5a1* in female mice,[35] suggesting that mechanisms of cooperativity may be specific to the testis. Another explanation for normal testis development in dKO mice is the maintenance of testosterone production during fetal development by continued expression of HSD17B1 that is able to compensate for the loss of HSD17B3 during fetal development.[33] Taken together, these observations suggest that androgen action during fetal testis development in dKO mice is supported by HSD17B1 and SRD5A2.

Adult dKO mice had grossly normal reproductive tracts but decreased testicular expression of the Leydig cell maturation marker *Hsd3b6*, consistent with altered Leydig cell maturation and function during *Hsd17b3* deficiency. The data suggested that the alternate pathway operates in the adult mouse testis but that it is not up-regulated in the testis during HSD17B3 deficiency. Intratesticular testosterone levels were preserved in both *Hsd17b3* KO and dKO, pointing to *Hsd17b3*-independent mechanisms of testosterone synthesis.[20] Importantly, testicular DHT was maintained in dKO mice and the mRNA expression of another SRD5A enzyme, *Srd5a2*, showed a >40-fold increase. The data suggested that the marked up-regulation of *Srd5a2* is a response to the loss of *Hsd17b3*, rather than the loss of *Srd5a1*. SRD5A2 is

particularly effective at catalyzing 5α-reduction at low levels of testosterone, such as is observed in the testis during puberty,[29,40] and thus it is reasonable to hypothesize that the testis responds to steroidogenic insufficiency by switching on SRD5A2. Studies in human prostate have shown that adult somatic cell suppression of SRD5A2 is regulated by DNA methyltransferase-dependent epigenetic modifications of the SRD5A2 promoter,[41] raising the intriguing possibility that, during *Hsd17b3* deficiency, demethylation of testicular *Srd5a2* could contribute to the increased expression of *Srd5a2*.

The testicular phenotype of dKO mice is one of steroidogenic compensation, similar to *Hsd17b3* KO mice.[20,22] dKO mice exhibited elevated circulating LH and testicular expression of *Lhcgr* and steroidogenic enzymes including *Star*, *Cyp11a1*, and *Cyp17a1* consistent with a phenotype of steroidogenic compensation by the Leydig cells.[20,22] The expression of steroidogenic enzymes was not further increased in dKO compared to *Hsd17b3* KO testes, and testicular steroids were not further stimulated by hCG, indicating that the Leydig cells are functioning to their maximum output in the absence of *Hsd17b3*. The preserved synthesis of testicular testosterone and DHT was not hCG-responsive in dKO mice, suggesting that the compensatory mechanisms in the testis are refractory to further LHCGR stimulation. Adult testes do not express HSD17B1, even in the absence of HSD17B3,[33] and therefore this enzyme cannot be responsible for the maintenance of testicular testosterone production in both the *Hsd17b3* KO and dKO testes, suggesting that other, as-yet unidentified, hydroxysteroid dehydrogenase enzymes are capable of converting androstenedione to testosterone in the adult mouse testis.[5,20,33]

Our analyses revealed that *Hsd17b3* deficiency is associated with an increase in alternate pathway steroids and DHT in the circulation. However, this does not occur in the testes, likely due to the marked up-regulation of testicular *Srd5a2* expression, which can maintain DHT production via the conversion from testosterone in the canonical pathway. We also showed that the loss of *Srd5a1* in the dKO mice caused a marked reduction in circulating levels of androsterone, 3β-diol and DHT compared to *Hsd17b3* KO mice, indicating that *Srd5a1* contributes to the maintenance of androgen bioactivity in peripheral tissues in conditions of steroidogenic insufficiency. Taken together, our findings suggest that the loss of HSD17B3 in the testis and the resulting phenotype of steroidogenic compensation is associated with an increase in the alternate pathway of androgen biosynthesis in peripheral tissues. These observations point to the existence of compensatory mechanisms in extra-gonadal tissues that act to maintain DHT biosynthesis when Leydig cell steroidogenesis is compromised.

We also assessed the levels of 11-keto steroids in the testis and circulation. These 11-keto steroids are synthesized from adrenal-derived 11-oxygenated steroids in target tissues[23] and are present at much lower levels than native androgens in males.[23] We were able to detect 11K-DHT, but not 11K-T, in the testis of adult mice, but the levels did not change in *Hsd17b3* KO or dKO mice. Circulating 11K-T was undetectable in mice and 11K-DHT was lowly abundant in WT mice; however, 11K-DHT was elevated in both *Hsd17b3* KO and dKO mice, suggesting the synthesis of this bioactive androgen is an extra-gonadal compensatory response to the loss of *Hsd17b3*. 11-keto androgens are up-regulated in castration-resistant prostate cancer[42] and in the fetal mouse testis when *Hsd17b1* and *Hsd17b3* expression is reduced,[27] suggesting that they can be increased in males when steroidogenesis is compromised. 11K-T can be efficiently converted to 11K-DHT by SRD5A2, but not by SRD5A1,[43] and both 11K-T and 11K-DHT can bind to the AR to elicit androgen responses.[28,44] Little is known about the androgenic potency of 11K-DHT in mouse tissues, but it is important to note that androgen bioactivity relies on multiple factors, including mechanisms of local tissue production and inactivation, an ability to bind to carrier proteins and to elicit classic genomic and/or rapid non-genomic AR-dependent responses. The fact that 11K-DHT, but not 11K-T, is up-regulated in the circulation, but not testes, of KO mice with a phenotype of androgen biosynthetic enzyme insufficiency and steroidogenic compensation points to the existence of intriguing mechanisms of co-operativity between androgen biosynthetic pathways in mice.

Our finding that SRD5A and the alternate pathway can support androgen production in conditions of steroidogenic insufficiency is relevant to the understanding of human male endocrine disorders. Masculinization of the human fetus involves both the canonical and alternate pathways of androgen biosynthesis.[12,17] Alternate pathway androgen precursors are not produced in the developing human testis and are instead synthesized predominantly in peripheral tissues and the placenta.[14] How the canonical and alternate pathways intersect and cooperate during human male sexual development is not clear, but our data suggest mechanisms of compensation between the two pathways to maintain androgen bioactivity. Human XY individuals with HSD17B3 deficiency can develop male characteristics during puberty[19,21]; however, whether the synthesis of DHT via the alternate pathway could promote androgen-dependent pubertal masculinization in conditions of human HSD17B3 deficiency is not known and yet is suggested by our findings in mice. Finally, ~10% of men with late-onset hypogonadism exhibit a phenotype of compensated hypogonadism, with high LH and normal testosterone,[45] similar to

steroidogenic compensation in HSD17B3-deficient adult mice.[20,22] Whether SRD5A and the alternate pathway, including an up-regulation of SRD5A2 in the testis, contribute to the maintenance of androgen bioactivity in this clinical setting is unknown.

In conclusion, observations from *Hsd17b3* KO and *Hsd17b3* and *Srd5a1* dKO mice have revealed striking mechanisms of compensation to maintain androgen bioactivity during fetal life and in adulthood in male mice. In the absence of *Hsd17b3* and *Srd5a1*, fetal sexual development and androgen production can be maintained by testicular HSD17B1[33] and there is a compensatory increase in testicular SRD5A2 expression at birth. In adult mice deficient in *Hsd17b3* alone or *Hsd17b3* and *Srd5a1*, the testes exhibit a phenotype of steroidogenic compensation, with elevated LH and precursor steroid production and continued testosterone production, likely via unknown enzyme(s) capable of synthesizing testosterone,[20,22] and DHT, likely via the marked upregulation of the SRD5A2 enzyme. In peripheral tissues, the absence of HSD17B3 causes 11K-DHT production to be switched on, and there is an increase in steroids produced via the alternate pathway of androgen production, suggesting that the canonical, alternate, and 11-keto steroid androgen production pathways can cooperate to contribute to androgen production. We conclude that mice have evolved multiple mechanisms, involving multiple pathways of androgen production, to maintain androgen biosynthesis throughout development and adulthood.

AUTHOR CONTRIBUTIONS

B. M. Lawrence, D. Rebourcet, and L. B. Smith conceived and designed the research; B. M. Lawrence, D. Rebourcet, A.-L. Gannon, S. Smith, M. K. Curley, A.-L Darbey, and R. McKay performed the research and acquired the data; B. M. Lawrence, L. O'Donnell, P. J. O'Shaughnessy, D. Rebourcet, and L. B. Smith analyzed and interpreted the data; B. M. Lawrence, L. O'Donnell, and L. B. Smith wrote the manuscript; D. Rebourcet and P. J. O'Shaughnessy revised the manuscript.

ACKNOWLEDGMENTS

The authors wish to thank Laura Milne, Eirini Matthaiou, and Nathan Jeffery from the University of Edinburgh (UK) and Shanu Parameswaran from the University of Newcastle (Australia) for their technical support, and Professor David Handelsman and Dr. Reena Desai from the ANZAC Institute (Australia) for steroid quantitation in transgenic mice. This work was funded by the National Health and Medical Research Council (NHMRC), the Department of Health (Australia), Project Grant APP1158344 (LBS, DR), and a UK Medical Research Council (MRC) Program Grant MR/N002970/1 (LBS).

DISCLOSURES

The authors declare no conflict of interest.

DATA AVAILABILITY STATEMENT

The data that support the findings of this study are available in the Materials and Methods, Results, and/or Supplemental Material of this article. Images used in the figures were created with BioRender.com, agreement numbers NO278I5F0T, VL278I6056, PF278I6AH5, ZI278I6J27, NB278I6YC9, OK278IFGLJ, XU278IH6UG, and DI27GXZCM9.

ORCID

Ben M. Lawrence https://orcid.org/0000-0002-7803-1611
Liza O'Donnell https://orcid.org/0000-0001-5848-6136
Anne-Louise Gannon https://orcid.org/0000-0001-6137-4063
Michael K. Curley https://orcid.org/0000-0002-3621-8007
Annalucia Darbey https://orcid.org/0000-0001-8541-5472
Rosa Mackay https://orcid.org/0009-0003-4395-2001
Peter J. O'Shaughnessy https://orcid.org/0000-0001-5651-7883
Diane Rebourcet https://orcid.org/0000-0002-7432-9269

REFERENCES

1. Andersson AM, Jorgensen N, Frydelund-Larsen L, Rajpert-De Meyts E, Skakkebaek NE. Impaired Leydig cell function in infertile men: a study of 357 idiopathic infertile men and 318 proven fertile controls. *J Clin Endocrinol Metab*. 2004;89:3161-3167.
2. Zarotsky V, Huang MY, Carman W, et al. Systematic literature review of the risk factors, comorbidities, and consequences of hypogonadism in men. *Andrology*. 2014;2:819-834.
3. Corona G, Rastrelli G, Di Pasquale G, Sforza A, Mannucci E, Maggi M. Endogenous testosterone levels and cardiovascular risk: meta-analysis of observational studies. *J Sex Med*. 2018;15:1260-1271.
4. Grino PB, Griffin JE, Wilson JD. Testosterone at high concentrations interacts with the human androgen receptor similarly to dihydrotestosterone. *Endocrinology*. 1990;126:1165-1172.
5. Lawrence BM, O'Donnell L, Smith LB, Rebourcet D. New insights into testosterone biosynthesis: novel observations from HSD17B3 deficient mice. *Int J Mol Sci*. 2022;23:15555.
6. Miller WL. Androgen biosynthesis from cholesterol to DHEA. *Mol Cell Endocrinol*. 2002;198:7-14.
7. Naamneh Elzenaty R, du Toit T, Fluck CE. Basics of androgen synthesis and action. *Best Pract Res Clin Endocrinol Metab*. 2022;36:101665.
8. Miller WL, Auchus RJ. The "backdoor pathway" of androgen synthesis in human male sexual development. *PLoS Biol*. 2019;17:e3000198.

9. Shaw G, Fenelon J, Sichlau M, Auchus RJ, Wilson JD, Renfree MB. Role of the alternate pathway of dihydrotestosterone formation in virilization of the Wolffian ducts of the tammar wallaby, Macropus eugenii. *Endocrinology*. 2006;147:2368-2373.
10. Wilson JD, Auchus RJ, Leihy MW, et al. 5alpha-androstane-3alpha,17beta-diol is formed in tammar wallaby pouch young testes by a pathway involving 5alpha-pregnane-3alpha,17alpha-diol-20-one as a key intermediate. *Endocrinology*. 2003;144:575-580.
11. Dhayat NA, Dick B, Frey BM, d'Uscio CH, Vogt B, Fluck CE. Androgen biosynthesis during minipuberty favors the backdoor pathway over the classic pathway: insights into enzyme activities and steroid fluxes in healthy infants during the first year of life from the urinary steroid metabolome. *J Steroid Biochem Mol Biol*. 2017;165:312-322.
12. Fluck CE, Meyer-Boni M, Pandey AV, et al. Why boys will be boys: two pathways of fetal testicular androgen biosynthesis are needed for male sexual differentiation. *Am J Hum Genet*. 2011;89:201-218.
13. Mahendroo M, Wilson JD, Richardson JA, Auchus RJ. Steroid 5alpha-reductase 1 promotes 5alpha-androstane-3alpha,17beta-diol synthesis in immature mouse testes by two pathways. *Mol Cell Endocrinol*. 2004;222:113-120.
14. O'Shaughnessy PJ, Antignac JP, Le Bizec B, et al. Alternative (backdoor) androgen production and masculinization in the human fetus. *PLoS Biol*. 2019;17:e3000002.
15. Fluck CE, Pandey AV. Steroidogenesis of the testis – new genes and pathways. *Ann Endocrinol (Paris)*. 2014;75:40-47.
16. Geissler WM, Davis DL, Wu L, et al. Male pseudohermaphroditism caused by mutations of testicular 17 beta-hydroxysteroid dehydrogenase 3. *Nat Genet*. 1994;7:34-39.
17. Goncalves CI, Carrico J, Bastos M, Lemos MC. Disorder of sex development due to 17-beta-hydroxysteroid dehydrogenase type 3 deficiency: a case report and review of 70 different HSD17B3 mutations reported in 239 patients. *Int J Mol Sci*. 2022;23:10026.
18. Faisal Ahmed S, Iqbal A, Hughes IA. The testosterone:androstenedione ratio in male undermasculinization. *Clin Endocrinol*. 2000;53:697-702.
19. Mendonca BB, Gomes NL, Costa EM, et al. 46,XY disorder of sex development (DSD) due to 17beta-hydroxysteroid dehydrogenase type 3 deficiency. *J Steroid Biochem Mol Biol*. 2017;165:79-85.
20. Rebourcet D, Mackay R, Darbey A, et al. Ablation of the canonical testosterone production pathway via knockout of the steroidogenic enzyme HSD17B3, reveals a novel mechanism of testicular testosterone production. *FASEB J*. 2020;34:10373-10386.
21. Hiort O, Marshall L, Birnbaum W, et al. Pubertal development in 17beta-hydroxysteroid dehydrogenase type 3 deficiency. *Horm Res Paediatr*. 2017;87:354-358.
22. Sipila P, Junnila A, Hakkarainen J, et al. The lack of HSD17B3 in male mice results in disturbed Leydig cell maturation and endocrine imbalance akin to humans with HSD17B3 deficiency. *FASEB J*. 2020;34:6111-6128.
23. Storbeck KH, O'Reilly MW. The clinical and biochemical significance of 11-oxygenated androgens in human health and disease. *Eur J Endocrinol*. 2023;188:R98-R109.
24. Yazawa T, Inaba H, Imamichi Y, et al. Profiles of 5alpha-reduced androgens in humans and eels: 5alpha-dihydrotestosterone and 11-ketodihydrotestosterone are active androgens produced in eel gonads. *Front Endocrinol (Lausanne)*. 2021;12:657360.
25. Davio A, Woolcock H, Nanba AT, et al. Sex differences in 11-oxygenated androgen patterns across adulthood. *J Clin Endocrinol Metab*. 2020;105:e2921-e2929.
26. Whiley PAF, Luu MCM, O'Donnell L, Handelsman DJ, Loveland KL. Testis exposure to unopposed/elevated activin a in utero affects somatic and germ cells and alters steroid levels mimicking phthalate exposure. *Front Endocrinol (Lausanne)*. 2023;14:1234712.
27. Whiley PAF, O'Donnell L, Moody SC, et al. Activin a determines steroid levels and composition in the fetal testis. *Endocrinology*. 2020;161:1-16.
28. Handelsman DJ, Cooper ER, Heather AK. Bioactivity of 11 keto and hydroxy androgens in yeast and mammalian host cells. *J Steroid Biochem Mol Biol*. 2022;218:106049.
29. Killian J, Pratis K, Clifton RJ, Stanton PG, Robertson DM, O'Donnell L. 5alpha-reductase isoenzymes 1 and 2 in the rat testis during postnatal development. *Biol Reprod*. 2003;68:1711-1718.
30. Mak TCS, Livingstone DEW, Nixon M, Walker BR, Andrew R. Role of hepatic glucocorticoid receptor in metabolism in models of 5alphaR1 deficiency in male mice. *Endocrinology*. 2019;160:2061-2073.
31. Mahendroo MS, Cala KM, Hess DL, Russell DW. Unexpected virilization in male mice lacking steroid 5 alpha-reductase enzymes. *Endocrinology*. 2001;142:4652-4662.
32. Shima H, Tsuji M, Young P, Cunha GR. Postnatal growth of mouse seminal vesicle is dependent on 5 alpha-dihydrotestosterone. *Endocrinology*. 1990;127:3222-3233.
33. Junnila A, Zhang FP, Martinez Nieto G, et al. HSD17B1 compensates for HSD17B3 deficiency in fetal mouse testis but not in adults. *Endocrinology*. 2024;165:bqae056.
34. Mahendroo MS, Cala KM, Landrum DP, Russell DW. Fetal death in mice lacking 5alpha-reductase type 1 caused by estrogen excess. *Mol Endocrinol*. 1997;11:917-927.
35. Mahendroo MS, Cala KM, Russell DW. 5 alpha-reduced androgens play a key role in murine parturition. *Mol Endocrinol*. 1996;10:380-392.
36. Okeigwe I, Kuohung W. 5-alpha reductase deficiency: a 40-year retrospective review. *Curr Opin Endocrinol Diabetes Obes*. 2014;21:483-487.
37. Mitchell RT, Mungall W, McKinnell C, et al. Anogenital distance plasticity in adulthood: implications for its use as a biomarker of fetal androgen action. *Endocrinology*. 2015;156:24-31.
38. Zielinski WJ, Vandenbergh JG. Testosterone and competitive ability in male house mice, Mus musculus: laboratory and field studies. *Anim Behav*. 1993;45:873-891.
39. Swerdloff RS, Dudley RE, Page ST, Wang C, Salameh WA. Dihydrotestosterone: biochemistry, physiology, and clinical implications of elevated blood levels. *Endocr Rev*. 2017;38:220-254.
40. Normington K, Russell DW. Tissue distribution and kinetic characteristics of rat steroid 5 alpha-reductase isozymes. Evidence for distinct physiological functions. *J Biol Chem*. 1992;267:19548-19554.
41. Bechis SK, Otsetov AG, Ge R, Wang Z, et al. Age and obesity promote methylation and suppression of 5α-reductase 2:

implications for personalized therapy of benign prostatic hyperplasia. *J Urol*. 2015;194:1031-1037.

42. Du Toit T, Swart AC. Inefficient UGT-conjugation of adrenal 11beta-hydroxyandrostenedione metabolites highlights C11-oxy C(19) steroids as the predominant androgens in prostate cancer. *Mol Cell Endocrinol*. 2018;461:265-276.
43. Barnard L, Nikolaou N, Louw C, Schiffer L, et al. The A-ring reduction of 11-ketotestosterone is efficiently catalysed by AKR1D1 and SRD5A2 but not SRD5A1. *J Steroid Biochem Mol Biol*. 2020;202:105724.
44. Pretorius E, Arlt W, Storbeck KH. A new dawn for androgens: novel lessons from 11-oxygenated C19 steroids. *Mol Cell Endocrinol*. 2017;441:76-85.
45. Tajar A, Forti G, O'Neill TW, et al. Characteristics of secondary, primary, and compensated hypogonadism in aging men: evidence from the European Male Ageing Study. *J Clin Endocrinol Metab*. 2010;95:1810-1818.

SUPPORTING INFORMATION

Additional supporting information can be found online in the Supporting Information section at the end of this article.

How to cite this article: Lawrence BM, O'Donnell L, Gannon A-L, et al. Compensatory mechanisms that maintain androgen production in mice lacking key androgen biosynthetic enzymes. *The FASEB Journal*. 2024;38:e70177. doi:10.1096/fj.202402093R